

HYDROGEOLOGICAL INVESTIGATION OF THE
RIETVLEI SANDSTONE, ROBERTSON, SOUTH
AFRICA

Neville Paxton

Submitted in fulfilment of the requirements for the degree

Magister Scientiae in Geohydrology

in the

Faculty of Natural and Agricultural Sciences

(Institute for Groundwater Studies)

at the

University of the Free State

Supervisor: Prof. Danie Vermuelen

Co-supervisor: Dr Modreck Gomo

January 2018

DECLARATION

I, Neville PAXTON, hereby declare that the dissertation hereby submitted by me to the Institute for Groundwater Studies in the Faculty of Natural and Agricultural Sciences at the University of the Free State, in fulfilment of the degree of Magister Scientiae, is my own independent work. It has not previously been submitted by me to any other institution of higher education. In addition, I declare that all sources cited have been acknowledged by means of a list of references.

I furthermore cede copyright of the dissertation and its contents in favour of the University of the Free State.



Neville PAXTON

28 January 2018

ACKNOWLEDGEMENTS

I would hereby like to express my sincere gratitude to all who have motivated and helped me in the completion of this thesis. The following individuals are thanked:

- Hannes Joubert, the director of Le Grand Chasseur for full support and promotion of scientific research, from project inception to finalisation.
- Julian Conrad for his support and insight.
- Dale Barrow for technical input.
- My wife Margha, for being my pillar of support, and for distracting me when absolutely necessary.
- To God, through whom all is possible.

ABSTRACT

The study site is located 15 km south west of Robertson and 10 km north west of McGregor. The Klipberg Mountain forms the southern boundary of the site and the Breede River, from which the bulk of irrigation water is currently sourced, makes up the northern border of the study site. Recent drought has necessitated a hydrogeological investigation to determine groundwater potential to augment the current supply, however little is known about the Rietvlei Formation in the area. The investigation comprised of a detailed desktop survey, making use of satellite imagery, geological maps, existing literature and hydrogeological maps. Areas of interest were selected for geophysical survey. This proved challenging due to rugged terrain typical of the Table Mountain Group (TMG), the presence of a high voltage power line over target areas, and the associated low conductivity of the quartzitic sandstone. A successful borehole sited on an electromagnetic survey did however provide the ideal geological setting for further sitings using lineament mapping and geological survey. Drilling followed by Pumping Tests of borehole with blow yields in excess of 15 000 L/hr followed allowing aquifer parameters to be determined. Radial acting flow proved to be the dominant flow regime of the Rietvlei Formation. An average transmissivity of 23.32 m²/day was estimated which matches existing literature, while the average storativity of 4.8×10^{-4} was slightly lower. The groundwater quality varies across the site with exceptional quality found within the only existing borehole, drilled into the Sewefontein Fault with an electrical conductivity (EC) of 13.8 mS/m. This borehole did not show connectivity to other boreholes during the Pumping Tests and comprised Na – HCO₃⁻ type water. The boreholes drilled into the Klipberg Mountain have electrical conductivities ranging from 22.9 mS/m to 207 ms/m and are Na – Cl type waters. A number of irrigation classifications deem the groundwater suitable for irrigation, while some boreholes are not suitable according to other classification methods. Regular sampling of both water and soil should be conducted to determine long term affect (if any). Fracture size increased with depth in the direction of the syncline axis. There is also an associated decrease in groundwater quality towards the axis of the syncline and away from the mountains where recharge occurs. Borehole siting in similar conditions where extensive folding and faulting have occurred should take this into consideration to improve probability of intersecting good quality groundwater.

LIST OF ABBREVIATIONS

AOI = Areas of Interest
BH = Borehole
BVG = Bokkeveld Group
CCGR = Coordinating Committee of Geohydrological Research
CDT = Constant Discharge Test
CMB = Chloride Mass Balance
DD = Drawdown
DFN = Discrete Fracture Network
DWAFF = Department of Water and Forestry
EC = Electrical Conductivity
EM = Electromagnetometer
FC = Flow Characterisation
GW = Groundwater
ID = Identification
IRAF = Infinite Radial Acting Flow
K = Hydraulic Conductivity
KR = Kelly's Ratio
MAP = Mean Annual Precipitation
Max = Maximum
MH = Magnesium Hazard
Min = Minimum
nr = number
pH = Potential of Hydrogen
PI = Permeability Index
RAF = Radially Acting Flow
REV = Relevant elementary volume
RWL = Rest Water Level
T = Transmissivity
TDS = Total Dissolved Solids
TH = Total Hardness
TMG = Table Mountain Group
SANAS = South African National Accreditation System
SANS = South African National Standards
SAR = Sodium Adsorption Ratio
SP = Sodium Percentage
WRC = Water Research Commission
WBS = Well Bore Storage

TABLE OF CONTENTS

LIST OF ABBREVAIATION	V
CHAPTER 1 : INTRODUCTION	1
1.1 AIMS AND OBJECTIVES	2
CHAPTER 2 : LITERATURE REVIEW	3
2.1 INTRODUCTION	3
2.2 CONCEPTUAL MODELS FOR FRACTURED AQUIFER SYSTEMS	3
2.2.1 Fracture Flow	3
2.2.2 Parameters Determined from Pumping Tests	6
2.2.3 Pumping Test Analysis	7
2.2.3.1 Homogeneous fractures (uniform aquifer)	7
2.2.3.2 Double Porosity	7
2.2.3.3 Single Vertical Fracture	8
2.3 CASE STUDIES OF THE TMG AQUIFER	9
2.3.1 Regional Case Studies	9
2.3.2 Recent Case Studies	11
2.3.2.1 Site Specific Case Studies	13
2.4 SUMMARY	17
CHAPTER 3 : SITE DESCRIPTION	19
3.1 REGIONAL SETTING	19
3.1.1 Relief and Surface Drainage	19
3.1.2 Climate	21
3.1.3 Regional Geology	21
CHAPTER 4 : METHODS AND MATERIALS	23
4.1 GROUNDWATER EXPLORATION	23
4.1.1 Identification of Areas of Interest	23
4.1.2 Geophysics	23
4.1.2.1 Resistivity Method	26
4.1.2.2 Electromagnetic Method	26
4.1.3 Geological Survey	27
4.1.4 Borehole Drilling	28
4.2 AQUIFER PUMPING TESTS	28
4.2.1 Pumping tests: in the field	28
4.2.2 Pumping Test Analysis	32
4.3 ASSESSMENT OF HYDROGEOCHEMISTRY AND GROUNDWATER QUALITY FOR IRRIGATION	37
4.3.1 Sampling Technique	37
4.3.2 Data analysis and interpretation	39
4.3.2.1 Classification of hydrochemical facies	39
4.3.2.2 Correlation Coefficient Analysis	41

4.3.2.3	Saturation indices (SI)	41
4.3.3	Assessment of irrigation groundwater quality	41
4.3.3.1	Sodium absorption ratio (SAR)	42
4.3.3.2	Salinity Classification	43
4.3.3.3	Sodium Percentage	43
4.3.3.4	Hardness classification	44
4.3.3.5	Kelly's Ratio (1963)	44
4.3.3.6	Magnesium Hazard:	44
4.3.3.7	Permeability Index (PI):	44
CHAPTER 5 : RESULTS AND DISCUSSION		46
5.1	GROUNDWATER EXPLORATION	46
5.1.1	Identification of Areas of Interest	46
5.1.2	Geophysics	48
5.1.2.1	Electromagnetometer Profile 1	48
5.1.2.2	Electromagnetometer Profile 2	49
5.1.3	Geological Survey	50
5.1.4	Drilling Results	52
5.1.5	Summary	56
5.2	PUMPING TESTS: ANALYSIS RESULTS	59
5.2.1	HBH1	59
5.2.1.1	Step Test: HBH1	60
5.2.1.2	Constant Discharge Test: HBH1	60
5.2.1.1	Observation Boreholes and Storativity	62
5.2.2	LGC_BH1	63
5.2.2.1	Step Test: LGC_BH1	64
5.2.2.2	Constant Discharge Test: LGC_BH1	64
5.2.2.3	Observation Boreholes and Storativity	66
5.2.3	LGC_BH2	67
5.2.3.1	Step Test: LGC_BH2	67
5.2.3.2	Constant Discharge Test: LGC_BH2	68
5.2.3.1	Observation Boreholes and Storativity	70
5.2.4	LGC_BH3	70
5.2.4.1	Step Test: LGC_BH3	71
5.2.4.2	Constant Discharge Test: LGC_BH3	72
5.2.4.1	Observation Boreholes and Storativity	74
5.2.5	LGC_BH5	74
5.2.6	Step Test: LGC_BH5	75
5.2.7	Constant Discharge Test: LGC_BH5	76
5.2.7.1	Observation Boreholes and Storativity	78
5.2.8	LGC_BH8	78
5.2.8.1	Step Test: LGC_BH8	79
5.2.8.2	Constant Discharge Test: LGC_BH8	80
5.2.8.1	Observation Boreholes and Storativity	82
5.2.9	Habata_2	82
5.2.9.1	Step Test: Habata_2	83
5.2.9.2	Constant Discharge Test: Habata_2	84
5.2.9.1	Observation Boreholes and Storativity	86
5.2.10	Habata_4	86
5.2.10.1	Step Test: Habata_4	87
5.2.10.2	Constant Discharge Test: Habata_4	88
5.2.10.1	Observation Boreholes and Storativity	90
5.2.11	Habata_8	90
5.2.12	Step Test: Habata_8	91
5.2.12.1	Constant Discharge Test: Habata_8	92
5.2.12.1	Observation Boreholes and Storativity	94
5.3	PUMPING TEST RESULTS SUMMARY	94

5.3.1	Connected Boreholes	94
5.3.2	Flow characteristics and aquifer Parameters	96
5.4	ASSESSMENT OF HYDROGEOCHEMISTRY AND GROUNDWATER QUALITY FOR IRRIGATION	99
5.4.1	Hydrochemical facies	100
5.4.2	Hydrogeochemical processes	104
5.4.2.1	Correlation analysis	104
5.4.2.2	Sodium against Chloride	105
5.4.2.3	Calcium and magnesium against Sulphate and Bicarbonate ions	106
5.4.2.4	Analysis of saturation indices	107
5.4.3	Assessment of irrigation groundwater quality	108
5.4.3.1	SAR and EC	108
5.4.3.2	Total Hardness (TH)	109
5.4.3.3	Sodium Percentage	109
5.4.3.4	Kelly's Ratio (KR)	109
5.4.3.5	Magnesium Hazard (MH)	110
5.4.3.6	Permeability Index (PI)	110
5.5	SUMMARY	111
CHAPTER 6 : CONCLUSION AND RECOMMENDATIONS		114
6.1	CONCLUSIONS	114
6.1.1	Groundwater Exploration	114
6.1.2	Groundwater Flow Characteristics and Aquifer Parameters	115
6.1.3	Hydrogeochemical Processes and Groundwater Quality	115
6.2	RECOMMENDATIONS	116
REFERENCES		117
APPENDIX A (MAPS)		122
APPENDIX B (DRILL LOGS)		127
128		
APPENDIX C (PUMPING TEST RESULTS)		137

LIST OF FIGURES

Figure 1: The extent of the Table Mountain Group and location of the study site.	9
Figure 2: Drilling setup at each borehole array line (Greef, 1990).	14
Figure 3: The proximity of borehole array lines included in Greef’s study (1990) in relation to the current study area and the Klipberg Mountain.....	16
Figure 4: Main rivers and catchments of the study area.....	20
Figure 5: Monthly average temperature (°C) (left), and monthly average rainfall (right).....	21
Figure 6: Piper diagram with groundwater hydrochemical facies (yellow triangles) and processes responsible for composition (coloured circles).	40
Figure 7: Geological map with AOI demarcated in blue, targeting the Rietvlei Sandstones (Klipberg Mountain).....	47
Figure 8: EMP_1 traverse (red line) with shallow (light blue) and deep (orange) measurements, as well as the location of Drill Target 1 at Station 13. The green lineament represents the primary fracture targeted.	49
Figure 9: EMP_2 (red line) with shallow (blue) and deep (orange) readings, as well as the location of Drill Target 2 at Station 11.....	50
Figure 10: Geological and topographic features selected to target for drilling.	51
Figure 11: Simplified borehole logs with water bearing fracture depths.	54
Figure 12: Some geological structures targeted and intersected during drilling.....	55
Figure 13: Geological map of the area with fault, axis and cross section locations.....	57
Figure 14: Conceptual model of the study area (Profile line A-B).	58
Figure 15: Pumping test at the existing borehole HBH1 and distribution of observation boreholes.	59
Figure 16: Step Test drawdown curve for HBH1 borehole.	60
Figure 17: Log-log plot of drawdown of HBH1 with diagnostic flow regimes.....	61
Figure 18: Derivate plot (primary axis) and drawdown plot (secondary axis) of HBH1 with RAF gradient marked with red line.	61
Figure 19: Recovery graph of HBH1 applying Theis to determine Transmissivity.	62
Figure 20: Pumping test at LGC_BH1 and distribution of observation boreholes.	63
Figure 21: Step Test drawdown curve for LGC_BH1 borehole.....	64

Figure 22: Log-log plot of drawdown of LGC_BH1 with diagnostic flow regimes.	65
Figure 23: Derivate plot (primary axis) and drawdown plot (secondary axis) of LGC_BH1 with IRAF gradient fit marked with red line.	65
Figure 24: Recovery graph of LGC_BH1 applying Theis to determine Transmissivity.	66
Figure 25: Pumping test at LGC_BH2 and distribution of observation boreholes.	67
Figure 26: Step Test drawdown curve for LGC_BH2 borehole.	68
Figure 27: Log-log plot of drawdown of LGC_BH2 with diagnostic flow regimes.	68
Figure 28: Derivate plot (primary axis) and drawdown plot (secondary axis) of LGC_BH2 with radial acting flow (RAF) occurring 0-180 minutes, fitted with red line.	69
Figure 29: Recovery graph of LGC_BH2 applying Theis to determine Transmissivity.	70
Figure 30: Pumping test at LGC_BH3 and distribution of observation boreholes.	71
Figure 31: Step Test drawdown curve for LGC_BH3 borehole.	72
Figure 32: Log-log plot of drawdown of LGC_BH3 with diagnostic flow regime.	72
Figure 33: Derivate plot (primary axis) and drawdown plot (secondary axis) of LGC_BH3 with IRAF gradient marked with red line.	73
Figure 34: Recovery graph of LGC_BH3 applying Theis to determine Transmissivity.	74
Figure 35: Pumping test at LGC_BH5 and distribution of observation boreholes.	75
Figure 36: Step Test drawdown curve for LGC_BH5 borehole. Notice how the 3rd step fails at 21.3 L/s.	76
Figure 37: Log-log plot of drawdown of LGC_BH5 with diagnostic flow regimes.	76
Figure 38: Derivate plot (primary axis) and drawdown plot (secondary axis) of LGC_BH5 with IRAF gradient fit marked with red line.	77
Figure 39: Recovery graph of LGC_BH5 applying Theis to determine Transmissivity.	78
Figure 40: Pumping test at LGC_BH8 and distribution of observation boreholes.	79
Figure 41: Step Test drawdown curve for LGC_BH8 borehole. Notice how the 4th step fails at 10.4 L/s.	80
Figure 42: Log-log plot of drawdown of LGC_BH8 with diagnostic flow regimes.	80
Figure 43: Derivate plot (primary axis) and drawdown plot (secondary axis) of LGC_BH8 with linear flow gradient fit marked with red line.	81

Figure 44: Recovery graph of LGC_BH8 applying Theis to determine Transmissivity.....	82
Figure 45: Pumping test at Habata_2 and distribution of observation boreholes.....	83
Figure 46: Step Test drawdown curve for Habata_2 borehole.....	84
Figure 47: Log-log plot of drawdown of Habata_2 with diagnostic flow regimes.....	84
Figure 48: Derivate plot (primary axis) and drawdown plot (secondary axis) of LGC_BH2 with IRAF gradient fit marked with red line.....	85
Figure 49: Recovery graph of Habata_2 applying Theis to determine Transmissivity.....	86
Figure 50: Pumping test at Habata_4 and distribution of observation boreholes.....	87
Figure 51: Step Test drawdown curve for Habata_4 borehole.....	88
Figure 52: Log-log plot of drawdown of Habata_4 with diagnostic flow regimes.....	88
Figure 53: Derivate plot (primary axis) and drawdown plot (secondary axis) of Habata_4 with IRAF gradient fit marked with red line.....	89
Figure 54: Recovery graph of Habata_4 applying Theis to determine Transmissivity.....	90
Figure 55: Pumping test at Habata_8 and distribution of observation boreholes.....	91
Figure 56: Step Test drawdown curve for Habata_8 borehole.....	92
Figure 57: Log-log plot of drawdown of Habata_8 with diagnostic flow regimes.....	92
Figure 58: Derivate plot (primary axis) and drawdown plot (secondary axis) of Habata_8 with bi-linear gradient fit marked with red line.....	93
Figure 59: Recovery graph of Habata_8 applying Theis to determine Transmissivity.....	94
Figure 60: Piper diagram indicating groundwater types.....	101
Figure 61: Stiff diagrams of the sampled boreholes, normalised to the same axis to gain a perspective on the relative salinity.....	102
Figure 62: Geological map with stiff diagrams and groundwater types (marked with colour polygons), as well as groundwater flow direction. Salinity as a measure of EC (mS/m) is plotted on the respective stiff diagram.....	103
Figure 63: Bivariate plot of Na⁺ against Cl⁻ for the study site. Arrows are used to indicate the ion-exchange processes when samples deviate from the 1:1 line.....	106
Figure 64: Bivariate plot of Ca²⁺ + Mg²⁺ against SO₄²⁻ + HCO₃⁻. Arrows emphasise the ion-exchange resulting in samples plotting off the 1:1 line.....	106
Figure 65: Wilcox diagram of groundwater for irrigation.....	108

LIST OF TABLES

Table 1: Aquifer parameters gained from existing literature.....	10
Table 2: Recharge estimates of Table Mountain Group study areas.....	11
Table 3: Summary of hydrogeological conditions of boreholes in the study conducted by Greef (1990).	15
Table 4: Stratigraphy, lithology and depositional environment of the Nardouw and Ceres Subgroups underlying the study area (adapted from Thamm and Johnson, 2006).	22
Table 5: Summary of common geophysical methods and their applicability/non-applicability for the TMG.....	25
Table 6: A summary of abstraction rates for step tests and constant discharge tests.....	31
Table 7: Diagnostic tools for groundwater flow characterisation.	36
Table 8: Result of laboratory analysis with parameters expressed in mg/L unless otherwise indicated, compared to SANS 241-1:2015 Drinking Water Standards. Light grey indicates concentration above aesthetic limit, while dark grey is above chronic limit.....	38
Table 9: Comparison of the range of the measured chemical parameters to SANS 241 (2015) Drinking Water Standards.....	42
Table 10: Summary of successfully drilled boreholes.....	53
Table 11: A summary of connectivity of boreholes and possible reasons for the link.....	96
Table 12: Summary of Aquifer Parameters determined from Pumping Test Analysis.....	98
Table 13: Descriptive statistics of laboratory results for the nine boreholes.	99
Table 14: Groundwater chemistry results, classified according to electrical conductivity (represented by orange bar, in ascending order).	99
Table 15: Pearson’s correlation matrix of pH, EC (mS/m), TDS and major ions (mg/L).	104
Table 16: Saturation Indices for the 9 borehole samples	107
Table 17: Total hardness values of groundwater samples in ascending order from left to right.	109

Table 18: Sodium percentages of groundwater samples in ascending order from left to right.
..... 109

Table 19: Kelly’s ratio values for groundwater samples in ascending order from left to right.
..... 110

Table 20: Magnesium hazard rating for groundwater samples in ascending order from left to right. 110

Table 21: Permeability index rating of groundwater samples in ascending order from left to right. 111

Table 22: Classification of groundwater suitability for irrigation. 113

CHAPTER 1: INTRODUCTION

A hydrogeological investigation is the first step in determining groundwater quality, yield potential, economic value, and storage capacity of an aquifer as a water resource. A hydrogeological investigation is a study of the geological and subsurface conditions responsible for groundwater flow and groundwater chemistry. A vast selection of resources and data contribute to the investigation, including: satellite and aerial imagery, topographical information, geophysical data, an assessment of the geological setting, drilling information, groundwater levels, groundwater quality data, recharge conditions and hydrogeological testing (both physical and chemical analysis). The data, both recent and historical, allows the hydrogeological environment to be characterised and conceptualised. This scientific approach to hydrogeological conceptualisation promotes informed groundwater management.

A hydrogeological investigation was conducted in the Western Cape of South Africa. The study site and setting is presented in **Map 1 (Appendix A)**. The study area comprises of Bokkeveld Group Formation in the low-lying areas and Rietvlei Formation forming the Klipberg Mountain to the south. Only one existing borehole was found in production at the study site. Vineyards and Citrus orchards are irrigated from an intricate canal system originating from the Breede River to the north of the study area.

A recent drought prompted a hydrogeological investigation to determine the potential of groundwater as an additional water source to supplement the restricted surface water supply. When given the option of groundwater development in the Table Mountain Group (TMG), of which the Rietvlei Formation forms the youngest unit, the older Peninsula Formation sandstones are the primary target. They are quartzitic, have more extensive fracture systems and water quality is generally considered good. The Nardouw Subgroup, of which the Rietvlei forms part, is recorded in various literature sources to be lower yielding, and yield poor quality groundwater with high iron and manganese levels. Recent literature on the TMG in respect to hydrogeological characterisation of the Rietvlei Formation is limited and the Klipberg Mountain which formed the primary target in this study has yet to be characterised hydrogeologically.

1.1 AIMS AND OBJECTIVES

The aim of the study is to characterise the hydrogeological conditions which determine the groundwater chemistry and aquifer flow characteristics within the Rietvlei Formation of the study area. This will be done by doing the following:

- Collation and interpretation of existing hydrogeological data.
- Determine geological factors controlling the occurrence of groundwater.
- Determine aquifer parameters by conducting pumping tests.
- Describe the hydrogeochemical processes controlling the evolution of groundwater chemistry and assess the suitability of the groundwater for irrigation.
- Development of a conceptual model of the hydrogeological conditions of the site.

CHAPTER 2: LITERATURE REVIEW

2.1 INTRODUCTION

An example of a large scale hydrogeological investigation was conducted by the Water Research Commission (WRC) of South Africa on the TMG – of which the Rietvlei Formation forms the youngest lithological unit. The WRC is a statutory body directed to sourcing suitable solutions for water related challenges. In 1999 the Coordinating Committee for Geohydrological Research (CCGR) advised that focus is placed on the TMG as a source of water supply (Pietersen and Parsons 2002). The objectives of the study were as follows:

- Determine the status of the existing knowledge of the TMG aquifer.
- Ascertain the role of geological structures on groundwater dynamics.
- Set a protocol of management scenarios for groundwater abstraction from the TMG.
- Quantify the impact of groundwater abstraction of the environment.
- Develop appropriate resource quantification methodologies.
- Research recharge and artificial recharge potential.

This culminated in “A Synthesis of the Hydrogeology of the Table Mountain Group – Formation of a Research Strategy”. The selection of the TMG for a study of such magnitude was due to the fractured aquifers potential to contribute large scale water supply for the Eastern and Western Cape. At the time of the above-mentioned study, it had primarily been exploited for irrigation and small scale domestic use in an unrestricted and poorly managed fashion (Pietersen and Parsons 2002).

2.2 CONCEPTUAL MODELS FOR FRACTURED AQUIFER SYSTEMS

2.2.1 Fracture Flow

A fractured aquifer is a rock in which water flows and is stored (to a limited extent) in discrete open spaces within the rock itself. These openings, or fractures, can be found in porous, permeable matrix blocks, known as dual porosity systems. Single porosity systems are those fractured aquifers that occur when the matrix is so impermeable that it is essentially inert. Flow then occurs

from the main fractures only (Kruseman and De Ridder 2000). When fractures are interconnected the system is referred to as a ‘fracture network’. The connectivity and aperture dimensions of fractures within the host rock influence the flow regime of groundwater. The following factors determine if the fracture network is a continuum, and this in turn indicates flow behaviour within the fractured media:

- Conductivity of matrix and of fracture.
- Fracture connectivity.
- The representative elementary volume (REV).

The REV is the smallest volume of porous material over which a measurement can be made that will yield a statistically representative value of the material as a whole (Bear and Bachmat 1987). When fractures are well connected, fracture flow dominates after which matrix flow starts contributing to the flow regime (Woodford 2002). This is typical of dual porosity systems and is common in TMG Aquifers. Van Tonder and Xu (1999) highlighted the following points as the determinants of fracture flow:

- Fracture connectivity.
- Wall roughness of apertures.
- The permeability and porosity of the host rock.
- Length and orientation of the fracture.
- Aperture width.
- Fill material and fill material properties.
- Channelling effect.

Aperture width has the greatest effect on hydraulic conductivity within a fractured aquifer. Hydraulic conductivity is defined as the rate of flow under a unit hydraulic gradient through a unit cross sectional area of aquifer (Ferris et al. 1962). This is evident in the cubic law, a theoretical condition where flow (Q) is proportional to the fractures aperture. The cubic law is a different version of ‘Darcy’s Law’ presented in equation (1).

$$Q = K \cdot \frac{\Delta h}{\Delta l} \cdot A \quad (1)$$

Where:

Q = Flow through an area over time [L^3T^{-1}]

A = Area of through flow [L^2]

Δh = Change in head over the length in question [L]

Δl = Length [L]

K = Hydraulic conductivity [LT^{-1}]

Hydraulic conductivity (K) can be solved as follows:

$$K = \frac{k\rho g}{\mu} \quad (2)$$

Where:

ρ = fluid density [ML^{-3}]

g = gravitational acceleration [LT^{-2}]

μ = dynamic viscosity [$ML^{-1}T$]

k = permeability [L^2]

For the cubic law, hydraulic conductivity is determined by:

$$K = \frac{(2b)^2 \cdot \rho g}{12\mu} \quad (3)$$

By placing equation 3 and $A = bh$ [L^2] into equation 1, the Poiseuille Equation (4) results:

$$Q = \frac{b^3 \cdot \rho \cdot h}{3 \cdot \mu} \cdot \frac{\Delta h}{\Delta l} \quad (4)$$

Where: b = aperture/width of fracture [L] and h = fracture height [L]

This infers that hydraulic conductivity in a fractured aquifer increases with average fracture length, fracture density, aperture width, and interconnectivity. It applies when laminar flow occurs (Reynold numbers <2300); simply put, Q is a function of the cube of the fracture aperture, hence the name ‘cubic law’ (Wendland 1996, cited in Van Tonder et al. 2002).

The aim of a single-well pumping test is to determine the performance of the borehole being tested as well as the sustainable yield of the borehole. The yield, specific capacity and observed drawdown over time are some of the values and information that can be gained from a pumping test. This in turn is related to the potential of the borehole and efficiency of the screens, which is then in turn used to specify the design of the abstraction equipment. Correctly conducted pumping tests can provide information on the hydraulic characteristics of an aquifer such as hydraulic conductivity, transmissivity, storativity, the depth of water bearing fractures and the presence of flow boundaries (Woodford 2002).

2.2.2 Parameters Determined from Pumping Tests

Pumping test data allows one to obtain transmissivity rather than hydraulic conductivity. Transmissivity is defined as the rate of flow under a unit hydraulic gradient through a unit width of given saturated aquifer thickness. Transmissivity is related to hydraulic conductivity as follows in equation (5):

$$T = Kb \quad (5)$$

Where: T is transmissivity [L^2/T], b is aquifer thickness and K is hydraulic conductivity.

Storativity of fractures is generally lower than that of the matrix (Van Tonder and Xu 1999, cited in Woodford 2002), suggesting that the radius of influence can extend over large areas and be of an irregular shape, dependent on orientation of the connected fracture system. When undergoing a pumping test, the storativity can change over time as conditions can move from confined to unconfined with the lowering piezometric level (Woodford 2002). The low storage of a fracture is illustrated simply by the following equation (6) adapted from Van Tonder *et al.* (2002):

$$V_f = h_f \cdot l_f \cdot b = 4000 \text{ m} \cdot 100 \text{ m} \cdot 0.003 \text{ m} = 1200 \text{ m}^3 \quad (6)$$

Where: V_f is fracture volume [L^3], h_f is fracture height [L], l_f is fracture length [L], and b is fracture aperture [L].

If abstracted at a rate of 12 m^3/hr this single fracture of relatively large dimensions will empty within 100 hours. This example assumes that there is no active recharge and that the matrix is not contributing any groundwater, which is unlikely in real world scenarios.

In a confined aquifer storativity is defined as the volume of water released from storage per unit surface area of the aquifer per unit decline of hydraulic head. Storativity can also be referred to as storage coefficient. It is defined by equation (7).

$$S = S_s b \quad (7)$$

Where: S is storativity [dimensionless], S_s is specific storage [L^{-1}] and b is aquifer thickness [L].

For unconfined aquifers storativity comprises the drainable porosity, referred to as specific yield. As the water table is lowered during pumping, water stored in the matrix or interstitial pore spaces is released by gravity drainage.

2.2.3 Pumping Test Analysis

There are various methods available for evaluating pumping test data, each with their own advantages and limitations. The data obtained from the method selected has to be interpreted using applicable analytical solutions, typically by applying computer aided curve matching techniques applicable to the flow regime of the aquifer. This in itself is part science, part user interpretation dependent – put simply by Kruseman and De Ridder (2000): “*the analysis of pumping test data is as much an art as a science*”. Flow regimes are briefly discussed in the subsections below.

2.2.3.1 Homogeneous fractures (uniform aquifer)

A dense network of uniform, closely spaced fractures can result in a continuum, similar in flow characteristics to that of a porous aquifer (Bäulme 2003). This unsteady-state radial convergent flow was described by Theis in 1935 and Cooper and Jacob in 1946.

2.2.3.2 Double Porosity

The double porosity concept was first developed by Barenblatt et al. (1960). Fractures are assumed to have high permeability and low porosity – thus having low storativity. The matrix on the other hand has a higher storativity due to a high porosity coupled with low permeability. Initial flow into the borehole is directly from the fractures. When the limited storativity of the fractures becomes depleted, the contribution of the matrix to flow increases significantly. Pumping test data from the highly fractured TMG often illustrates the double porosity flow regime concept (Woodford 2002).

Radial acting flow from the matrix and fractures takes place into the pumped borehole, indicating a continuous, homogenous or radial acting fracture network (Bäulme 2003).

2.2.3.3 Single Vertical Fracture

A set of parallel, vertical fractures (or a dyke) can be represented by a single vertical fracture with a specified aperture width and length. The pumping well intersects this fracture which is otherwise part of a homogenous and confined aquifer. Four distinct flow phases can occur within the pumped fractured aquifer. These were determined by Cinco and Samaniego (1981) and later classified by Barker (1988) and are briefly discussed below.

- Linear flow: Due to the pressure drop within fractures, linear flow is directly proportional to the abstraction rate taking place, typically within faults or dykes of low permeability.
- Bilinear flow: If the matrix is permeable enough, flow perpendicular to the single fracture takes place from the formation into the fracture.
- Radial flow: When the cone of depression is circular in shape (aerial extent), typically occurring in fully penetrating boreholes in homogenous aquifers. The start of radial flow is also the point in time where the representative elementary volume (REV) acts homogeneously.
- Spherical flow: In the case of an isotropic aquifer medium, the cone of depression takes the shape of a sphere (Gringarten and Ramey 1973). Spherical type flow can be considered a temporary type of flow in a partially penetrating borehole – anisotropy in an aquifer will result in the circular shape becoming ellipsoid, with the cone of depression eventually reaching the bottom of the aquifer, followed by radial flow (Van Tonder et al. 2002).

A rational conceptual model of flow within a fractured rock aquifer is necessary to apply the appropriate methods of pumping test data analysis to determine representative aquifer characteristics and the hydraulic properties (Woodford 2002).

2.3 CASE STUDIES OF THE TMG AQUIFER

The TMG extends over a massive area in the Eastern and Western Cape (**Figure 1**), occurring in various thicknesses and within various rainfall regimes. The northern most part of the TMG, near Vanrhynsdorp borders desert areas with an average rainfall of less than 150 mm/yr., while in the central southern, higher lying areas of Ceres and Worcester rainfall can exceed 2000 mm/yr. (Rosewarne 2002a).

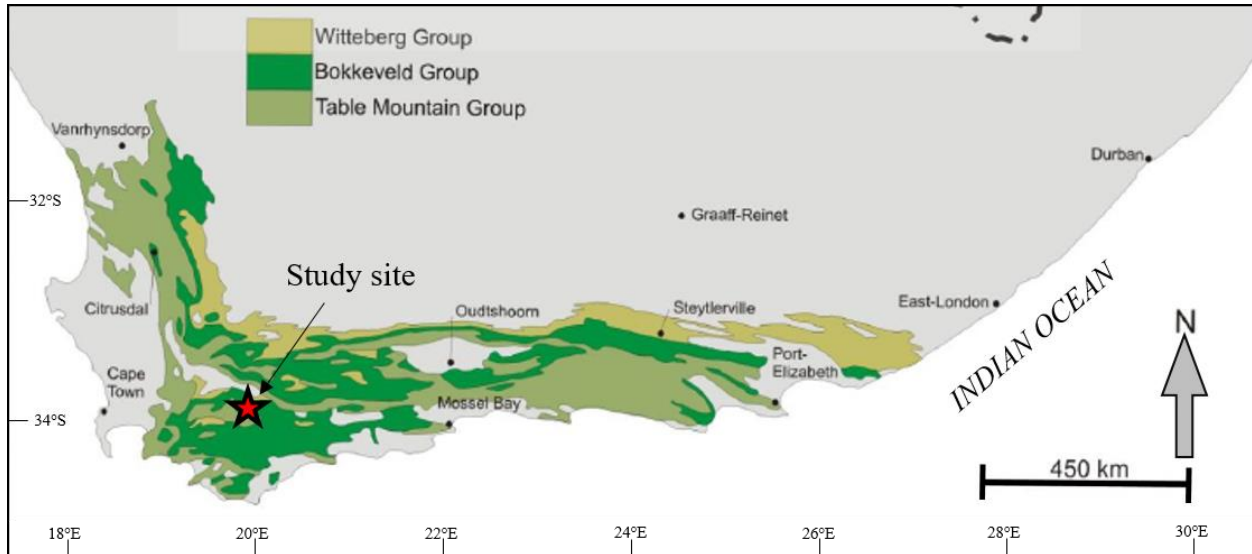


Figure 1: The extent of the Table Mountain Group and location of the study site.

The tectonic and structural control factors of the TMG result in an aquifer with variable hydraulic properties. The hydraulic conductivity varies from low (in the absence of faulting or fracturing) to zones that are highly fractured and transmissive. Due to the extensive fractured nature into which high yielding boreholes are drilled, it is challenging to accurately determine the hydraulic conductivity of single fractures within the TMG (Rosewarne 2002). The TMG Aquifer has been the focus of many hydrogeological investigations due to its regional extent and water supply potential.

2.3.1 Regional Case Studies

The large scale hydrogeological investigation conducted by the Water Research Commission (WRC) on the TMG was primarily to supply municipalities overlying the TMG (or in close proximity) with new or additional water sources. **Table 1** presents aquifer parameters determined from these investigations.

Table 1: Aquifer parameters gained from existing literature.

Area	Analysis Method	Transmissivity (m/day)	Storativity	Formation	Source
Citrusdal	FC*	<10 to 200	1×10^{-4} to 1×10^4	Peninsula	Umvoto and SRK (2000)
Hex Valley	Gringarten and Witherspoon	56	-	Rietvlei and Gydo Shale	Rosewarne (1989)
Klein Karoo	FC	10 to 200	10^{-1} to 10^2	Peninsula & Nardouw	Kotze (2000)
Kleinmond-Botrivier	Jacob and FC	70 - 320	1 to 5×10^4	Nardouw	Parsons (2001)
St Francis	Gringarten and Witherspoon	165 to 2485	1.8 to 3.3×10^{-3}	Nardouw	Rosewarne (1989)
Struisbaai	Jacob	15 to 200	8.6×10^{-3}	Peninsula & Nardouw	Weaver (1999)
Uitenhage	Not stated	~10 - 400	2×10^{-4} to 5×10^2	Peninsula & Nardouw	Maclear (2001)

FC = Flow characterization programme developed by IGS, Bloemfontein

In Rosewarne's (2002) characterisation of the TMG Aquifers, the following points of relevance were made:

- The continental stresses involved in forming the TMG of today provided large scale deformation and fracturing to significant depth (>2000 m).
- The uniform, brittle nature of the quartzitic sandstones of the TMG results in the rock to be easily fractured, while plastic deformation occurs more readily in the younger and often adjacent Bokkeveld Group (BVG).
- Groundwater within the TMG is acidic, and usually low in total dissolved solids, decreasing the chances of apertures being blocked by mineral deposition (to a lesser degree for shallow fractures).

Due to the regional heterogenic nature of the TMG, storativity estimates for the formation as a whole vary. The following presents estimates given at the time of the TMG Synthesis Study (2002):

- Weaver (2000) estimated a value of 10^{-2} for the TMG within 200 km of the City of Cape Town.

- Hartnady and Hay support a storativity value of 10^{-1} (in Weaver 2001).
- Kotze supports a storativity range of 10^{-2} to 5×10^{-2} (Kotze 2000).

The above-mentioned values indicate that a conservative estimate for the bulk storativity of the Peninsula and Nardouw Formations is in the range of 0.01 to 1×10^{-3} (Rosewarne 2002). According to Parsons (2001) there is no comprehensive study of recharge of the TMG. This limits the ability to determine the exploitability of the TMG aquifer. Parsons (2002) estimates recharge of high lying areas with excess rainfall of 600 mm/yr. to be in excess of 20%, with 5 % assigned to drier lower lying areas. Excluding a great deal of the volume of subsurface TMG and only using the outcropping area and thickness, this storativity range shows that the TMG could include tens of billions of cubic metres of groundwater within its fractured matrix (Rosewarne 2002).

TMG sandstones often form topographic highs due to their quartzitic and weathering resistant nature. The resultant orographic precipitation (rain and snowfall) is significantly higher than precipitation in valleys. The low-lying areas often comprise of the more easily weathered argillaceous rocks such as the Bokkeveld Group (BVG) or Malmesbury Group. Recharge estimates for study areas are presented in **Table 2**.

Table 2: Recharge estimates of Table Mountain Group study areas.

Area	Method	Recharge (% of MAP)	Formation	Source
Hermanus	CMB and Seasonal GW levels	11 - 30 %	Peninsula	Kotze (1998)
Hex River		12%	TMG and BVG	Rosewarne (1979)
Kammnassie Mountains	Not stated	16%	Peninsula	Kotze (2000)
Little Karoo		5%	Nardouw	
Uitenhage	Not stated	15%	TMG	Meyer (1999)
Agter-Witzenberg	CMB	25%	Peninsula	Maclear (1996)
	Isotopes	50%	Nardouw	Weaver (1999)

MAP = Mean Annual Precipitation; GW = Groundwater; CMB = Chloride Mass Balance

2.3.2 Recent Case Studies

The connectivity of fracture networks plays an important role in characterising the flow regime of groundwater within a fractured network (Pollard and Aydin 1988, cited in Lin et al. 2014). The development of the discrete fracture network (DFN) has allowed flow and transport of groundwater to be predicted in fractures. Data on fracture orientation, length, aperture, infill

properties, density and connectivity are necessary to develop DFN models. The connectivity of fractures is however not measurable in the field, thus generated fracture networks are necessary in the analysis.

Lin L., Lin H. and Xu (2014) developed an investigative approach with the objective to generate random realisation and analysis of fracture connectivity founded on the fracture characteristics of a wellfield. A conceptual model was developed using pumping test data, fracture network characteristics logged in the field, and remote sensing fracture identification. The Boschklouf Wellfield drilled into the Peninsula Formation of the TMG, east of Citrusdal in the Western Cape provided the study site for the research.

In the field, outcrops, quarries, and road cuts often provide the only, albeit limited source of fracture characterisation, and are insufficient in providing the length of the fractures. Xu et al. (2014) made use of remote sensing techniques to determine fracture length. Identified lineaments are considered crucial as they represent surface manifestations of subsurface fracture networks of transmissive fractured aquifers (Degnan and Clark 2002, cited in Xu et al. 2014).

Limitations for lineament mapping include varying interpretation techniques between individuals and limited rock exposures. To mitigate this, multiple interpreters were employed, and the results were combined into one shapefile. The selected study site of the Boschklouf wellfield provides ample TMG outcrop to accommodate lineament mapping. Multiple nodes were applied to each lineament to avoid straight-line inaccuracy resulting from the use of only two nodes. Fracture characterisation in the field, specifically dip angle, spacing, aperture width and dip azimuth was used to correlate the lineament mapping.

The resulting conceptual model by Xu et al. (2014) was developed by random generation of fracture realities developed for TMG aquifers. Statistical data derived from field measurements and imagery was applied. This allows the fracture connectivity pattern to be studied and compared to groundwater flow observations.

The study concluded that a large portion of fractures are present in the form of separated fracture networks or clusters. These fracture clusters are inferred to be hydraulically disconnected other than through the borehole itself (Xu et al. 2014). The conceptual model has been verified by analytical models and is considered applicable to TMG aquifers by the authors, particularly unconfined and well exposed sandstone formations (Xu et al. 2014).

2.3.2.1 Site Specific Case Studies

In 1990 Greef conducted a study in the Poesjesnels Valley, the lower lying area just west of the study site comprising of the BVG shales and sandstones. The objectives of the study were to determine factors contributing to the increasing salinity of the Breede River and provide mitigation methods to curb the serious issue. The deterioration of the Breede River water quality had been taking place for more than twenty years with data showing that the salt load of tributary rivers was increasing. This was directly attributed to increasing agricultural activities (Greef 1990). At the time of the study rainfall was measured to be 50.87 million m³ on the higher lying sandstone outcrops and 32.89 million m³ on the BVG within the valley. Evaporation was determined to be high in the valley, reaching an average of 10 mm per day (Greef 1990). Greef's study focussed on surface water and groundwater contribution to the primary flow channels.

Six areas were selected for drilling to determine the groundwater influence on the mineralisation in the river. The areas were selected in order to sample the widest varieties of soil type, slope, agricultural development and spatial distribution possible. The drilling program comprised of percussion boreholes (100m and 35m depths for observation boreholes), diamond core boreholes (50m deep), auger holes (4m deep) and excavation pits. The boreholes were set up in transects (**Figure 2**), referred to as borehole line arrays, in order to intersect different lithologies, and their associated groundwater characteristics. It must be noted that drilling only took place in the valley, intersecting the Bokkeveld Group.

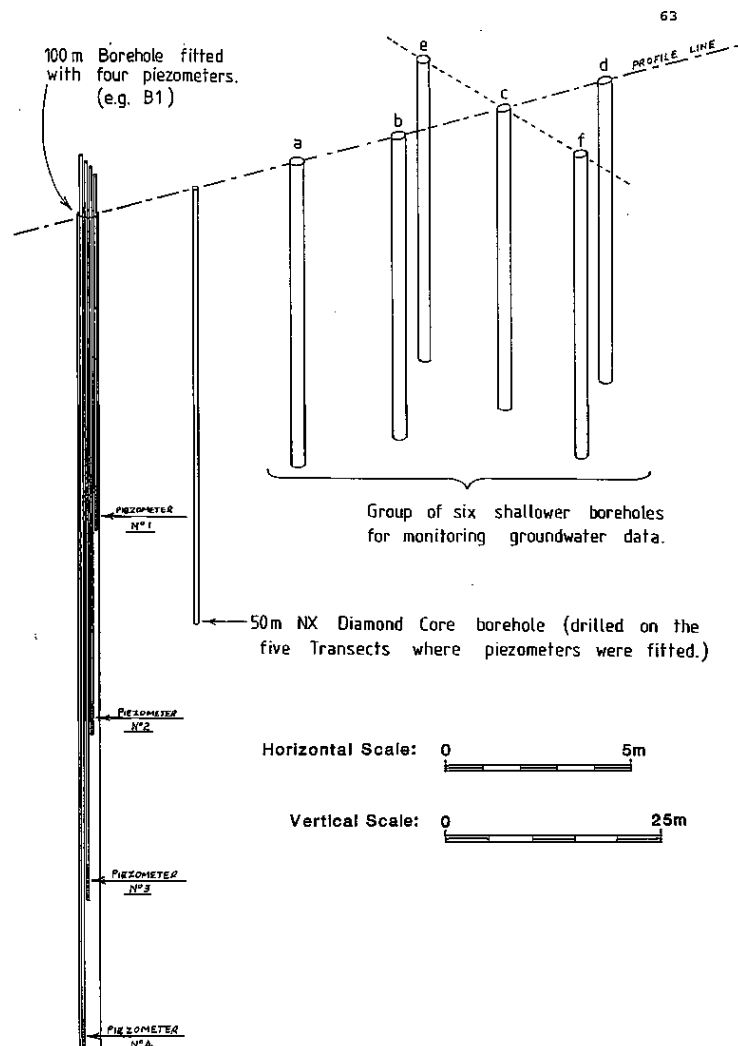


Figure 2: Drilling setup at each borehole array line (Greef, 1990).

Pumping tests were conducted on the percussion boreholes with some resulting in high yields. Groundwater samples were also analysed and were classed as Na - Cl type waters. Boreholes drilled within close proximity to the TMG had significantly less mineralised groundwater. A summary of the borehole geology and pumping test results is presented in **Table 3**. The approximate location of the boreholes drilled in Greef's study and the proximity to the boreholes used in this research is presented in **Figure 3**.

Table 3: Summary of hydrogeological conditions of boreholes in the study conducted by Greef (1990).

Borehole	Formation	Yield (L/sec)	T (m²/day)	Flow Conditions	Data Analysis Method	Electrical Conductivity (mS/m)
A1	Tra-Tra Shale and Hex River Sandstone	4	15.5	Radial	Jacob	602
A2	Tra-Tra Shale and Hex River Sandstone	13	15.8	Radial	Jacob	1006
B1	Waboomberg Shale and Boplaas Sandstone	14	-	-	-	273
B2	Waboomberg Shale and Boplaas Sandstone	23.5	68	Linear	Jenkins and Prentice	956
B5	Waboomberg Shale and Boplaas Sandstone	17.5	-	-	-	590
C1	Tra-Tra Shale and Hex River Sandstone	4.4	-	-	-	939
C2	Tra-Tra Shale and Hex River Sandstone	12.5	8	Radial	Theis	1250
D1	Tra-Tra Shale and Hex River Sandstone	7.2	15	Radial	Theis	440
D2	Tra-Tra Shale and Hex River Sandstone	3.45	-	-	-	320
E1	Voorstehoek	12	14.5	Radial and leaky aquifer	Theis and Seward	690
F1	Tra-Tra Shale and Hex River Sandstone	<0.01	Not enough flow	-	-	356

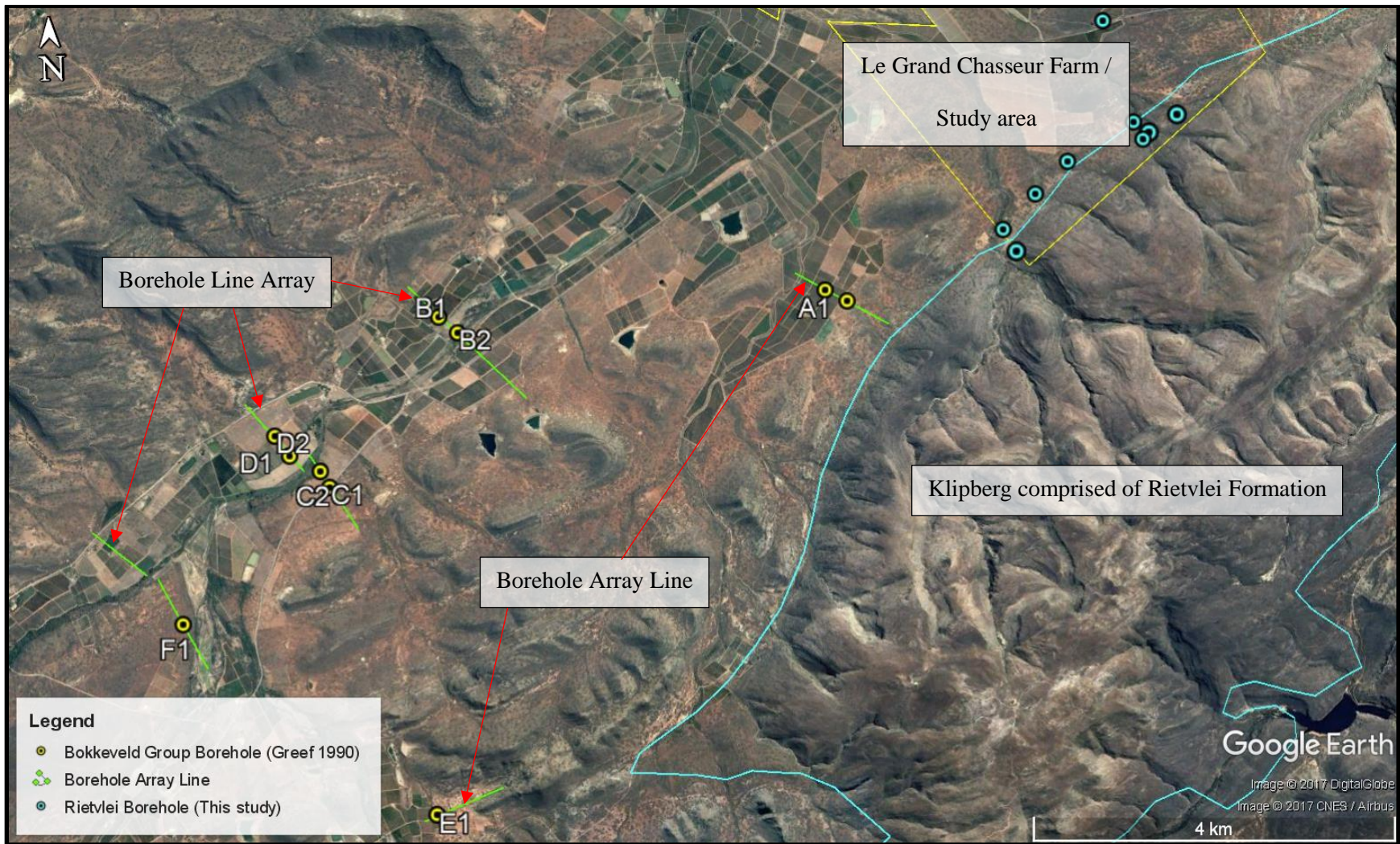


Figure 3: The proximity of borehole array lines included in Greef’s study (1990) in relation to the current study area and the Klipberg Mountain.

Greef (1990) conducted joint line surveys indicating that the primary fracture direction crosses the valley at a NW-SE orientation (120° to 140°). They cross cut the fold axis of the syncline and Sewefontien Fault at right angles. The main fractures are vertical to sub-vertical. This was determined with down the hole geophysical techniques as well as outcrop fracture surveys. Greef (1990) concluded from this that the fracture system within the Poesjesnels Valley and surrounding mountains is likely to promote groundwater movement from the higher lying areas (with associated higher hydraulic head), through and across the BVG, and into the river catchment. He confirmed this by conducting an isotope analysis, finding a clear correlation between the ¹⁸O in deeper boreholes and the Poesjesnels River.

Greef (1990) also recommended that the potential of the TMG sandstones be investigated for the purpose of groundwater development. A subsequent lowering of total dissolved solids (TDS) in the valley could also result when TMG groundwater is used for irrigation.

The awareness of the increasing salinity in major rivers in South Africa was growing. The primary concern was the long term detrimental impact on agricultural soils. In 1997, Kirchner et al. conducted another study on the area titled 'Causes and Management of the Salinity in the Breede River Valley, South Africa'. In this follow up study to Greef (1990) the potential of the TMG sandstones were again highlighted. Kirchner et al. (1997) described the soil cover on the TMG to be either very thin, or absent, resulting in the rainfall recharging the aquifer directly. The water abstracted from the TMG was found to have a very low ion concentration, with TDS values as low as 3 mg/L measured (Kirchner et al. 1997). Evaporation at that time was measured to be 1 800 mm/yr using the A-pan method, while rainfall in the town of Robertson, 11.5 km north east of the site, had an average rainfall of 270 mm/yr.

2.4 SUMMARY

When given the option of groundwater development in the TMG, the Rietvlei sandstones are rarely the priority target formation due to the feldspathic and argillaceous texture. Peninsula Formation sandstones are more favourable as they are highly quartzitic, have more extensive fracture systems and water quality is considered very good (Kotze 2000). In comparison the Nardouw Subgroup, of which the Rietvlei forms part is recorded to be lower yielding, slightly poorer quality, and the accompanying high manganese and iron concentrations require careful management. The

Skurweberg Formation is the preferable target of the Nardouw Subgroup. Studies have been focussed on municipal areas, or areas of intensive farming – the study area for this research falls into neither of these categories and the existing surface water schemes are sufficient for the present localised agricultural activities. Recent literature on the TMG is somewhat limited in respect of characterisation of the Rietvlei Formation.

CHAPTER 3: SITE DESCRIPTION

3.1 REGIONAL SETTING

The study site is located 15 km south west of Robertson and 10 km north-west of McGregor (**Map 1, Appendix A**). The Klipberg Mountain forms the southern boundary of the site and the Breede River, from which the bulk of irrigation water is currently sourced, makes up the northern boundary of the farm.

3.1.1 Relief and Surface Drainage

The study site comprises of gently sloping ground which becomes increasingly rocky and steep towards the Klipberg in the South and the Sandberg in the north east. The north western sections of the study area are flat with thicker soils.

There are no perennial rivers flowing through the farm, however during periods of sufficient rainfall, primarily in the winter months, episodic rivers form in the Klipberg Mountain and flow in a north westerly direction, along the primary fracture zones. The stream channels are easily visible in both the field and on satellite imagery, marked by deeply eroded stream channels in the fractured Rietvlei Sandstones of the Klipberg. The study area overlies two quaternary catchments within the Breede Water Management Area, namely the H40G to the west and the H40J to the east presented in Figure X. Bordering the northern most section of the farm lies the Poesjenels River, flowing in a north easterly direction to join up with the Breede River flowing in a north westerly direction.

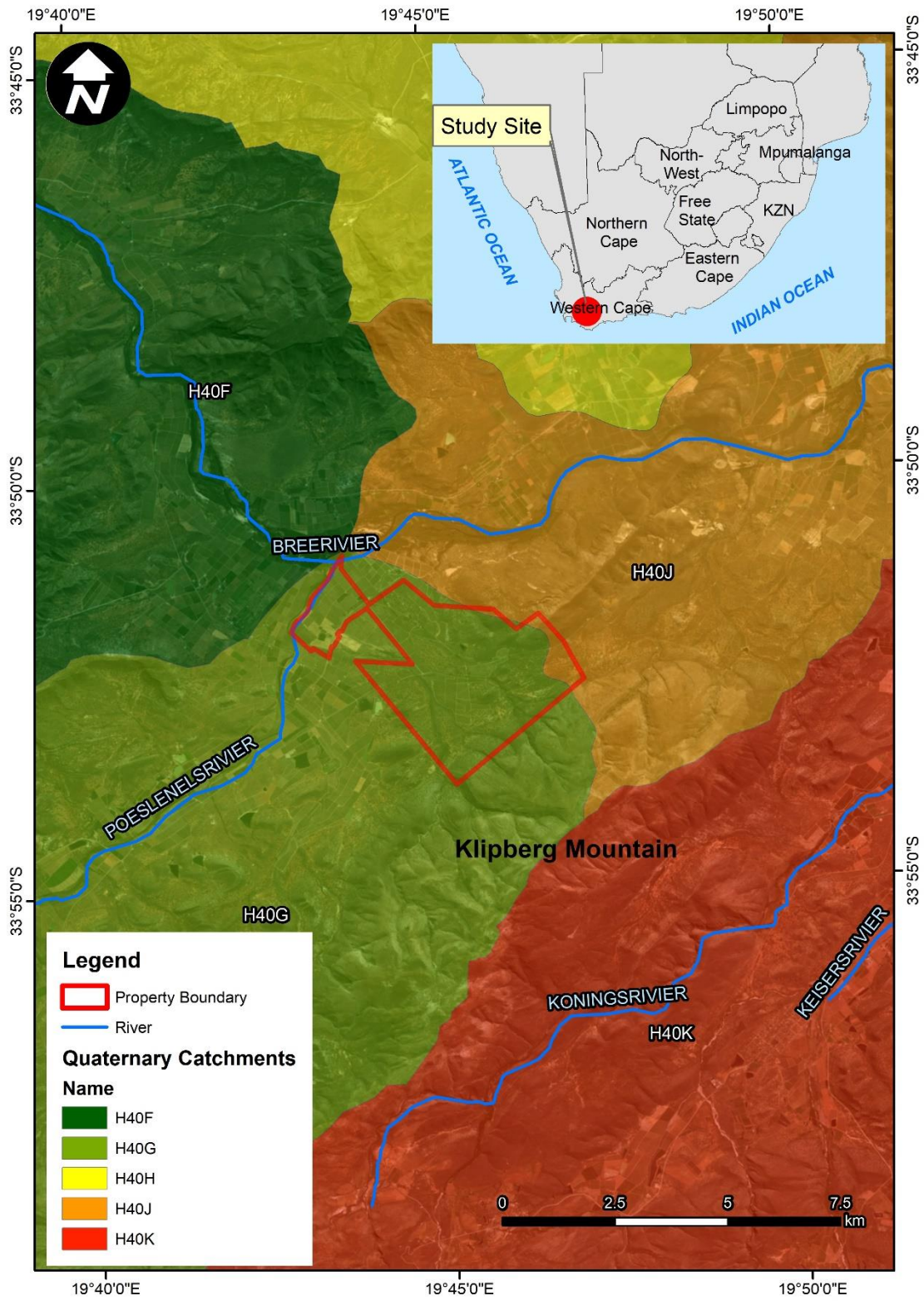


Figure 4: Main rivers and catchments of the study area.

3.1.2 Climate

The study area is located in a Mediterranean climate, with cool wet winters, and hot dry summers. Average temperature ranges from 21 °C in January to 10 °C in June. Rainfall predominantly occurs in the winter months from April to September. June and August receive the most rain on average with 35 mm and 34 mm respectively. On average 301 mm rainfall occurs per year **Figure 5**.

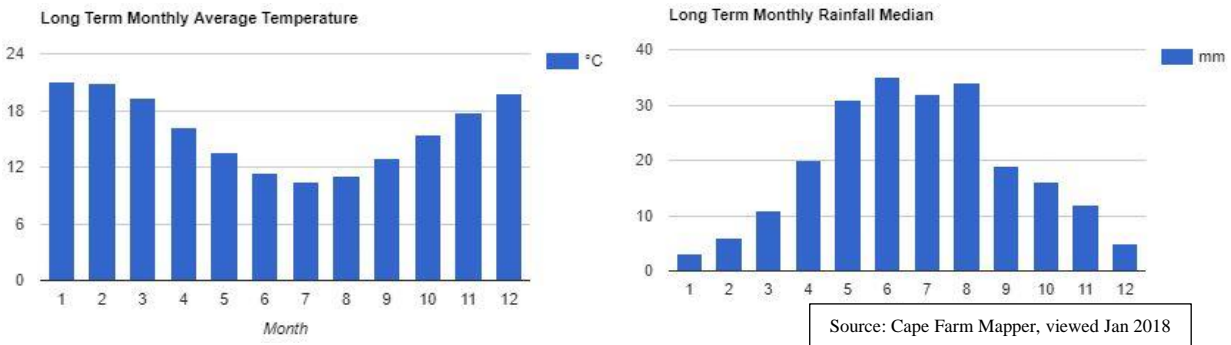


Figure 5: Monthly average temperature (°C) (left), and monthly average rainfall (right).

3.1.3 Regional Geology

The study area and surrounds are underlain by sandstones, shales, siltstones and mudrocks of the Table Mountain Group (TMG) and the BVG. The paleo environments for these sedimentary formations ranged from shallow marine to fluvial, with a minor glacial component.

The TMG is divided into several formations typical of early Palaeozoic cratonic sheet sandstone (Thamm and Johnson 2006). These highly fractured sandstones have an outcrop area of 37 000 km² and range in thickness from 900 m to 4000 m (Lin 2007). The primary stratigraphic units of the TMG are the Piekernierskloof, Graafwater, Peninsula, Pakhuis, Cedarburg and Nardouw Formations in order of oldest to youngest. The Rietvlei sandstones which make up the Klipberg Mountain to the south of the study site are the upper-most layer of the Nardouw Formation. The Rietvlei Formation comprises of light-coloured, feldspathic, quartzitic sandstone up to 200 m thick. The depositional environment is thought to be that of a nearshore process on a stable, shallow marine shelf, which graded into a vast fluvial coastal plain along the northern basin (Rust 1967; Thamm 1984; Theron and Thamm 1990; cited in Thamm and Johnson, 2006).

Theron's (1972) comprehensive stratigraphic study documented the depositional environment of the Bokkeveld Group (BVG). The BVG overlies the TMG, and comprises of a cyclic, upward

coarsening alternation of mudstone and fine-grained sandstone units. The Ceres Subgroup which occurs on this study site comprises three upward coarsening cycles that are recognised throughout the Bokkeveld Basin, namely; the Gydo and Gamka Formations (lower cycle), the Voorstehoek and Hex River Formations (middle cycle), and the Tra-Tra and Bo-Plaas Formations (upper cycle). The approximate thicknesses of these Formations west of 21° longitude line, are given in **Table 4**. Abundant marine invertebrate fossils are found in the Ceres Subgroup, providing ample evidence of the marine depositional environment (Theron and Loock 1988, cited in Thamm and Johnson, 2006).

Table 4: Stratigraphy, lithology and depositional environment of the Nardouw and Ceres Subgroups underlying the study area (adapted from Thamm and Johnson, 2006).

Age	Subgroup	West of ~21° Longitude			
		Formation	Thickness (m)	Lithology	Depositional Environment
Devonian (345 – 395 Ma)	Ceres	Boplaas	70	Sandstone	Delta front, shallow marine
		Tra-Tra	85	Mudrock, Siltstone	Offshore shelf, prodelta slope
		Hex River	60	Sandstone	Delta front, shallow marine
		Voorstehoek	200	Mudrock, siltstone	Offshore shelf, prodelta slope
		Gamka	70	Sandstone	Delta front, shallow marine
		Gydo	150	Mudrock, siltstone	Offshore shelf, prodelta slope
Silurian (395 – 435 Ma)	Nardouw	Rietvlei	200	Sandstone	Shallow marine
		Skurweberg	300	Sandstone	Fluvial, braid-plain, shallow marine
		Goudini	200	Sandstone	Shallow marine, fluvial braid plain

The highly fractured and faulted present-day structure of the TMG is the product of two major tectonic events, namely the Permo - Triassic Cape Orogeny and the fragmentation of southwestern Gondwana during the Mesozoic (De Beer 2001). The Cape Orogeny was responsible for thickening the sequence in areas of high strain, while the extensional faulting later disrupted the lateral continuity of the sequence (De Beer 2001). The age of the rocks and regional metamorphism which the TMG has been subjected to has resulted in very low to no primary porosity; however, the secondary tectonic extensional processes resulted in the TMG becoming a major fractured aquifer system for South Africa (Rosewarne 2002).

CHAPTER 4: METHODS AND MATERIALS

4.1 GROUNDWATER EXPLORATION

A desktop study was the first phase of groundwater exploration. This comprised of an examination of relevant literature, satellite and aerial photo imagery, and analysis of regional and local geological and hydrogeological maps. Areas of interest (AOI) were then selected to undergo further investigation by a site visit and geophysical survey. A borehole sited in the Bokkeveld Group proved dry and another one sited in the Rietvlei Sandstones, sited using an electromagnetometer proved high yielding (6 L/s blow yield). Due to challenging conditions for further geophysical survey in the TMG member, geological survey took precedence. Geological settings similar to that of the successful borehole were targeted. Primary and secondary fractures identified on satellite imagery, were confirmed in the field as ideal targets. This coupled with close proximity to episodic streams and cross cutting, large quartz veins proved successful with boreholes producing blow yields ranging from 15 000 L/hr to an excess of 80 000 L/hr.

4.1.1 Identification of Areas of Interest

Areas of Interest (AOI) were identified during the desktop study. The 1:250 000 Geological Map of Worcester (Thomas 1997, Map nr. 3319 Worcester) was then used to gain regional perspective of underlying geology and assess the presence, or lack thereof, of regional targets (**Map 2, Appendix**).

The 1: 500 000 Hydrogeological Map Series for Cape Town, Map number 3317, (Meyer 2001), adapted by DWAF (now Department Water and Sanitation 2012) and WRC was then overlain on the study site. Regional aquifer type and average yields (**Map 3, Appendix**) and the expected groundwater quality (**Map 4, Appendix**) were analysed. A combination of the abovementioned map layers and satellite imagery allowed areas to be selected for geophysical exploration and detailed geological survey, referred to as AOI.

4.1.2 Geophysics

The application of geophysics to the TMG has been somewhat limited due to challenges posed by rugged terrain. Various methods have been applied to the TMG, a short summary of which are

given in **Table 5**. This summary is not a comprehensive list, rather a short description of some of the challenges faced when using the popular geophysical methods in the TMG.

Table 5: Summary of common geophysical methods and their applicability/non-applicability for the TMG.

Method	Measured	Principle	Primary Application	Limitation in TMG
Seismic	Seismic wave propagation and reflection.	Pulsed acoustic energy is generated at the surface by weight drops, reflected or refracted at density changes in the subsurface. If velocity/density information is available, measurement time of the acoustic energy can be interpreted as different geological units.	Discontinuities in hard rock terrain, weathered zones (S-waves) and water table depth (P-waves). Regional geological studies. Oil exploration.	Only applicable for horizontal or gently dipping strata. TMG dips steeply and is often extensively folded. Layers must be of equal or increasing velocity with depth to enable measurement. TMG is often overlain by less dense formations such as BVG*.
Gravity	Variations in earth's gravitational field.	Measures local scale variations in the earth's gravitational field as a result of mass density changes in the subsurface.	Economic ore and oil exploration. Regional geological studies.	Gravity stations on steep slopes should be avoided. Is not directly related to groundwater associated structures - primarily used for cavity detection in karst environments.
Magnetic	Variations in earth's natural magnetic field.	Measurement of the earth's magnetic field allows delineations of formations with anomalous magnetic properties.	Oil exploration. Regional geological studies. Hydrogeological investigations.	Not useful in sedimentary formations without magmatic intrusions. In exceptional cases the weathered zone of faults can have a magnetic signature, however the hydrous ferric oxide which precipitates in faults of the TMG is not magnetic.
Electromagnetic (EM)	Measures magnitude of a secondary EM field generated from AC [#] induced into the subsurface by a primary EM field.	The difference between the secondary and primary EM field can be directly related to the electrical properties of the subsurface which vary with porosity, saturation and total dissolved solids in the water.	Cavity detection. Economic ore body exploration. Contaminant mapping. Weathered and fault zones.	Does not easily distinguish between rocks of low, and very low conductivity. Groundwater in the TMG is often low in TDS** - difference in conductivity between water saturated zones and the host quartzite is difficult to distinguish. Ideal to distinguish quartzitic TMG and the more argillaceous TMG, also Malmesbury and BVG.
Resistivity	Electrical current is transmitted into subsurface and resulting potential difference is measured.	The potential difference is used to calculate the apparent lateral and vertical resistivity of the subsurface.	Differentiate between fresh and salt water, sandy aquifers and clay material, water bearing fractured rock and solid host rock.	Sharp corners and rough terrain need to be avoided for accuracy, often difficult in TMG terrain. When possible, this method provides invaluable information on fault locality and dip.

BVG* = Bokkeveld Group; AC[#] = Alternating current; TDS = Total dissolved solids. Source: adapted from Fraser and Stemmet (2002) and (ed Kirsch 2009)

The resistivity method is the most widely accepted geophysical method for application on the TMG (Fraser and Stemmet 2002).

4.1.2.1 Resistivity Method

The resistivity method was initially used to locate lateral and vertical changes in electrical properties that may be related to changes in the formation properties. The contact zone of the Rietvlei Formation and Gydo Formation, the former having a higher resistivity than the latter more argillaceous material, formed an ideal target for the resistivity method.

The setup used involved laying out two multi-core cables with 16 electrode take-outs every 10 m in the Wenner array configuration. These cables are laid out on the surface in a straight line (topography allowing). The electrode is hammered into the ground and connected to the multicore cable with a short jumper cable. The multi-core cables are connected to the ABEM electrode selector ES 464 that controls the measurement sequence. The electrode selector is connected to the ABEM Terrameter SAS1000 that is powered by a car battery. The Terrameter unit is responsible for collecting the apparent resistivity measurements.

This method was also the first-choice tool for geophysics due to the presence of a high voltage power line crossing the study site. The power line trending from west to east is in close proximity (<100m) and parallel to the contact of the Rietvlei and Gydo Formations contact zone. Electric fields (telluric currents) and noise caused by electrically active infrastructure can be compensated for by applying a bias potential to balance the potential electrodes before energising the current electrodes. This discrimination circuitry and programming separates self potentials, direct current voltages, and noise from external sources (ABEM 2010). After numerous attempts to correctly set up the multi core cables however, the resistivity survey was terminated. The thin overburden above the Rietvlei Sandstone resulted in poor to no contact of a large portion of the electrodes with the subsurface. The poor contact would have resulted in a large error percentage and low confidence data.

4.1.2.2 Electromagnetic Method

The electromagnetic survey was then carried out using a Geonics EM34-3 Electromagnetometer which measures the ground conductivity of the subsurface. The EM34-3 induces a changing electromagnetic (EM) field with a known frequency into the subsurface using a sender coil. This

changing EM field induces current flow in conductive subsurface areas (for example a saturated fracture within a weathered zone), which is measured by the receiver coil. This is then automatically converted to ground conductivity. The ground conductivity measured has a direct correlation with formation porosity and groundwater salinity; i.e. if porosity of the formation or groundwater salinity increases, this will be reflected as a higher ground conductivity measurement (Telford et al. 1990). The coils can be operated in vertical or horizontal co-planar fashion with a specified separation of 10 m, 20 m, or 40 m. For this study 40 m separation was used. This enables the measurement of the ground conductivity to up to depths of 30 m and 60 m (depending on the conductivity of the subsurface) for the vertical and horizontal coil orientations respectively (McNeill 1980).

Fractured zones within hard-rock generally display a positive conductivity anomaly when using the electromagnetic induction techniques, for both dry and water bearing fractures. Depending on geological conditions, the dry fracture and open zones of advanced weathering are less resistive than the surrounding intact rock (Kirsch 2009). Two AOI were surveyed using the electromagnetometer with a 40 m coil separation and vertical and horizontal co-planar coil orientation. Noise from the power line was minimised by surveying the furthest section from the power line and reducing the instrument sensitivity by using a higher conductivity range.

4.1.3 Geological Survey

Due to the limited suitability of geophysical techniques in the TMG (**Table 5**) and interference resulting from overlying power lines, geological survey was incorporated to site drilling targets. Satellite image interpretation of regional fractures (represented by lineaments) which were confirmed in the field formed the basis of the geological siting techniques. Multiple nodes were applied to each lineament to avoid straight-line inaccuracy resulting from the use of only two nodes as recommended by Xu et al. (2014). The contact zone of the Gydo Formation and Rietvlei Formation with cross cutting features formed primary targets. Quartz veins were found trending both north east to south west, and parallel to the syncline axis (west to east). Episodic stream beds if proximal to some or all of the above-mentioned features were also targeted.

4.1.4 Borehole Drilling

Air percussion drilling was used to drill targets. The overburden, primarily comprising loose sandy soil to clayey sand with minor colluvial boulders was cased off with 219 mm solid steel casing. Boreholes were drilled to end depth with a 203 mm diameter hammer (open borehole). Drill depths ranged between 80 m and 120 m. Drill sites with blow yields in excess of 20 000 L/hr were selected for pumping tests - with the exception of LGC_BH8 with a blow yield of 15 000 L/hr, selected due to its proximity to infrastructure.

4.2 AQUIFER PUMPING TESTS

Aquifer Pumping Tests conducted according to the recommended methods of SANS10299-4 (2003) have been conducted on selected boreholes for two primary objectives: 1) to determine the aquifer parameters and thus characterise hydrogeological conditions of the Rietvlei Aquifer, and 2) to determine sustainable yields of the boreholes for long term use. For the purpose of this paper, the first objective is discussed, as characteristics of the Rietvlei Formation of the study area is relatively undefined. Aquifer parameters give a good indication of the physical environment of groundwater flow, which plays an important role in the quality of the groundwater. Once this has been determined, groundwater development in Rietvlei Formation can be fine-tuned at an earlier stage to improve cost efficiency of projects. Note that the term boreholes and wells are used interchangeably throughout the chapter in order to match local and international literature.

4.2.1 Pumping tests: in the field

A Pumping Test is a controlled field test conducted to determine aquifer parameters for a single well aquifer. Pumping tests are critical in well field management as they are the only hydrogeological tests that provide indications of the groundwater reservoir, and reservoir boundaries (Van Tonder et al. 2002). They incorporate the largest volume of rock due to the extended period of abstraction, and therefore allow the most reliable hydraulic properties to be estimated (Bäumle 2003). A large number of pumping tests, together with monitoring boreholes, allow a statistical analysis of the formation specific to the area to be performed.

Pumping tests were conducted according to the “Test-pumping of water boreholes; Part 4” set by the South African National Standard (SANS 10299-4, 2003). A summary of the method used is

given below, however for a full explanation of the methods used as set out by these standards, it is recommended that the complete document be viewed.

In the case where more than one borehole exists in close proximity, the additional boreholes can be used to gain more aquifer parameters. With software specifically designed for interpreting pumping test data, the following can be determined:

- Aquifer characteristics for example storativity and transmissivity.
- The presence of recharge boundaries and flow barriers.
- Ideal spatial setting of production boreholes for the application and management of a wellfield.
- Recommended abstraction rates to which borehole should be appropriately equipped.

The pumping test applied at the study site comprised three field tests in consecutive order as follows:

- **Step Test:** Used to determine the discharge rate needed for the CDT which will fully stress the aquifer – used to estimate the sustainable yield of the borehole in the Flow Characteristics (FC) Programme. Data from the Step-drawdown Test can also be used to determine borehole efficiency and transmissivity (T). It is conducted in steps (typically four), each comprising one hour of pumping at a certain constant rate, followed immediately by another hour at a higher rate until the end of the fourth step. If data from the four steps is insufficient, the hydrogeologist can extend the Step Test. More steps with pumping intervals of up to two hours can gain better data, so long as the steps are long enough to be able to disregard effects of wellbore storage (Kruseman and De Ridder 2000). The rates for the different intervals should be chosen so that the first step is lower than the required rate, the third step is equal to the expected yield and the final step is higher than that. In most cases the blow yield of a borehole is used to select the rate for the first step. The planned abstraction rates for the following steps can be changed according to the water level response of the preceding step.
- **Constant Discharge Test (CDT):** This test determines the volume of groundwater that the borehole can yield for the long term. It also allows the transmissivity and storativity (if observation boreholes are incorporated) of an aquifer to be determined. The length for

which this test is conducted depends on the planned use of the borehole, and is related to the boreholes importance as a resource. The hydrogeologist can also set the time range, however the longer the test, the more reliable the data. The CDTs in this study were conducted for 24 hour periods. The abstraction rate must be constant throughout the duration of the test, and the response of water levels is recorded at certain time intervals (set by SANS 10299-4, 2003).

- **Recovery Test:** This test represents the natural inflow of groundwater into the borehole, with measurements starting at the end of the CDT, when the pump is switched off. The pump must be fitted with a non-return valve to ensure that no water enters the borehole from the discharge pipe as this will have an effect on water levels. The water level is ideally monitored until 95% of the total drawdown has recovered, or until the duration of the CDT has been reached (whichever happens first). In this case recovery tests were terminated when the rate of water level rise (recovery) was linear (data was sufficient for estimating aquifer parameters), and never before 8 hours had passed.

The following points are important in the rationale behind the field testing at Le Grand Chasseur:

- Boreholes with blow yields above 20 000 L/hr were selected to undergo pumping tests, (with the exception of LGC_BH8). A summary of pumping tested boreholes is provided in **Table 6**.
- Drilling and pumping tests were undertaken in phases; therefore, the selection of observation boreholes was dependent on the completed boreholes at the time.
- Observation boreholes were selected according to geological setting, and proximity to tested boreholes. An overlap of one observation borehole across the different tests, was applied to allow cross referencing of connected boreholes, yet still be practical in the field as distances between boreholes was often over 1 km in rugged terrain.

Table 6: A summary of abstraction rates for step tests and constant discharge tests.

BH ID	BH Depth (m)	Rest Water Level (mbgl [#])	Blow Yield (L/hr)	Steps (L/s)	CDR* (L/s) for 24 hr	Total DD** for CDT (m)	Total Recovery	% Recovery	Time of recovery (mins)
HBH1 (Existing)	51.9	10.38	unknown	2; 2.7; 3.5; 4.7	5	18.46	14.18	77	480
LGC_BH1	99.4	7.19	36 000	3.35; 6.7; 10; 15	14	37.53	32.18	86	480
LGC_BH2	97.1	7.92	35 000	3.24; 6.5; 9.7; 14.6	12	76.13	66.62	88	480
LGC_BH3	71	10.39	80 000	7.4; 14.8; 22.2; 33.3	30	17.26	11.63	67	480
LGC_BH5	98.4	8.51	70 000	7.4; 14.8; 21.31 (fail)	8	24.26	19.67	81	480
LGC_BH8	90.5	11.49	15 000	2.3; 4.6; 6.9; 10.4	7	49.94	46.1	92	480
Habata_2	120.2	25.26	20 000	1.8; 3.7; 5.5; 7.4	4.4	22.05	20.11	91	1440
Habata_4	96.8	19.32	80 000	7.3; 14.7; 22.2 (fail)	11	24.7	23.03	93	1320
Habata_8	102.76	19.06	40 000	1.8; 3.7; 5.5; 11.5 (fail)	7.3	33.36	29.06	87	1200

mbgl[#] = metres below ground level

CDR* = Constant Discharge Rate

DD** = Drawdown

fail = water level reaches pump inlet

4.2.2 Pumping Test Analysis

Aquifer parameters and flow characteristics were determined from the pumping test data. The Flow Characterisation (FC) Program (developed by Van Tonder et al. 2001) was used to determine hydraulic parameters.

The Cooper-Jacob (1946) method is applied to radial acting drawdown data in the FC Program to characterise flow characteristics and gain hydraulic parameters. The Cooper-Jacob equation is a modified version of the Theis (1935) equation, the changes to which are shown in equations (2) to (5).

$$s = \frac{Q}{4\pi T} w(u) \quad (2)$$

$$u = \frac{r^2 S}{4Tt} \quad (3)$$

Where

- Q is abstraction rate [L^3/T]
- r is distance of observation borehole to pumping borehole [L]
- s is drawdown [L]
- S is storativity [dimensionless]
- t is change in time since start of abstraction [T]
- T is transmissivity [L^2/T]
- $w(u)$ represents the Theis borehole function for non-leaky confined aquifers [dimensionless]

A smaller value for u tends towards a more accurate approximation of the Theis function. Driscoll (1986) makes use of $u \leq 0.05$ while Kruseman and de Ridder (2000) make use of $u \leq 0.01$. The Theis function $w(u)$, may also be calculated using equation (4).

$$w(u) = -0.5772 - \ln(u) + u - \frac{u^2}{2 \cdot 2!} + \frac{u^3}{3 \cdot 3!} + \frac{u^4}{4 \cdot 4!} + \dots \quad (4)$$

Equation (4) may then be approximated using two terms as follows in equation

$$w(u) \cong -0.5772 - \ln(u) \quad (5)$$

Cooper and Jacob combined (2) and (5) to form the linear equation (6).

$$s = \frac{Q}{4\pi T} \left(-0.5772 - \ln \left(\frac{Sr^2}{4Tt} \right) \right) \quad (6)$$

By converting to decimal logarithms, the straight line Cooper - Jacob equation results (7).

$$s = \frac{2.303Q}{4\pi T} \log \left(\frac{2.25Tt}{Sr^2} \right) \quad (7)$$

Drawdown (s) is then plotted as a function of logarithmic time on a semi-log plot, and a straight line is drawn through the data where radial flow occurs. Transmissivity (T) is determined using equation (8).

$$T = \frac{2.303Q}{4\pi \Delta s} \quad (8)$$

Where

- Δs is the gradient of the fitted line.

Transmissivity estimates determined from single-well tests in unconfined aquifers are affected by pumping test duration, constant discharge rate, and the analyst (Halford et al. 2006). Even when applying the Cooper - Jacob method, unconfined aquifers are affected by vertical anisotropy and specific yield as flow regime changes from fractures to matrix (Halford et al. 2006).

Recovery data was thus taken as the most reliable data due to the lack of anthropogenic interference. The Theis recovery method (1935) was applied to determine the transmissivity of the aquifers by matching a straight line to the recovery data measured against equivalent time (t') on a semi-logarithmic plot (Willman et al. 2007). Recovery is the natural inflow of water into the

borehole released instantaneously from storage with the decline in hydraulic head. The Theis (1935) equation is presented in equation (9).

$$s' = \frac{2.303Q}{4\pi T} \left[\log\left(\frac{t}{t'}\right) - \log\left(\frac{S}{S'}\right) \right] \quad (9)$$

Where

- s' is recovery or recovery [L]
- Q is abstraction rate [L^3/T]
- T is transmissivity [L^2/T]
- t is elapsed time since start of abstraction [T]
- t' is elapsed time since abstraction ceased [T]
- S is storativity during abstraction [dimensionless]
- S' is storativity during recovery [dimensionless]

The Theis recovery equation (9) is applied by plotting recovery (s') as a function of $\log(t')$ on a semi-logarithmic plot with a straight line fitted to the late time recovery data. T is then calculated with (10).

$$T = \frac{2.303Q}{4\pi\Delta s'} \quad (10)$$

Where

- $\Delta s'$ is the gradient of the fitted line to residual drawdown.

Recovery is plotted against $\log(t')$, resulting in late time residual drawdown plotting on the left side of the graph. A straight-line fit is made to the early residual drawdown data in a semi-log axes, in the Diagnostic Plots spreadsheet of the FC Program. Early time data (the right side of the data plots) can depart from the ideal aquifer conditions as skin effect and wellbore storage have a role to play. In this study area however, borehole development and open borehole construction lead to negligible skin effect, as seen in the semi-logarithmic plot of recovery. Diagnostic tools used in

the log-log and semi-log plots for flow regime characterisation are presented in **Table 7** (adapted from Van Tonder et al. 2002).

The following assumptions are made when applying both Theis and Cooper-Jacob solutions:

- Storage releases groundwater instantaneously with decline in hydraulic head.
- Diameter of borehole is small, that is wellbore storage can be neglected.
- Unsteady flow.
- Flow into the borehole is horizontal.
- The value u' is small.
- The tested borehole is fully penetrating.
- The aquifer has infinite areal extent.
- The aquifer is of uniform thickness, is homogenous and isotropic.

Table 7: Diagnostic tools for groundwater flow characterisation.

Plot	Slope / Feature of derivative line	Time	Flow Characteristic	Possible fracture setting
Log-log	1	Early time	-Wellbore storage (WBS).	-n/a – water stored in the borehole itself, not the aquifer.
	0.5		-Linear flow.	-Linear fracture within an inert-low conductive matrix. Typical of sub vertical fractures, faults or dykes.
	0.25		-Bilinear flow.	-Flow from fracture and formation. Indicative of a good fracture network with matrix contribution.
	0.5	Late time	-2 parallel no-flow boundaries, or 3 equidistant no-flow boundaries.	-Limited fracture extent.
1	-Limited reservoir, with four closed boundaries.		-Cone of depression reaches a geological boundary of lower permeability surrounding the borehole.	
Semi-log	Straight line	Typically middle to late (before or after boundary conditions)	-Radial acting flow (RAF).	-Occurs when the aquifer is considered to be homogenous, when a fractured reservoir is considered to be a continuum. Occurs in well connected, fracture networks.
	Doubling slope	After RAF	-One no-flow boundary.	-Fracture is limited.
	Quadrupling slope	After RAF	-Two perpendicular no-flow boundaries.	-No-flow boundaries are perpendicular to fracture.
Derivative	Downward then upward	Dependent on fracture depth and Q	-Position of a fracture reached, followed by dewatering of fracture.	-Limited fracture extent.
	Strong downward trend	Late time	-Recharge/fixed head boundary.	-Aquifer is receiving recharge during test, such as induced from surface water bodies.
	Dip in derivative	Early time (after WBS)	-Double porosity aquifer.	-Flow regime changes from linear to bi-linear, groundwater from fracture and matrix.
	Straight horizontal line	Typically middle to late (before or after boundary conditions)	-Radial Flow.	-Occurs when the aquifer is considered to be homogenous, when a fractured reservoir is considered to be a continuum.
	Doubling of slope	After radial-flow period	-1 no-flow boundary.	-Occurs in well connected, fracture networks.
	Slope of = 1	Late time	-Closed boundary.	-Fracture/s have a limited extent.

4.3 ASSESSMENT OF HYDROGEOCHEMISTRY AND GROUNDWATER QUALITY FOR IRRIGATION

In groundwater management, quality of groundwater is as important as yield. Various hydrogeochemical groundwater types can result from water and host rock interactions. A sound conceptual understanding of the hydrogeological processes, mineralogy, and geological setting is important, as this determines the groundwater's suitability for industrial, agricultural, or domestic use. This is done by identifying the possible processes responsible for the hydrogeochemistry and comparing them to the actual measured groundwater chemistry. A diagnostic approach has been applied to achieve this, making use of graphical and statistical methods.

Boreholes were drilled into stable hard rock formations, with the casing depth ranging between 6 and 16 m. No screens were installed - the boreholes are thus considered "open boreholes". Groundwater samples taken from these boreholes are therefore a representation of multiple water bearing fractures. The drilling and pumping tests discussed in this study targeted the Rietvlei Formation Sandstones, and it was in this rock that water bearing fractures were intersected.

4.3.1 Sampling Technique

Groundwater samples were collected at the end of the CDT. Two samples were collected into 330 ml polyethylene bottles directly from the discharge pipe. Bottles were rinsed thoroughly three times with the groundwater itself. The bottles were filled to the brim and sealed, kept in cool temperatures and sent to a SANAS accredited laboratory for inorganic analysis. Microbiological content was not sampled due to the remoteness of the study and the planned purpose being for irrigation only. An ionic balance error of $\pm 5\%$ was used to indicate the analytical precision for the measurements conducted in the lab (Domenico and Schwartz 1998). All concentrations were measured in milligrams per litre (mg/L) unless otherwise indicated. The laboratory results are provided in **Table 8** where they are compared to SANS 241-1: 2015 Drinking Water Guidelines to highlight elevated parameters.

Table 8: Result of laboratory analysis with parameters expressed in mg/L unless otherwise indicated, compared to SANS 241-1:2015 Drinking Water Standards. Light grey indicates concentration above aesthetic limit, while dark grey is above chronic limit.

Analyses	HBH01	LGC_BH1	LGC_BH2	LGC_BH3	LGC_BH5	LGC_BH8	Habata 2	Habata 4	Habata 8	SANS 241-1:2015
pH (at 25 °C)	6.2	6.6	6.3	6.2	6.7	6.4	5.3	5.8	5.8	≥5 - ≤9.7 Operational
Conductivity (mS/m) (at 25 °C)	13.8	44.3	129.6	90.6	69.0	137.8	207.4	99.3	22.9	≤170 Aesthetic
Total Dissolved Solids	88.0	265.0	830.0	541.0	413.0	819.0	1327.0	636.0	146.0	≤1200 Aesthetic
Sodium (Na)	8.8	50.9	134.9	93.0	52.8	213.2	255.3	101.8	16.7	≤200 Aesthetic
Potassium (K)	5.6	8.8	16.3	15.5	9.6	17.3	25.8	15.9	8.2	N/A
Magnesium (Mg)	3.3	8.5	32.8	21.9	11.5	33.1	47.0	21.4	3.7	N/A
Calcium (Ca)	8.3	16.1	43.3	40.6	15.9	30.0	40.8	29.5	8.1	N/A
Chloride (Cl)	15.0	70.5	263.0	239.0	80.6	374.6	480.0	262.0	40.0	≤300 Aesthetic
Sulphate (SO4)	5.0	32.0	147.0	61.0	21.0	108.0	288.0	136.0	33.0	≤250 Aesthetic ≤500 Acute Health
Nitrate Nitrogen (N)	<0.36	<0.36	<0.36	<0.36	<0.36	<0.36	<0.36	<0.36	<0.36	≤11 Acute Health
Total Alkalinity (CaCO3)	39.0	57.6	49.0	41.8	44.4	56.3	6.3	46.0	30.0	N/A
Fluoride (F)	0.5	0.3	0.3	0.2	0.3	0.3	0.1	0.0	0.0	≤1.5 Chronic Health
Manganese (Mn)	0.6	1.2	2.9	0.1	1.4	1.6	6.7	0.1	2.2	≤0.1 Aesthetic ≤0.4 Chronic Health
Iron (Fe)	0.2	0.3	4.3	0.2	0.3	4.4	32.4	0.3	0.4	≤0.3 Aesthetic ≤2 Chronic Health
Copper (Cu)	<0.02	<0.02	<0.02	<0.02	<0.02	<0.02	<0.02	<0.02	<0.02	≤2 Chronic Health
Zinc (Zn)	<0.03	<0.03	<0.03	<0.03	<0.03	<0.03	<0.03	<0.03	<0.03	≤5 Aesthetic

4.3.2 Data analysis and interpretation

4.3.2.1 Classification of hydrochemical facies

The chemical composition of groundwater provides an indication of the processes under which groundwater flow and reactions take place – groundwater changes chemical composition as it moves through the aquifer over time. Graphical methods use the main ionic components of groundwater to display the similarities or differences of water samples (Appelo and Postma 2005).

Trilinear diagrams are used to group ions (in milliequivalents per litre) as a function of their concentration. Major cations (Ca^{2+} , Mg^{2+} , $\text{Na}^+ + \text{K}^+$) are plotted on one triangle (typically on the left side), while the anionic components (SO_4^{2-} , Cl^- , and $\text{HCO}_3^- + \text{CO}_3^{2-}$) are plotted on another triangle (typically the triangle to the right). The points at which the anionic and cationic concentration plot on the two separate triangles are superimposed on a single diamond shape in the centre. This allows the groundwater sample to be represented by one point (on the central diamond) with the position of the point providing an indication of the processes involved to result in such a composition. This is known as the Piper diagram, an example of which is presented in **Figure 6**. A brief description of the four main water types and where they occur on the diagram is provided (Piper 1944).

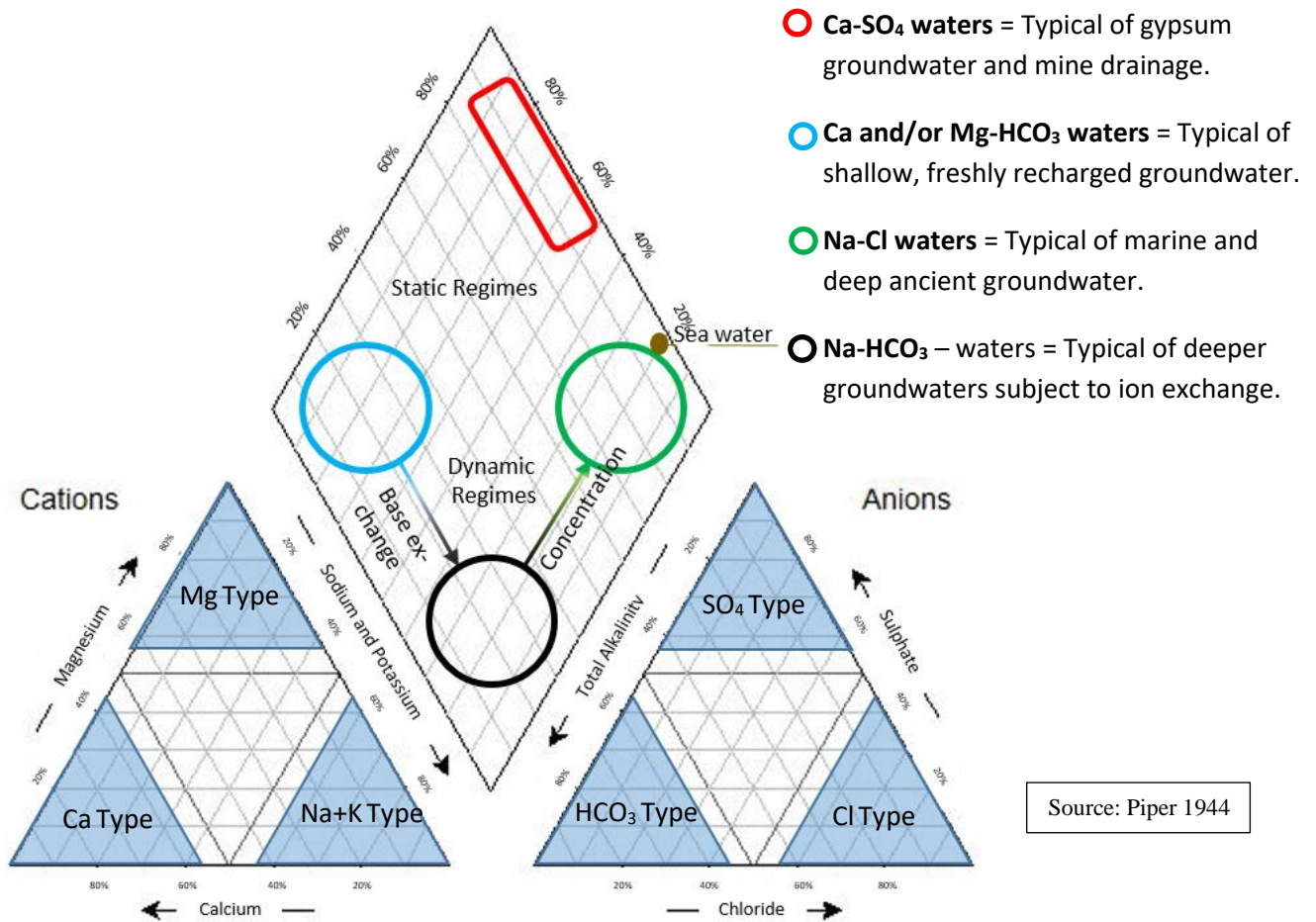


Figure 6: Piper diagram with groundwater hydrochemical facies (yellow triangles) and processes responsible for composition (coloured circles).

Stiff diagrams were also used. This simple graph comprises three different horizontal axes – cations plotted on the left and anions on the right, in milliequivalents per litre (meq/L). The structure of a stiff diagram can vary, depending on the order of the parameters, however it is customary to have Na⁺ on the left and Cl⁻ on the right of the top axis. Ca²⁺ and HCO⁻ make up the second axis, which provides an indication of the dissolution of CaCO₃. On the third axis Mg²⁺ to the left and SO₄²⁻ to the right depict the last common major components of groundwater. An optional fourth axis of different components for different studies can be included (Appelo and Postma, 2005). Lines connect the values of the different components and result in a shape that is typical of a certain water composition. The shape allows for easy comparison and grouping of similar groundwater compositions. Both Piper and Stiff diagrams were made using the WISH software (Lukas version 3.02.189).

4.3.2.2 Correlation Coefficient Analysis

A correlation coefficient analysis was conducted to determine the relationship between two chemical parameters. Simply put, it is a measure of how one variable can be used to predict another (Aref and Roosta 2016). A Pearson's correlation matrix using pH, EC, TDS and major ions was prepared to understand the relationship between different ionic species. Those chemical parameters that showed either a high positive, or high negative correlation are important in determining the process involved in resulting in a specific groundwater quality.

4.3.2.3 Saturation indices (SI)

Saturation indices measures departure of certain mineral phases from thermodynamic equilibrium and can thus be used to formulate hypotheses related to the mineral phase's reactivity in the aquifer. If the SI for a mineral phase is zero, then there exists a state of equilibrium between the groundwater and the host rock; if $SI > 0$, supersaturation of the groundwater with respect to the specific mineral phase exists; and $SI < 0$ indicates subsaturation of the mineral phase within the groundwater. This is useful in predicting in which direction the reaction will go; if $SI < 0$ then dissolution of the mineral phase will take preference (if present), while for supersaturation, precipitation of the mineral phase will be dominant (Appelo and Postma 2005). The geochemical software PHREEQC (Appelo and Postma, 2017 - version 3.3.12.12704) was used to calculate the SI for the 9 borehole samples. The default thermodynamic database phreeqc.dat provided the data for calculation.

4.3.3 Assessment of irrigation groundwater quality

The primary purpose for the groundwater development in this study is for irrigation. If groundwater is of such a quality that it may be potable, the necessary measures will be implemented to adhere to the required standard. For this reason, a comparison of the ranges of the measured chemical parameters to SANS 241 was made (**Table 9**) for an overall view of potential of groundwater for drinking.

For irrigation alone however, salinity of the groundwater is a major factor in determining the suitability of the groundwater. Soils that are initially saline necessitate removal of excess salts. Non-saline soils may become saline due to salts accumulating over time from improper soil management and irrigation techniques. The following hydrochemical parameters of groundwater

were used to determine its potential for irrigation namely; sodium adsorption ratio (SAR), salinity (classified according to electrical conductivity), total hardness (TH), sodium percentage (SP), hardness, Kelly’s Ratio (KR), magnesium hazard (MH) and permeability index (PI). Saline irrigation water may limit crop yields by limiting uptake of water into the plant by decreasing soil permeability and influencing the osmotic processes necessary for a plant’s metabolic processes (Todd 1980). Sodium in particular is the determining factor in the majority of these ratings. Sodium undergoes ion exchange with calcium and magnesium by adsorbing on to soil particles. This causes soil dispersion resulting in the breakdown of soil aggregates, with soil becoming harder and compact when dry, adversely affecting infiltration rates of water and air.

Table 9: Comparison of the range of the measured chemical parameters to SANS 241 (2015) Drinking Water Standards.

Analyses	Min	Max	SANS 241-1:2015
pH (at 25 °C)	5.3	6.7	≥5 - ≤9.7 Operational
Conductivity (mS/m) (at 25 °C)	13.8	207.4	≤170 Aesthetic
Total Dissolved Solids (mg/l)	88	1327	≤1200 Aesthetic
Sodium (mg/l as Na)	8.8	255.3	≤200 Aesthetic
Potassium (mg/l as K)	5.6	25.8	N/A
Magnesium (mg/l as Mg)	3.3	47	N/A
Calcium (mg/l as Ca)	8.1	43.3	N/A
Chloride (mg/l as Cl)	15	480	≤300 Aesthetic
Sulphate (mg/l as SO4)	5	288	≤250 Aesthetic ≤500 Acute Health
Total Alkalinity (mg/l as CaCO3)	6.25	57.57	N/A
Manganese (mg/l as Mn)	0.11	6.67	≤0.1 Aesthetic ≤0.4 Chronic Health
Iron (mg/l as Fe)	0.18	32.4	≤0.3 Aesthetic ≤2 Chronic Health

4.3.3.1 Sodium absorption ratio (SAR)

Sodium absorption ratio (SAR): Water used for irrigation with a high sodium content can be a concern due to the long-term effect sodium can have on the soil. This is known as the sodium hazard and is expressed as the sodium adsorption ratio (SAR). The SAR represents the ratio of sodium to calcium and magnesium, the latter two are important as they counter the negative effects of sodium. The continued use of sodium rich waters leads to sodium binding with the soil particles, making them compact and hard when dry – and thus infiltration and percolation rates decrease.

Clay rich soils are most susceptible to this due to their fine texture and polar nature. If the soil comprises calcium and magnesium, in large enough quantities, this can mitigate the sodium hazard (Fipps 1998.). The effects of high SAR values can be reduced by increasing the calcium content of the water by adding gypsum. Reducing the HCO_3 concentration also aids in reducing the effects of salinity, accomplished by acidifying the water. To calculate SAR equation (11) is applied (Richards 1954).

$$SAR = \frac{Na}{\sqrt{Ca + Mg/2}} \quad (11)$$

4.3.3.2 Salinity Classification

Irrigation with highly saline water can severely limit the choice of crop and be problematic towards seed germination. Elevated salt content in arid areas is common, as salt content is increased due to high evaporation rates. Plants can only transpire “pure” water and thus useable water within the soil decreases as salinity increases. Transpiration is directly related to yield of a crop - irrigation with a highly saline water directly lowers potential crop yield (Kumar et al. 2014). Richards (1954) classified salinity as a measure of electrical conductivity (EC) into four classes namely C1 (0 – 25 mS/m), C2 (25 – 750 mS/m), C3 (750 – 225 mS/m) and C4 (> 225 mS/m). The EC classification together with the SAR classification are plotted together on the Wilcox diagram to provide an indication of the potential for the irrigation water to result in saline soil.

4.3.3.3 Sodium Percentage

The undesirable effects of sodium on soil permeability is also classified according to sodium percentage. A sodium percentage of 60% in irrigation water increase soils properties to breakdown due to sodium build-up (Fipps1998). Sodium percentage, as presented in equation (12) is a measure of this. All units are presented as meq/L.

$$Na (\%) = \frac{(Na^+ + K^+) \times 100}{(Ca^{2+} + Mg^{2+} + Na^+ + K^+)} \quad (12)$$

4.3.3.4 Hardness classification

Total Hardness (TH) is considered an important classification for both drinking water and irrigation water as it provides an indication of mixing water quality. Hardness is an indicator of the potential of water to form calcium carbonate precipitation and scale formation, which can block outlets of plumbing or irrigation systems. The following equation (13) was used to calculate TH (Todd 1980).

$$TH (CaCO_3) = 2.497 Ca^{2+} + 4.1115 Mg^{2+} \quad (13)$$

Units in the above equation are presented in mg/L.

4.3.3.5 Kelly's Ratio (1963)

Kelly's ratio (KR) is a measure of sodium against calcium and magnesium with the concentration units in milliequivalents per litre. A KR value exceeding one indicates an excess of sodium in water and is generally considered unsuitable for irrigation. Equation (14) presents the formula.

$$KR = \frac{Na^+}{Ca^{+2} + Mg^{+2}} \quad (14)$$

4.3.3.6 Magnesium Hazard:

The alkali earth metals within groundwater are generally at equilibrium. However, if soils are irrigated with alkaline earth rich waters, crop yield can be reduced. Szalbolcs and Darab (1964) propose the Magnesium Hazard classification with the following formula (15):

$$MH = \frac{Mg^{2+}}{Ca^{2+} + Mg^{2+}} \times 100 \quad (15)$$

Units are measured in meq/L. A MH value over 50 is considered harmful for applying as irrigation.

4.3.3.7 Permeability Index (PI):

The permeability index considers ions that influence the permeability of soils, namely sodium, bicarbonate, calcium and magnesium. Continual application of water enriched in these salts can

decrease soil permeability of an area. The equation for PI is as follows (16) with ion concentration measured in meq/L.

$$PI = \frac{Na^{2+} + \sqrt{HCO_3^-}}{Ca^{2+} + Mg^{2+} + Na^+} \times 100 \quad (16)$$

The PI is made up of three classes: Class I (PI < 75%), Class II (25-75%) and Class III (PI > 75%). Class I and II are suitable for irrigation while Class III is unsuitable (Doneen 1964).

CHAPTER 5: RESULTS AND DISCUSSION

5.1 GROUNDWATER EXPLORATION

5.1.1 Identification of Areas of Interest

Two areas of interest (AOI) were selected as depicted in **Figure 7** below. Each AOI met some or all of the criteria summarized below:

- The AOI is within the average yield range of 2.0 L/sec - 5.0 L/sec (**Map 3, Appendix A**).
- The AOI is within the expected groundwater quality range of 0 – 70 mS/m (**Map 4, Appendix A**).
- The topography in certain areas is favourable for infrastructure development.
- Episodic drainage channels are within close proximity, representing deeper fracturing and preferential groundwater flow paths.
- Geological lineaments - both primary and secondary fracturing/lineaments from regional data and satellite imagery - cross the AOI.

Geophysical methods were then conducted in the AOI where possible.

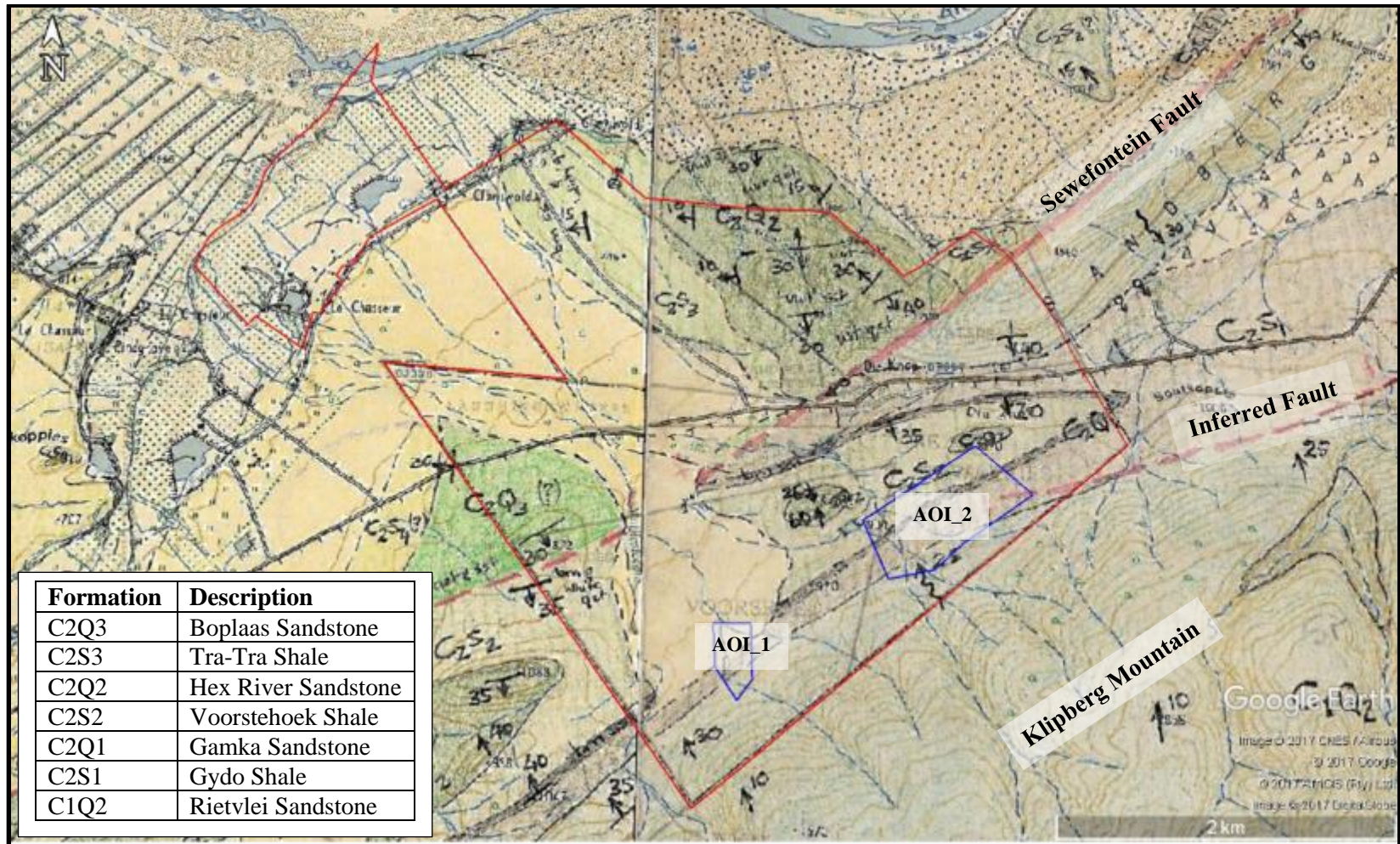


Figure 7: Geological map with AOI demarcated in blue, targeting the Rietvlei Sandstones (Klipberg Mountain).

5.1.2 Geophysics

5.1.2.1 Electromagnetometer Profile 1

Electromagnetometer Profile 1 (EMP_1) was conducted in a west to east direction within AOI_1 (**Figure 8**). Favourable targets for this traverse included the contact between the Rietvlei Formation and the Gydo Formation.

Drill Target 1 was sited at station 13 where the horizontal co-planar coil measurement reached a positive high of 29 mS/m after a gradual increase from station 9. A station is a point at which a reading is taken with a specific coordinate. The station is user specified. Geology type and required detail should be taken into consideration when determining spacing between stations. This gradual increase in conductivity represents a near vertical fractured zone. The vertical coil orientation, represented by the light blue line, as well as the horizontal coil orientation, decrease gradually, representing the thinning or pinching out of the argillaceous Gydo Formation towards the south (**Figure 8**). Station 13 is the peak of a gradually increasing deeper (horizontal measurement) reading, and is thus deemed to represent higher conductivity at depth. A medium sized water bearing fracture (6 cm diameter drill chips) was intersected at 65 m within the sandstone at this station. The high measurement of 42 mS/m at station 5 was ignored, as this peak is at the start of the survey, closest to the power line, and is not a gradual or large increase in conductivity. Confidence level in Station 13 was higher as it is located favourably close to a non-perennial stream, a potential source of preferential recharge. The stream bed is orientated in the same direction as the primary strike of fractures in the study area, that is 120° to 140° (NW-SE) represented by a green lineament in **Figure 8**.



Figure 8: EMP_1 traverse (red line) with shallow (light blue) and deep (orange) measurements, as well as the location of Drill Target 1 at Station 13. The green lineament represents the primary fracture targeted.

5.1.2.2 Electromagnetometer Profile 2

Electromagnetic Profile 2 (EMP_2) was conducted in AOI_2 towards the east of the farm (Figure 9). AOI_2 is an area of the farm with little to no infrastructure and good potential for agricultural development. The geological targets in this traverse include, an inferred fault and the syncline fold axis.

Drill Target 2 was selected at station 11 where the highest conductivity reading of 30 mS/m was found. This was deduced to be a weathered zone within the BVG, potentially hosting groundwater. From station 11 northwards, there is a decline in the conductivity readings, likely indicative of a magnetic anomaly which has been mapped at the 1:250 000 scale which trends north south across AOI_2, mapped at the 1:250 000 scale (Appendix A, Map 2).

This target was given first priority due to its, agricultural development potential, favourable spatial setting and geophysical anomaly.

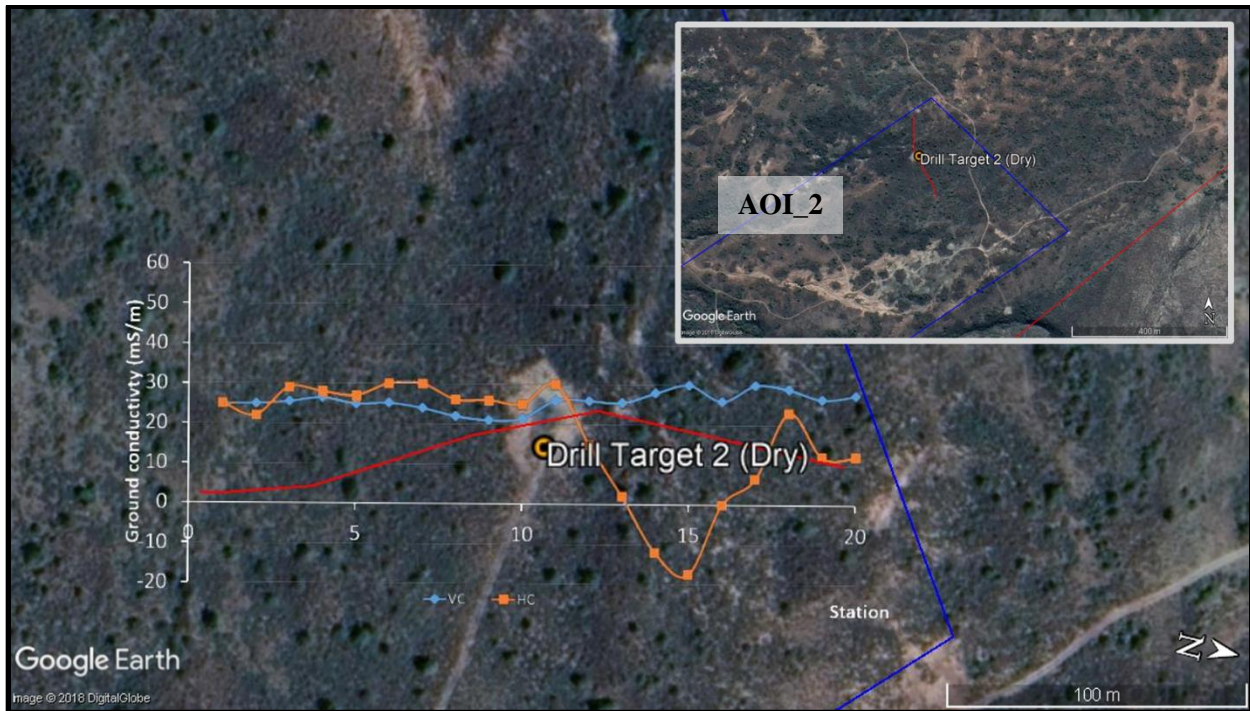


Figure 9: EMP_2 (red line) with shallow (blue) and deep (orange) readings, as well as the location of Drill Target 2 at Station 11.

5.1.3 Geological Survey

Drilling of Drill Target 2 intersected fractures at 9 m, 7 m, and 18 m within the BVG - none of which were water bearing. Drilling was terminated after 170 m as Rietvlei sandstone had not yet been intersected, and little weathering or fracturing was intersected at depth. As this borehole did not intersect any water strikes and was drilled into BVG, it is not discussed further in characterising the hydrogeological conditions of the Rietvlei Formation. Drill Target 1 was then drilled, and proved successful, with a blow yield of 6 L/s (discussed in **Section 5.1.2.1**). Similar settings as that of Drill Target 1 were selected using satellite imagery. The rugged terrain, however made geophysical surveying impractical in these settings and geological surveying took preference to site boreholes. The Klipberg Mountain, made up of Rietvlei Sandstones as well as features mentioned in **Section 5.1.1** resulted in new target features selection. The targets features were mapped in situ and on satellite imagery as shown in **Figure 10**.

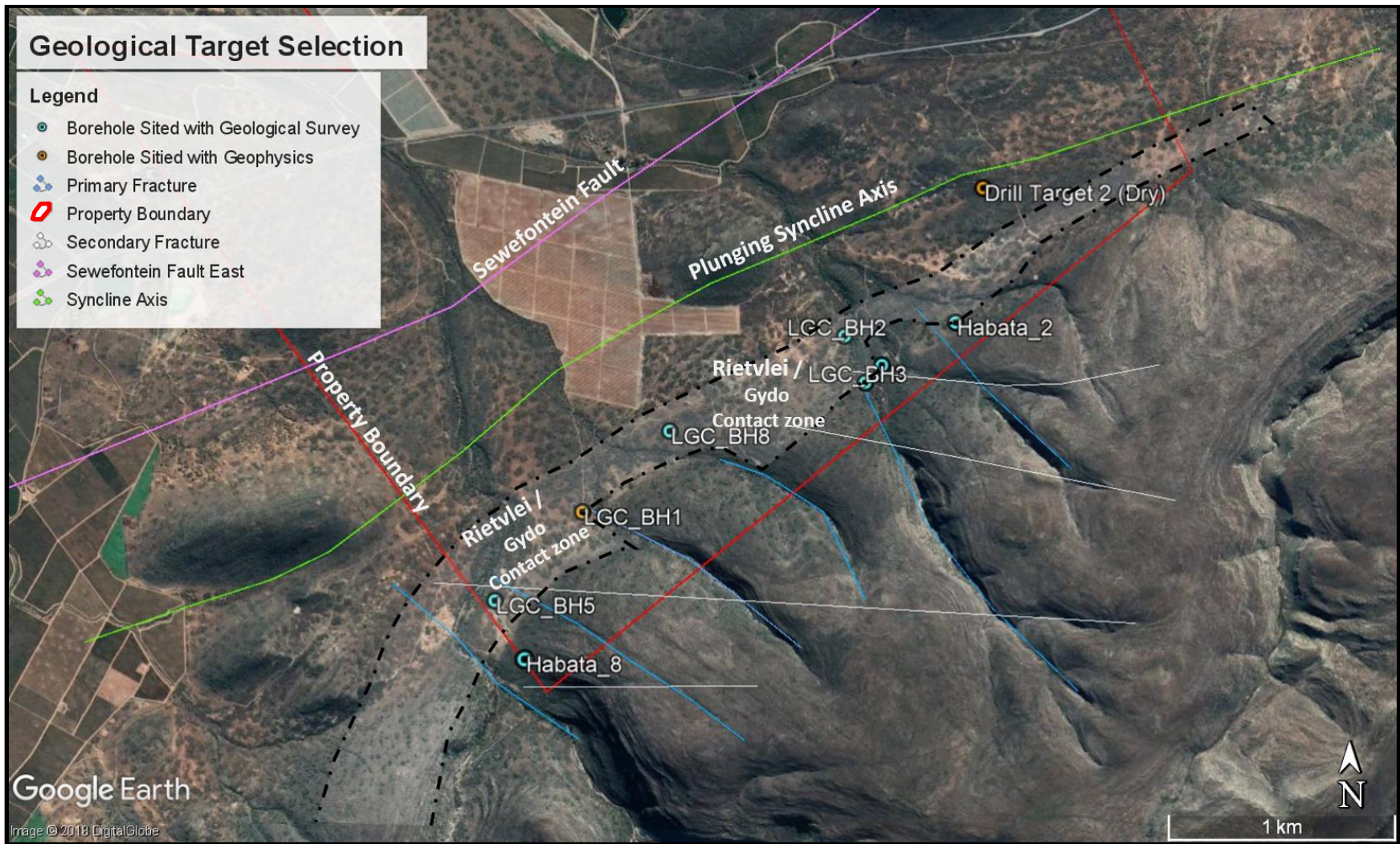


Figure 10: Geological and topographic features selected to target for drilling.

5.1.4 Drilling Results

Drilling using the percussion method was sufficient due to limited overburden thickness and lack of clay and boulders. Steel casing of 219 mm outer diameter was inserted to case off the loose overburden. Once intact bedrock was intersected, the borehole was left as an open hole of 203 mm diameter to end depth. In some cases, such as that of LGC_BH3, LGC_BH5 and Habata_4, the blow yields of 80 000 L/hr, 70 000 L/hr and 80 000 L/hr respectively prevented drilling to depths beyond the deepest water bearing fracture. Water bearing fractures were generally found in two zones within the Rietvlei Formation. Minor to major strikes at depths of 30 – 42 m and major strikes predominantly occurring at depths of 55 – 85 m. In the presence of Gydo Shales, water was intersected at the contact with the Rietvlei formations for LGC_BH3 and LGC_BH5. A summary of the drilling details is presented in **Table 10**. Although some fractures within the 30 - 42 m range were smaller in size and lower yielding, no fracture zones within the Rietvlei Sandstones were dry. The major water strikes were predominantly found in the 55 – 85 m zone. In such cases as LGC_BH2, LGC_BH3 and Habata_4 these strikes were associated with massive quartz veining. Habata_2 and LGC_BH5 had major water strikes in the same zone, however fractures lacked quartz infill. The size of the fractures ranged from 3 cm to 14 cm across the widest width of angular sandstone chips, referred to as minor to large water bearing fractures in the drill logs. Simplified drill logs are presented in **Figure 11** with complete logs presented in **Appendix B (Drill Logs)**. Some targets identified during the geological survey and intersected during drilling are presented in **Figure 12**.

Table 10: Summary of successfully drilled boreholes.

BH ID	BH Depth	Rest Water Level (mbgl)	Water Strikes (mbgl)	Blow Yield (L/hr)	Casing depth (m)
HBH1 (Existing)	51.9	10.38	Unknown	unknown	9.4
LGC_BH1	99.4	7.19	16, 30, 65 , 70, 92	36 000	16.6
LGC_BH2	97.1	7.92	16, 40, 44, 62 , 83	40 000	10
LGC_BH3	71	10.39	30, 54, 58, 78	80 000	12.3
LGC_BH5	98.4	8.51	30, 70	70 000	15.3
LGC_BH8	115	11.49	64	15 000	6
Habata_2	120.2	25.26	66, 71-72	20 000	6
Habata_4	96.8	19.32	29,42, 60,72, 85	80 000	7
Habata_8	102.76	19.06	66, 72-84	40 000	6

Note: Main water strikes are in bold.

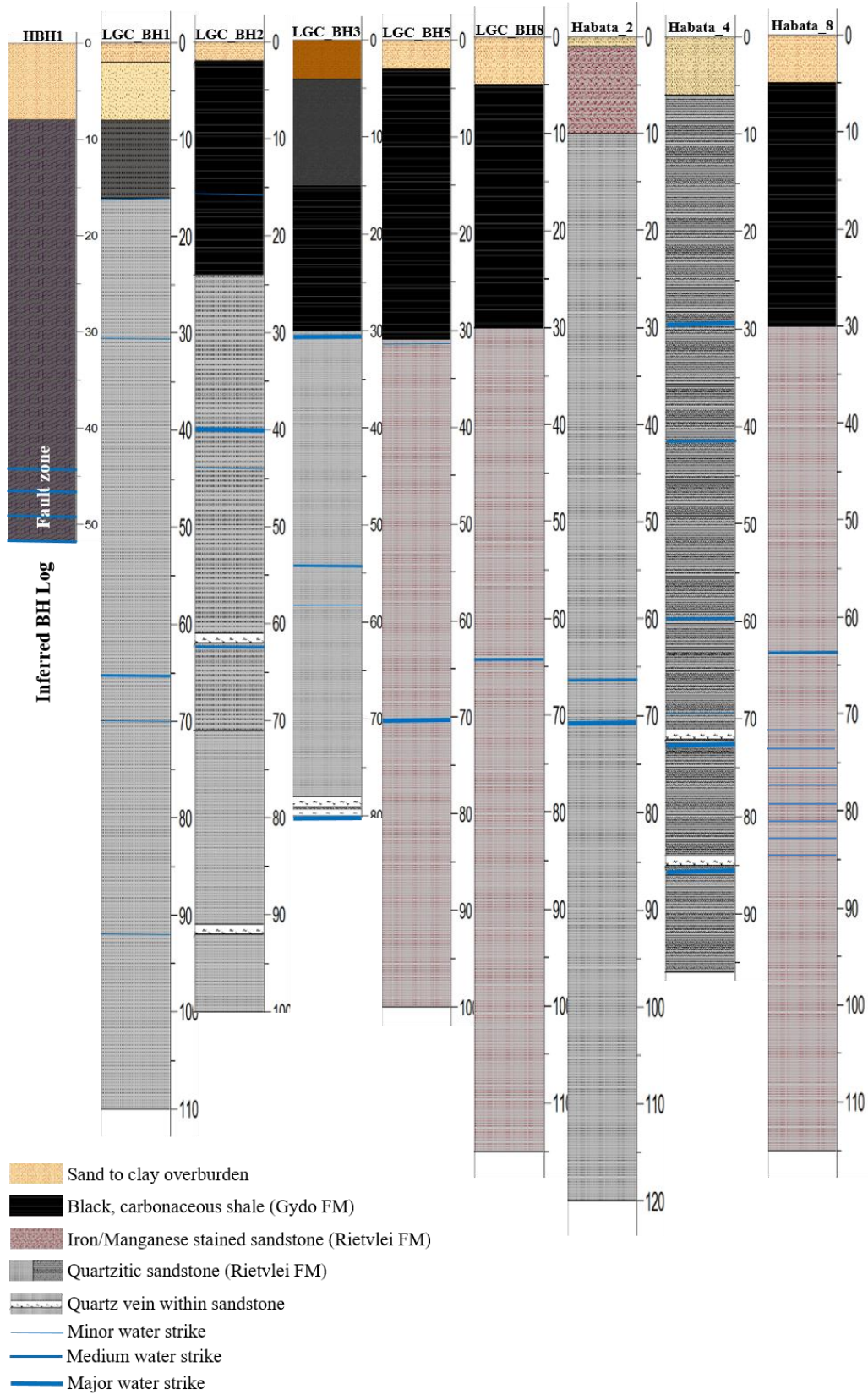


Figure 11: Simplified borehole logs with water bearing fracture depths.



Figure 12: Some geological structures targeted and intersected during drilling.

5.1.5 Summary

Due to the rugged terrain and quartzitic nature of the TMG, geophysical survey was somewhat limited. One electromagnetic profile which provided a successful drill target did however indicate the geological settings that provide high potential for groundwater development. Satellite imagery and geological field mapping was then applied in selecting drilling positions. Boreholes drilled with the air percussion method ranged in depth of 80 – 120 m. Two main water bearing fracture zones were found; 30 – 42 m and 55 – 85 m. Drill chips ranged in size from 3 -14 cm, with all fractures within the Rietvlei Formation being water bearing. Major water strikes were predominantly in the deeper zone (55 – 85 m), in some cases associated with massive quartz veining.

Data from the drill logs, have been used to develop a conceptual model. The location of the cross section is given in **Figure 13**, while the cross section itself is presented in **Figure 14**.

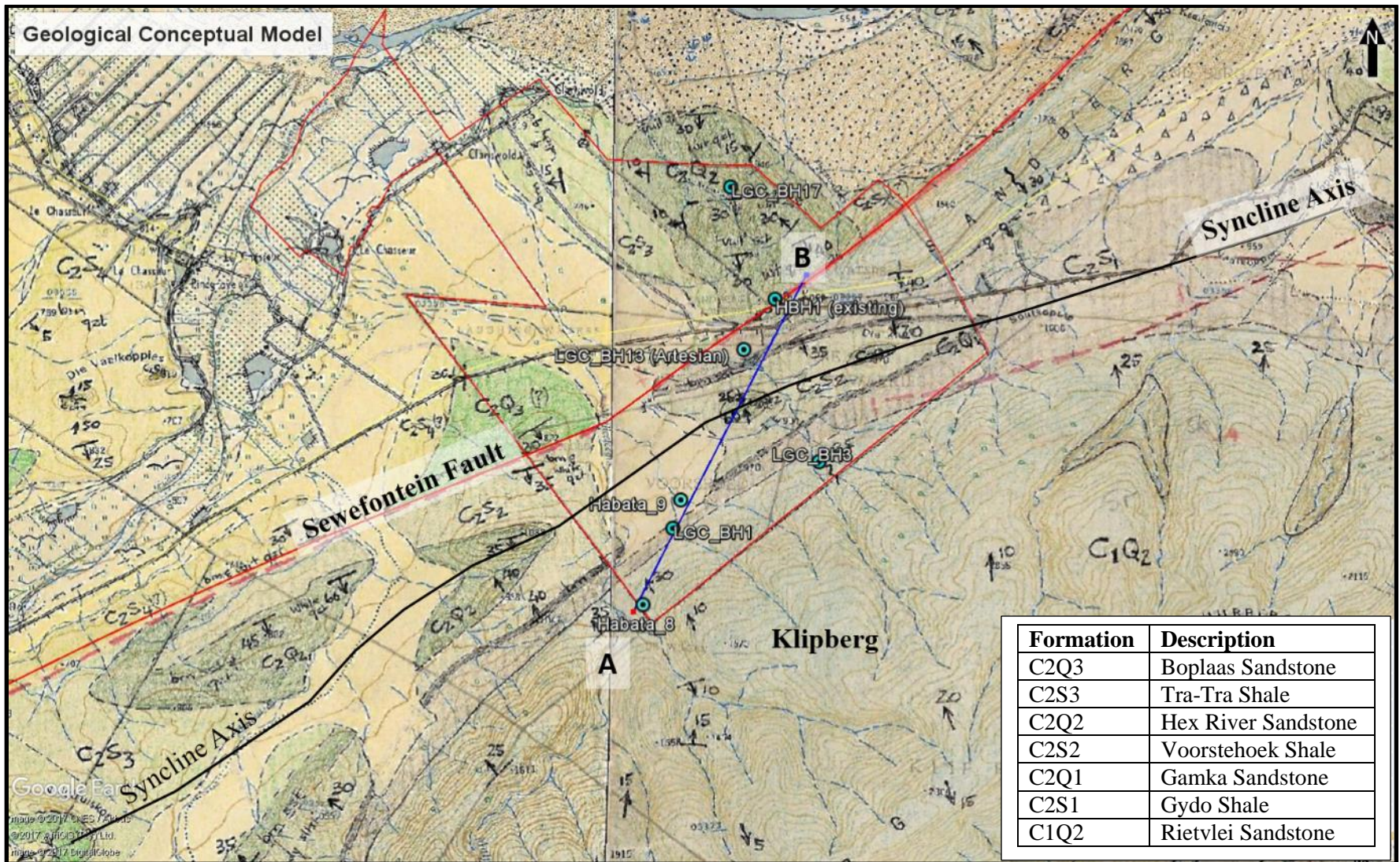


Figure 13: Geological map of the area with fault, axis and cross section locations.

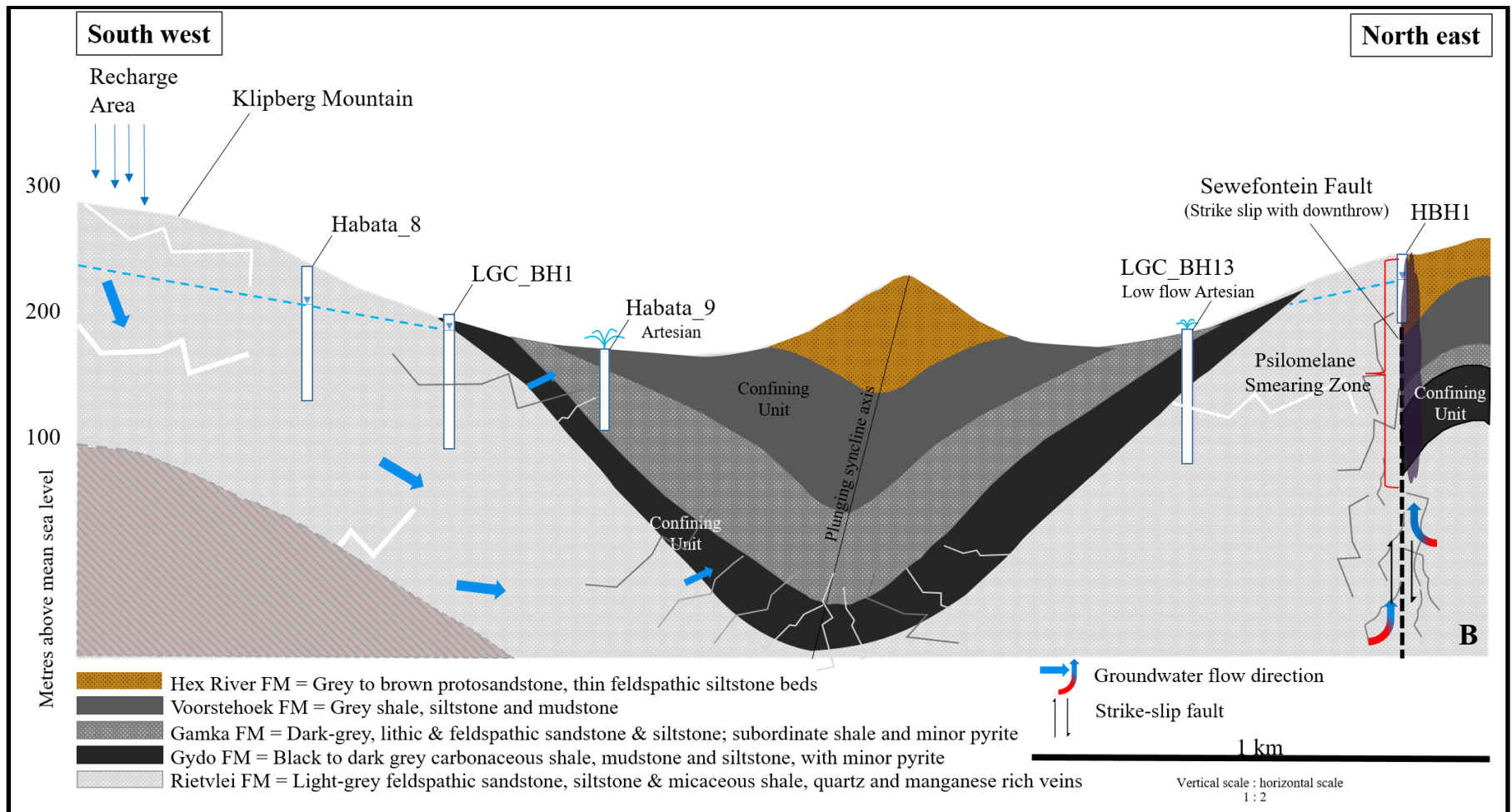


Figure 14: Conceptual model of the study area (Profile line A-B).

5.2 PUMPING TESTS: ANALYSIS RESULTS

Each borehole was analysed individually. Observation boreholes were used primarily to define boreholes with least interference on proximal boreholes as well as determine storativity. The goal was to develop a well-field with both production boreholes and backup boreholes for irrigation. The plots used to analyse each borehole are discussed in the subsections below. Raw CDT data used for the analysis is presented in **Appendix C (Pumping test Results)**.

5.2.1 HBH1

A pumping test was conducted on HBH1, the only production borehole at the time of this study. HBH1 is located in an area with distinct outcropping psilomelane (manganese hydroxide), and according to the 1: 50 000 geological map, is located within the Sewefontein Fault. Data such as drill logs and blow yields of existing boreholes are often non-existent. A conceptual understanding of the geological setting is thus ever more important in carrying out the interpretation of the pumping test. The locality of the tested borehole (HBH1) and observation boreholes is depicted in **Figure 15**.

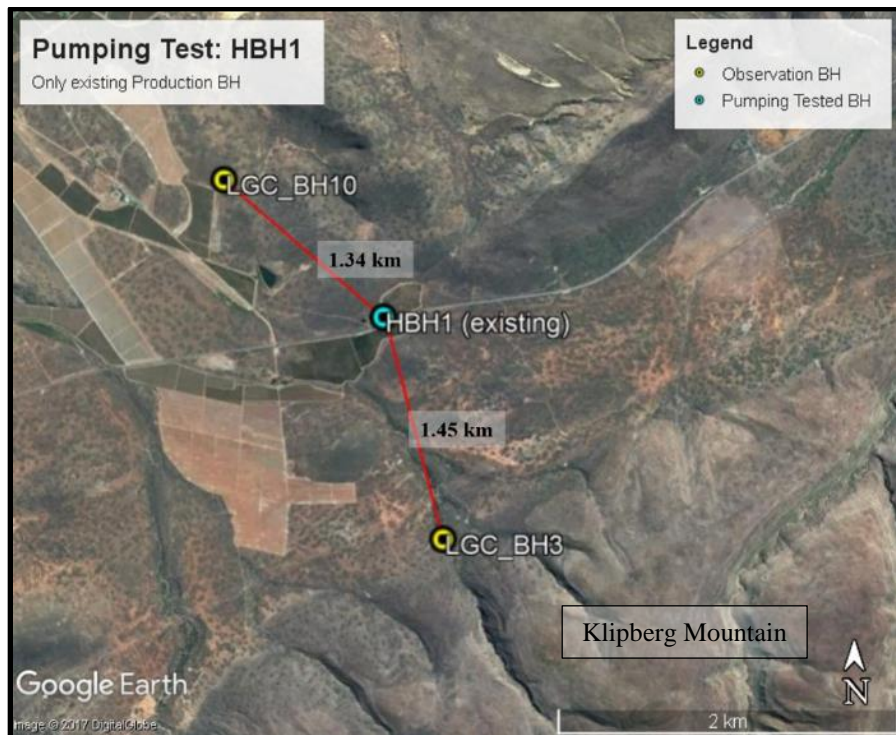


Figure 15: Pumping test at the existing borehole HBH1 and distribution of observation boreholes.

5.2.1.1 Step Test: HBH1

The Step Test commenced on the 10 June 2016. The rest water level (RWL) was 10.38 mbgl and the test pump was installed at 46 mbgl in the borehole with a depth of 51.9 m. The water level was drawn down to 11.3 m below the RWL at the end of the fourth step, conducted at a rate of 4.7 L/s. The fourth step incurred a drawdown of on average 5 cm per 10 minutes. No data was available on the depth of the main water strikes. A constant discharge rate of 5 L/s was selected to stress the borehole sufficiently and simulate peak demand abstraction rates. An initial transmissivity of 26 m²/day was estimated from Step Test data. As the boreholes is relatively shallow and located within a fault, the fracture zone was assumed to be within the deepest ten metres of the borehole. **Figure 16** shows the time-series drawdown relative to the different pumping rates during the Step Test.

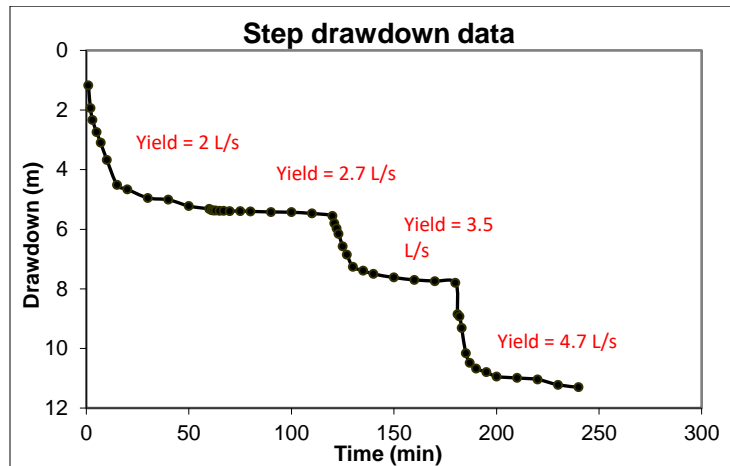


Figure 16: Step Test drawdown curve for HBH1 borehole.

5.2.1.2 Constant Discharge Test: HBH1

The CDT was conducted at a rate of 5 L/s for the 24 hour CDT period. The Theis Plot of the drawdown with time for the 24 hour CDT is shown in a log –log plot (**Figure 17**). The gradients of the drawdown are used to characterise the different flow regimes over the time of abstraction.

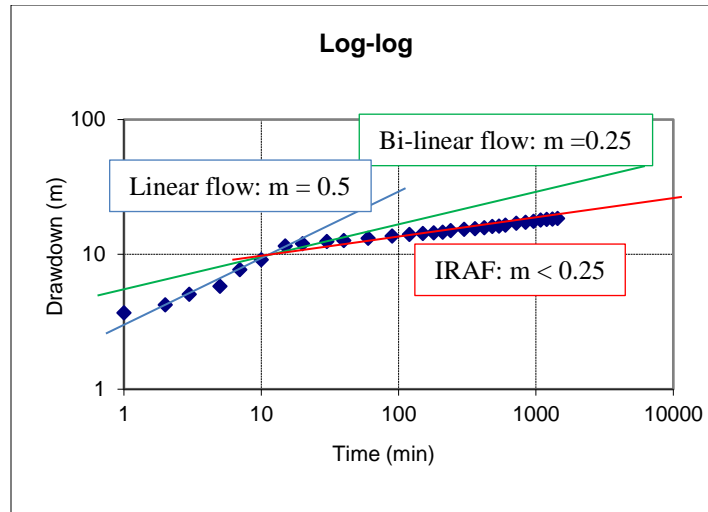


Figure 17: Log-log plot of drawdown of HBH1 with diagnostic flow regimes.

The log-log plot (**Figure 17**) of drawdown indicates linear flow by a 0.5 gradient (3-15 min). There is a brief period of bilinear flow from 15 to 40 minutes as indicated by a 0.25 gradient. From 40 - 150 minutes, there appears to be radial acting flow (RAF) as indicated by a horizontal slope (parallel to time axis) of the first derivative of drawdown (**Figure 18**). The changing flow regimes provide ample evidence of a well-connected fracture network. At approximately 180 and 420 minutes, flow boundaries are met. These represent dewatering of fractures – given the geological setting of the borehole, these possibly represent fault splays.

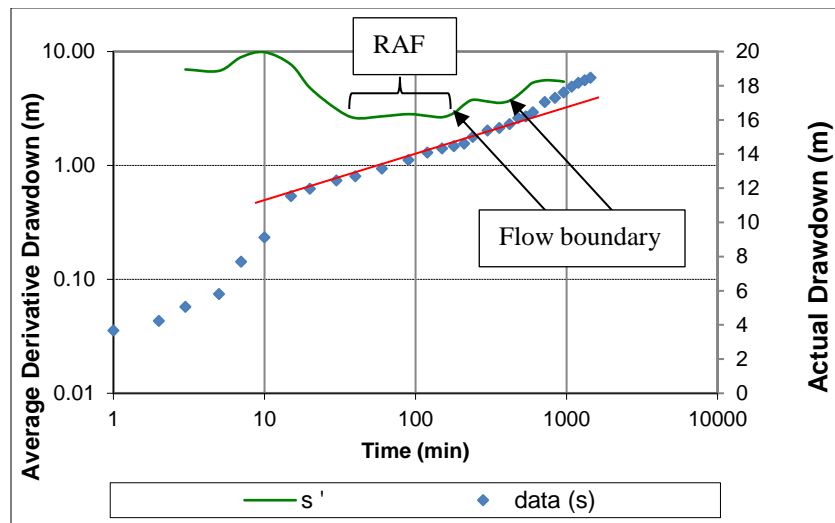


Figure 18: Derivate plot (primary axis) and drawdown plot (secondary axis) of HBH1 with RAF gradient marked with red line.

The Cooper-Jacob method was applied to the RAF portion (40-150 mins) of the drawdown curve. The diagnostic gradient was not fitted to the end of the data, rather to the middle to late time data. As this borehole is drilled into an extensive fault, with a lateral displacement of approximately 4 km, it is possible that recharge is being promoted from the upper reaches of the fault in mountains during the intermediate to end time of the test. This is an external effect, and fitting of diagnostic plots should not be applied in such instances. The diagnostic curve was thus fitted to the section representing RAF and a transmissivity of 25.2 m²/day was estimated.

The recovery data is presented in **Figure 19** together with the fitted curve used to determine the transmissivity (T) using the Theis recovery method. A T value of 22 m²/day was estimated using the recovery data which correlates well to the transmissivity of 26 m²/day and 25.2 m²/day estimated using the Step Test and CDT data respectively.

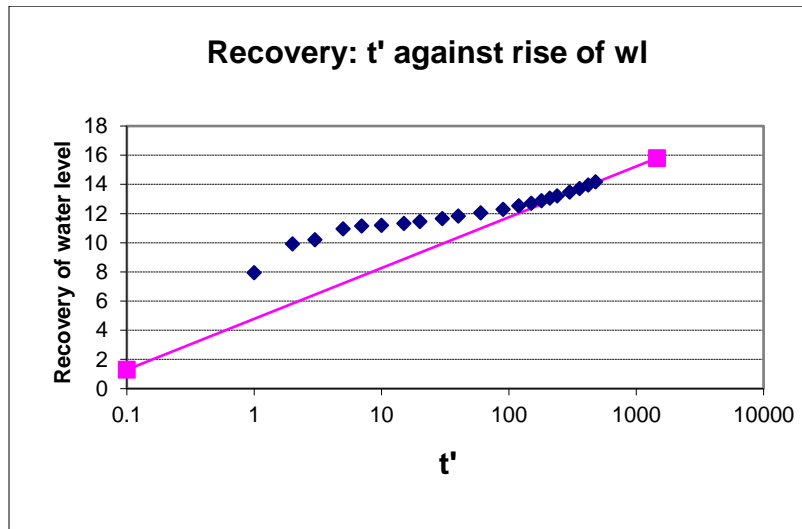


Figure 19: Recovery graph of HBH1 applying Theis to determine Transmissivity.

A comparison of the transmissivity values determined using Cooper-Jacob and Theis is given in **Table 12**. The two T values correlate well, indicating that the natural inflow during recovery is representative of the RAF used to determine the T value in the Cooper-Jacob method.

5.2.1.1 Observation Boreholes and Storativity

LGC_BH3 and LGC_BH10 were selected as observation boreholes to determine connectivity or lack thereof in different limbs of the syncline, and between the different formations. LGC_BH3 was drilled directly into the Rietvlei Sandstone, in the southern limb, while LGC_BH10 was drilled

into the Hex River Formation north of the Sewefontein Fault (not within the syncline). No drawdown was measured in the observation boreholes LGC_10 and LGC_BH3, thus storativity could not be estimated. This indicates that connectivity of this fault structure, the Hex River Formation to the north and Rietvlei Formation to the south is minimal or none-existent. HBH1 was included as an observation borehole in many pumping tests to confirm this, due to its importance as an already equipped production borehole.

5.2.2 LGC_BH1

LGC_BH1 was the first borehole drilled into the Rietvlei Formation. It was drilled to a depth of 110m with a minor water strike at 16 m depth (Gydo/Rietvlei contact) and a major water bearing strike at 30 m and 65 m within the Rietvlei Sandstone. The blow yield was estimated at 36000 L/hr. Four observation boreholes were included in the pumping test with the spatial distribution shown in **Figure 20**.

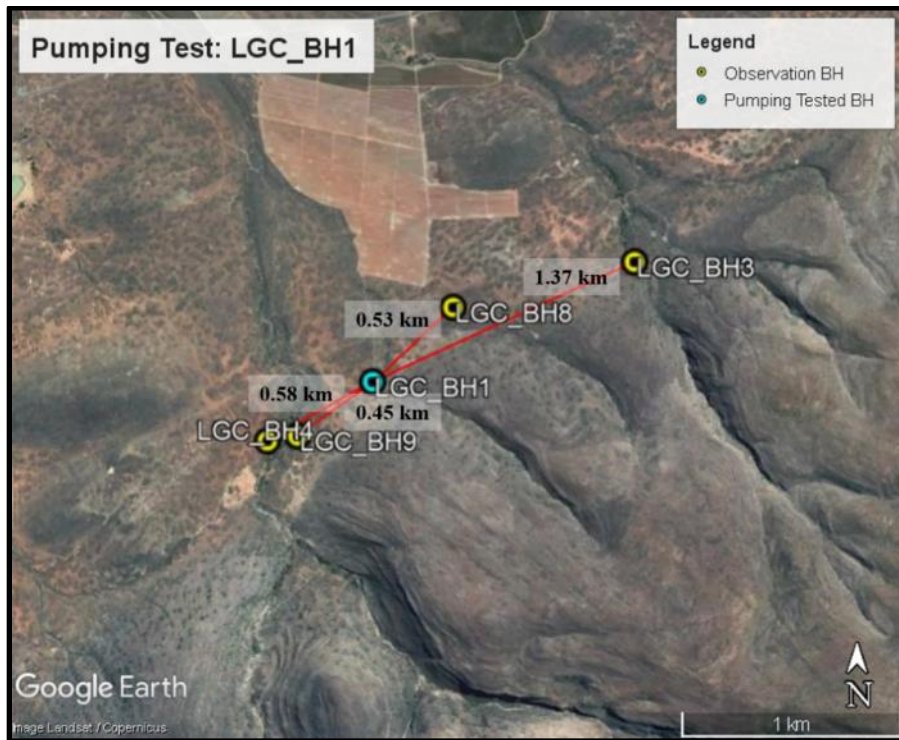


Figure 20: Pumping test at LGC_BH1 and distribution of observation boreholes.

5.2.2.1 Step Test: LGC_BH1

The Step Test commenced on the 31 May 2016. The rest water level (RWL) was 7.19 mbgl and the test pump was installed at 95 mbgl in the borehole with a measured depth of 99.4 m. Total drawdown after four steps was 35.84 m with the fourth step conducted at a rate of 15 L/s (**Figure 21**). The Step Test provides an indication of what abstraction rate can be applied to fully stress the borehole without exceeding water bearing fractures. Step test data also provides data to enable estimation of hydraulic parameters - T was estimated as 21 m²/day.

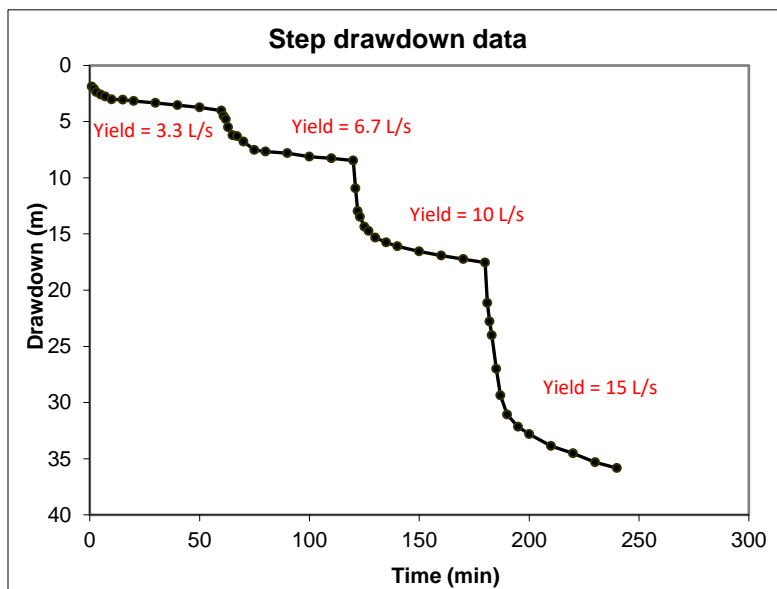


Figure 21: Step Test drawdown curve for LGC_BH1 borehole.

5.2.2.2 Constant Discharge Test: LGC_BH1

The test lasted the full 24 hours (1 440 minutes) at a rate of 14 L/s and the water level was drawn down to a maximum of 37.53 m below the rest water level at the completion of the CDT. The log-log plot of the drawdown with time for the 24 hour CDT is shown in **Figure 22**.

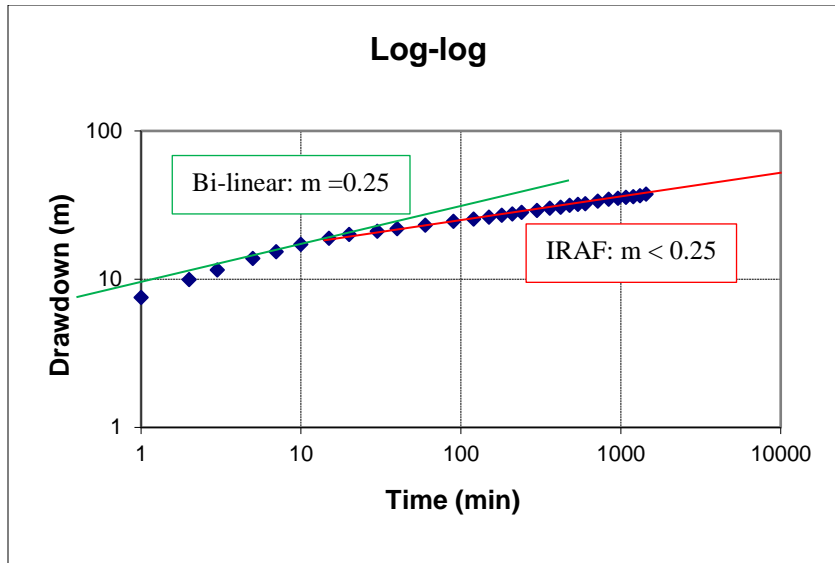


Figure 22: Log-log plot of drawdown of LGC_BH1 with diagnostic flow regimes.

The log-log plot indicates bi-linear flow during the first 15 minutes. From 15 – 540 minute a gradient of less than 0.25 is present, representing IRAF. This is again evident in the drawdown and derivative graph (**Figure 23**), with the derivative curve being horizontal during this time range. At approximately 720 mins there is a minor increase and decrease in the drawdown rate. This coincides with the depth of the first water bearing fracture (16 m), and likely represents the dewatering of the fracture. The change in flow regime from bi-linear to IRAF represents a well-connected fracture network, with flow from both fractures and matrix.

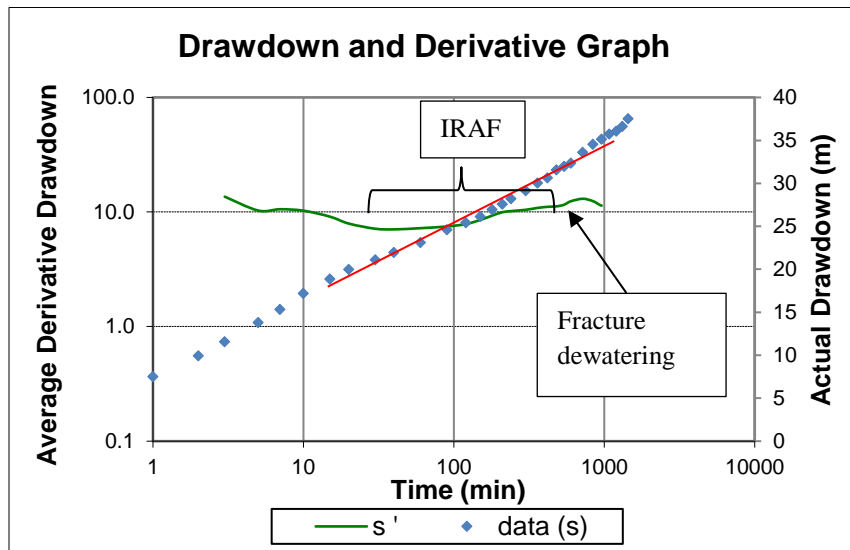


Figure 23: Derivate plot (primary axis) and drawdown plot (secondary axis) of LGC_BH1 with IRAF gradient fit marked with red line.

The Cooper-Jacob method was applied to the IRAF portion (15-540 mins) of the drawdown curve to estimate Transmissivity. A T of 20.5 m²/day was estimated. This correlates well with the T of 21 m²/day estimated from Step Test data.

The recovery data is presented in **Figure 24** together with the fitted curve used to determine the T value using the Theis recovery method. A T of 25.3 m²/day results.

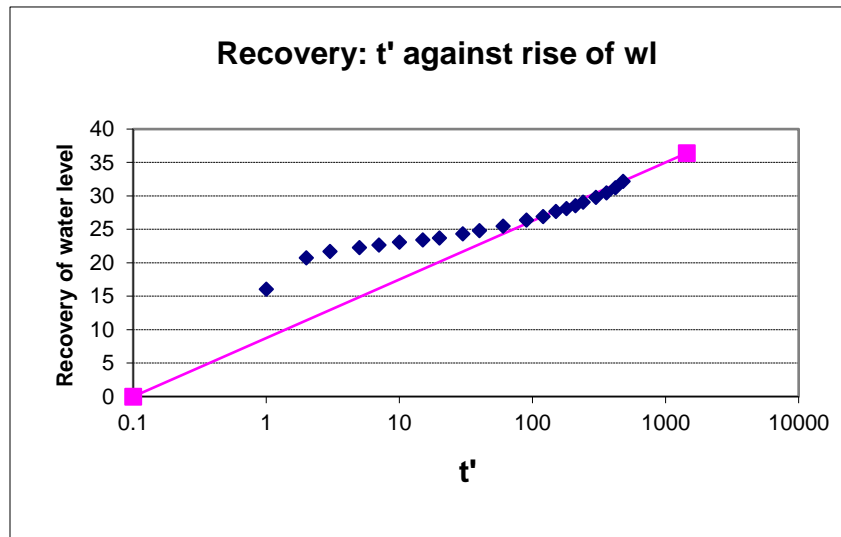


Figure 24: Recovery graph of LGC_BH1 applying Theis to determine Transmissivity.

A comparison of the transmissivity values determined using Cooper-Jacob and Theis is given in **Table 12**. The two T values correlate well, indicating that the natural inflow during recovery is representative of the IRAF used to determine the T value in the Cooper-Jacob method. The recovery is similar to that of the recovery of HBH1. Although this borehole is not drilled into a mapped fault, the fracture network is extensive and well connected to result in similar aquifer parameters to that of HBH1.

5.2.2.3 Observation Boreholes and Storativity

A drawdown was measured in LGC_BH8 and LGC_BH9, 528 m and 444 m away from LGC_BH1 respectively. Applying the Theis Recovery method a storativity of 1.4×10^{-4} to 3.6×10^{-4} is estimated. The measured drawdown over such a distance is important, as it gives evidence of the extent of the connected fracture networks present within the Rietvlei Formation.

5.2.3 LGC_BH2

LGC_BH2 was drilled to a depth of 110m, with the main water bearing fractures found at 16 m, 40 m, 44 m, 62 m and 83 m, within the Rietvlei Sandstone. Blow yield was reported by the driller as 35 000 L/hr. The location of LGC_BH2 and the observation borehole LGC_BH3 is shown in **Figure 25**.



Figure 25: Pumping test at LGC_BH2 and distribution of observation boreholes.

5.2.3.1 Step Test: LGC_BH2

The Step Test commenced on the 21 May 2016. The rest water level (RWL) was 7.92 mbgl and the test pump was installed at 89 mbgl in the borehole with a measured depth of 97.12 m. Water level was drawn down to 20.73 m below the RWL at the end of the fourth step, conducted at a rate of 14.6 L/s (**Figure 26**). During the third step conducted at 9.7 L/s a drawdown of only 5 cm was measured from 135 – 180 min. The final step with an abstraction rate of 14.6 L/s depicted a different picture, with a notable downward trend in the period of 200 – 240 minutes, with a drawdown of 3.15 m.

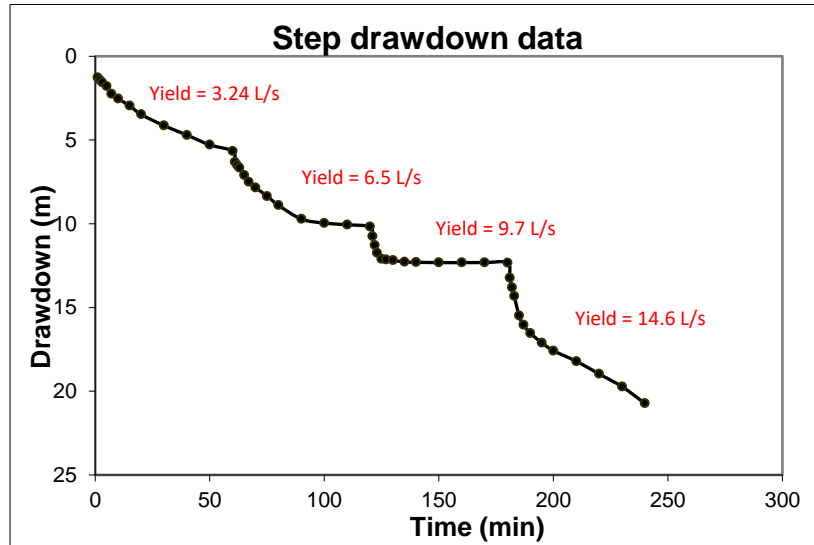


Figure 26: Step Test drawdown curve for LGC_BH2 borehole.

5.2.3.2 Constant Discharge Test: LGC_BH2

Based on the borehole response to the Step Test, an abstraction rate of 9.7 L/s was seen as too low, and that of 14.6 L/s as too high. The CDT was conducted at a rate of 12 L/s with the objective of stressing the borehole without dewatering fractures. Water level was drawn down to 76.13 m below the rest water level at the completion of the CDT. The log-log plot of the drawdown with time for the 24 hour CDT is shown in **Figure 27**.

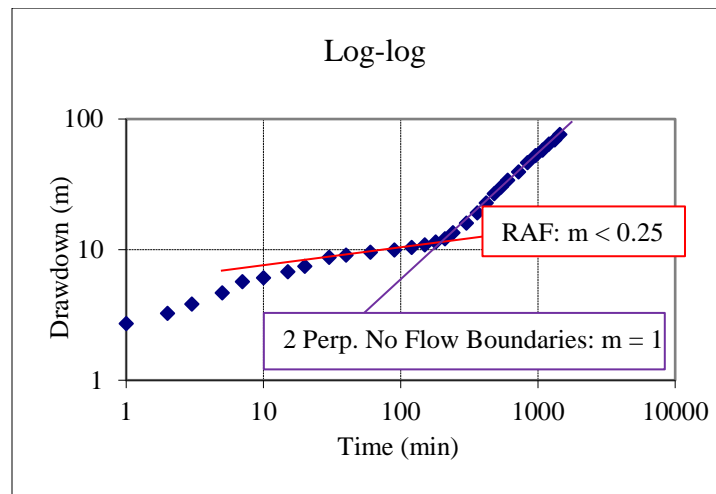


Figure 27: Log-log plot of drawdown of LGC_BH2 with diagnostic flow regimes.

Radial acting flow (RAF) occurs from 0 – 180 minutes, with a quadrupling of slope from 180 – 1440 minutes. This represents the drawdown curve reaching two no-flow perpendicular

boundaries. In the semi-log Cooper-Jacob and Derivative Plot (**Figure 28**) the derivative curve clearly depicts a decrease followed by an increase in the rate of drawdown at approximately 60 minutes typical of dewatering of a fracture.

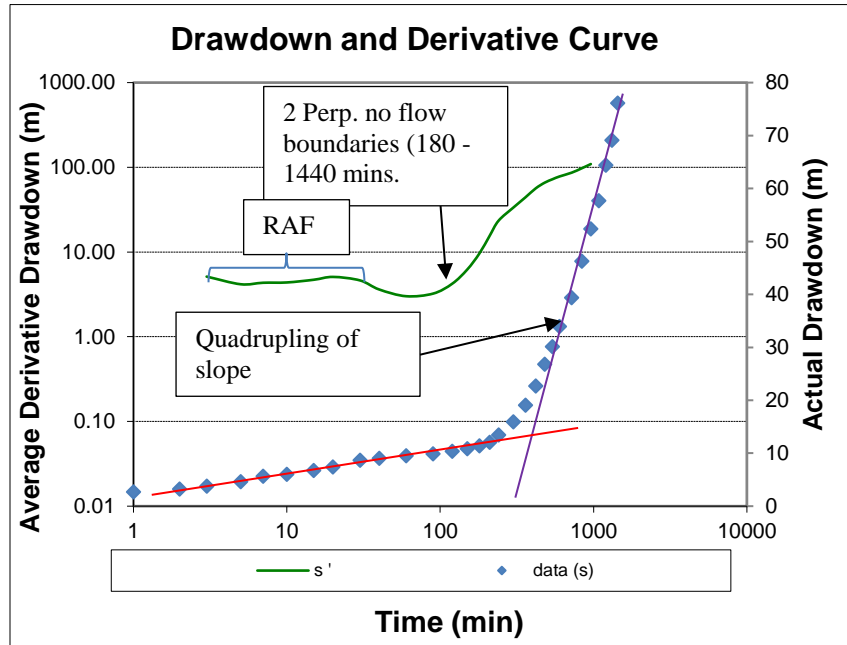


Figure 28: Derivate plot (primary axis) and drawdown plot (secondary axis) of LGC_BH2 with radial acting flow (RAF) occurring 0-180 minutes, fitted with red line.

The Cooper-Jacob method was applied to time 0 – 180 minutes, before fracture dewatering to estimate Transmissivity of the RAF regime. A transmissivity of 41.3 m²/day was estimated.

The recovery data is presented in **Figure 29** together with the fitted curve used to determine the T value using the Theis recovery method. A T of 38.7 m²/day was estimated using the recovery data. This correlates well with the transmissivity estimated using Cooper-Jacob for the drawdown of the radial acting flow.

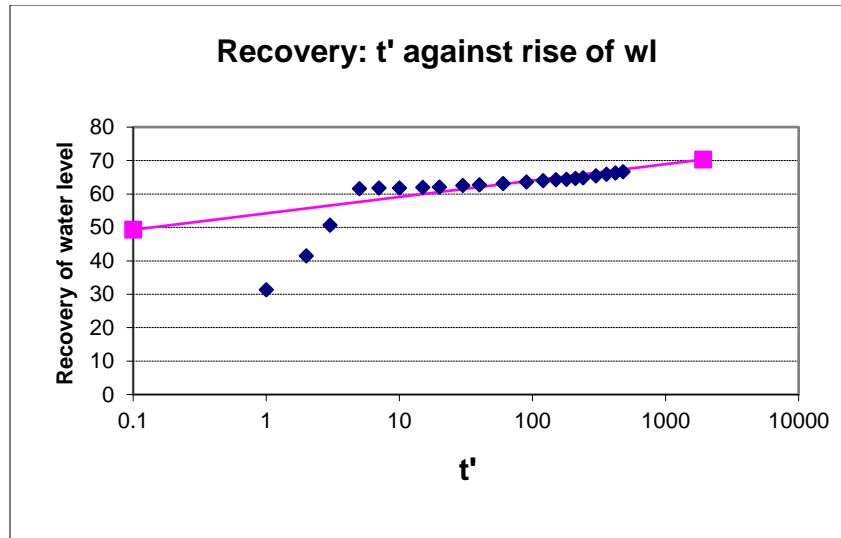


Figure 29: Recovery graph of LGC_BH2 applying Theis to determine Transmissivity.

5.2.3.1 Observation Boreholes and Storativity

LGC_BH3 was used as an observation borehole, which is located 230 m south of LGC_BH2. No drawdown was measured in the observation borehole, thus storativity was not calculated.

5.2.4 LGC_BH3

LGC_BH3 was drilled to a depth of 80m. Drilling was terminated due to water pressure preventing deeper drilling beyond this depth. Blow yield was reported to be in excess of 80 000 L/hr. Main water bearing fractures were found at 31 m, 54 m, and 78 m, within the Rietvlei Sandstone. The location of LGC_BH3 as well as observation boreholes (and distances) is given in **Figure 30**.

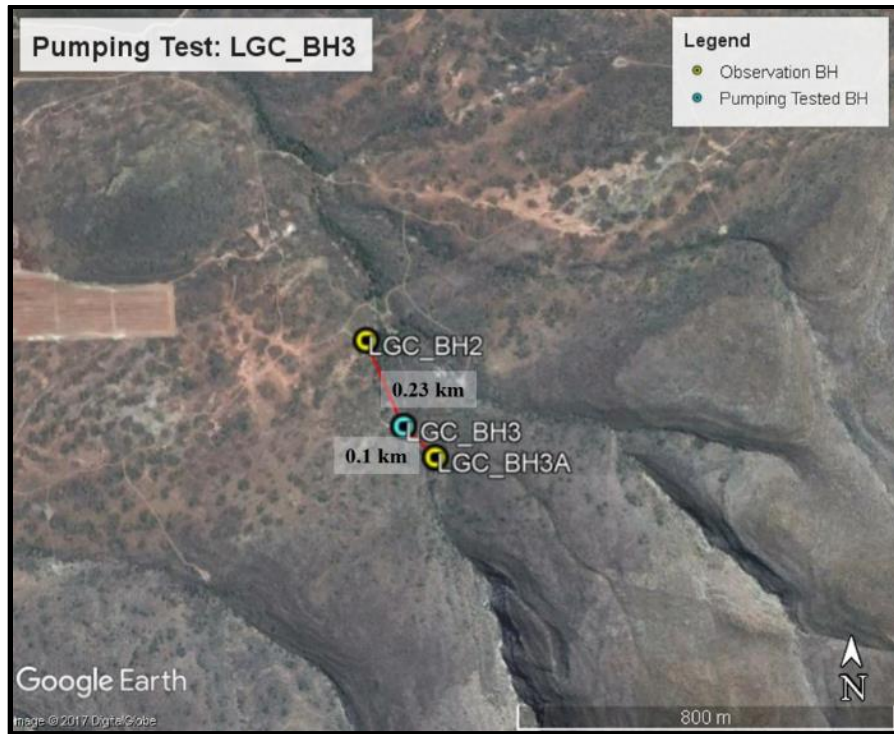


Figure 30: Pumping test at LGC_BH3 and distribution of observation boreholes.

5.2.4.1 Step Test: LGC_BH3

The Step Test was conducted on the 19 May 2016. The rest water level (RWL) was 10.39 mbgl and the test pump was installed at 65 mbgl in the borehole with a measured depth of 71m. The water level was drawn down to 12.33 m below the RWL at the end of the fourth step, conducted at a rate of 33.3 L/s (maximum pump abstraction rate). **Figure 31** shows the time-series drawdown relative to the different pumping rates during the Step Test. Due to the decreasing rate of drawdown during the last step, and overall drawdown of 12.33 mm for the four steps, the rate of 30 L/s was selected for CDT. The step test provided an initial T of $112\text{m}^2/\text{day}$, indicating a highly transmissive fracture network.

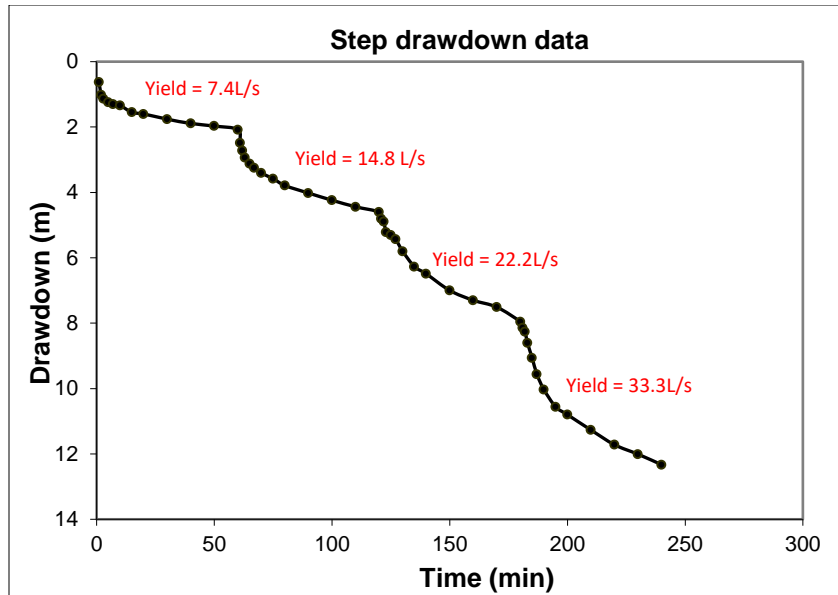


Figure 31: Step Test drawdown curve for LGC_BH3 borehole.

5.2.4.2 Constant Discharge Test: LGC_BH3

The 24 hour CDT (1 440 minutes) conducted at rate 30 L/s resulted in 17.26 m total drawdown. The log-log plot is shown in **Figure 32**. The gradient (m) of the drawdown is used to characterise the different flow regimes over the time of abstraction.

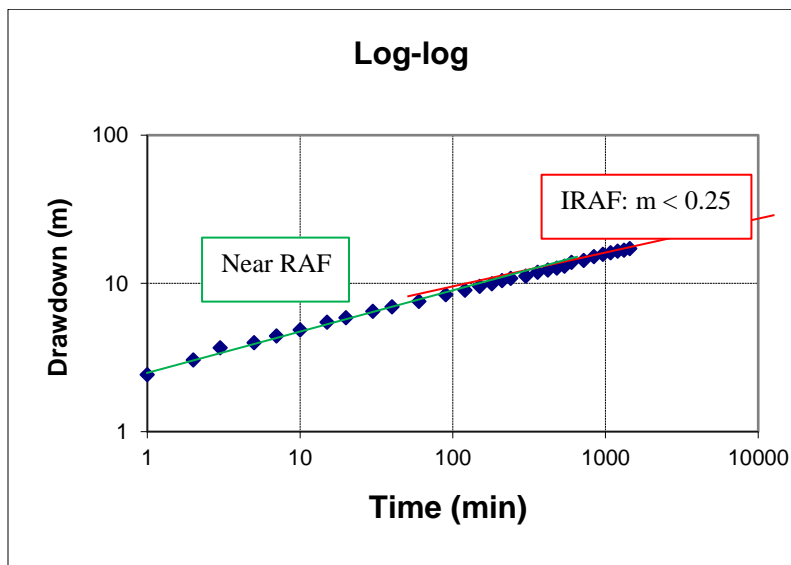


Figure 32: Log-log plot of drawdown of LGC_BH3 with diagnostic flow regime.

The log-log plot (**Figure 32**) of drawdown indicates near radial acting flow during the first 720 minutes of the CDT, after which IRAF flow occurs to the end of the test. The first derivative curve

in **Figure 33** shows this gradual increase in drawdown over the length of test with a near horizontal line from 720 – 1440 minutes, representing IRAF.

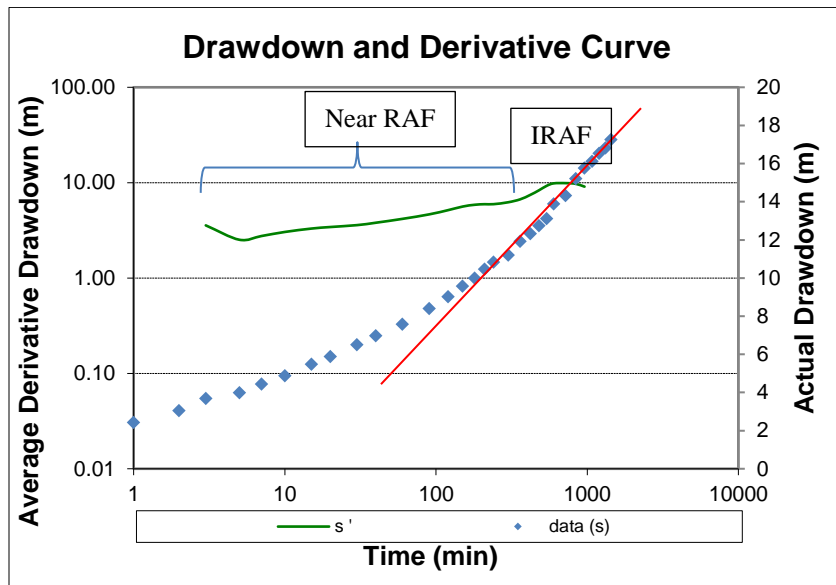


Figure 33: Derivate plot (primary axis) and drawdown plot (secondary axis) of LGC_BH3 with IRAF gradient marked with red line.

The Cooper-Jacob method was used with the curve matching at the late time IRAF regime resulting in a T estimate of $54.8 \text{ m}^2/\text{day}$.

The recovery data is presented in **Figure 34** together with the fitted curve used to determine the T value using the Theis recovery method. A transmissivity of $83.6 \text{ m}^2/\text{day}$ was estimated using the recovery data.

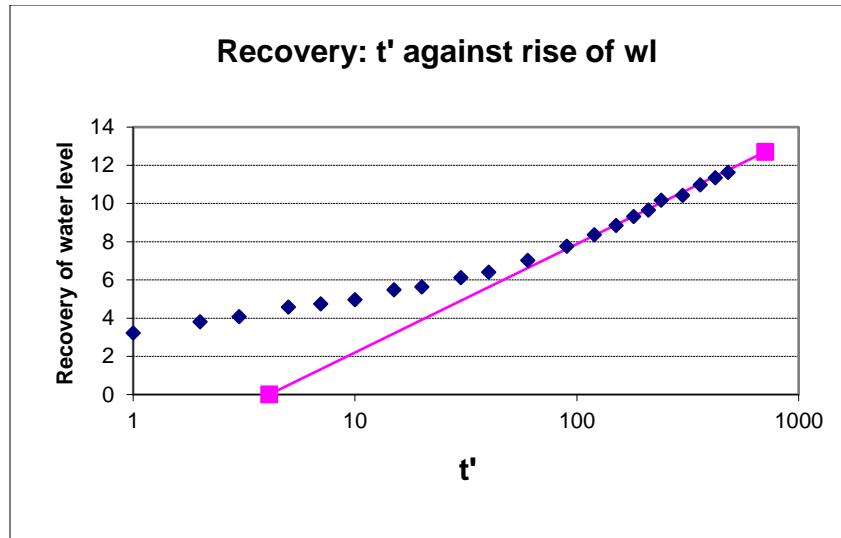


Figure 34: Recovery graph of LGC_BH3 applying Theis to determine Transmissivity.

5.2.4.1 Observation Boreholes and Storativity

A drawdown was measured in the observation boreholes LGC_BH3a and LGC_BH2, 100 m and 230 m away from LGC_BH3 respectively. Applying the Theis solution a storativity of 7×10^{-4} is estimated.

5.2.5 LGC_BH5

Drilled south of an ephemeral stream bed, LGC_BH5 was drilled to a depth of 100m, with a blow yield of 80 000 L/hour and minor water strikes at 29-31 m at the shale/sandstone contact, and a major strike at 71 m. The location of LGC_BH5 and spatial distribution of observation boreholes is given in **Figure 35**.

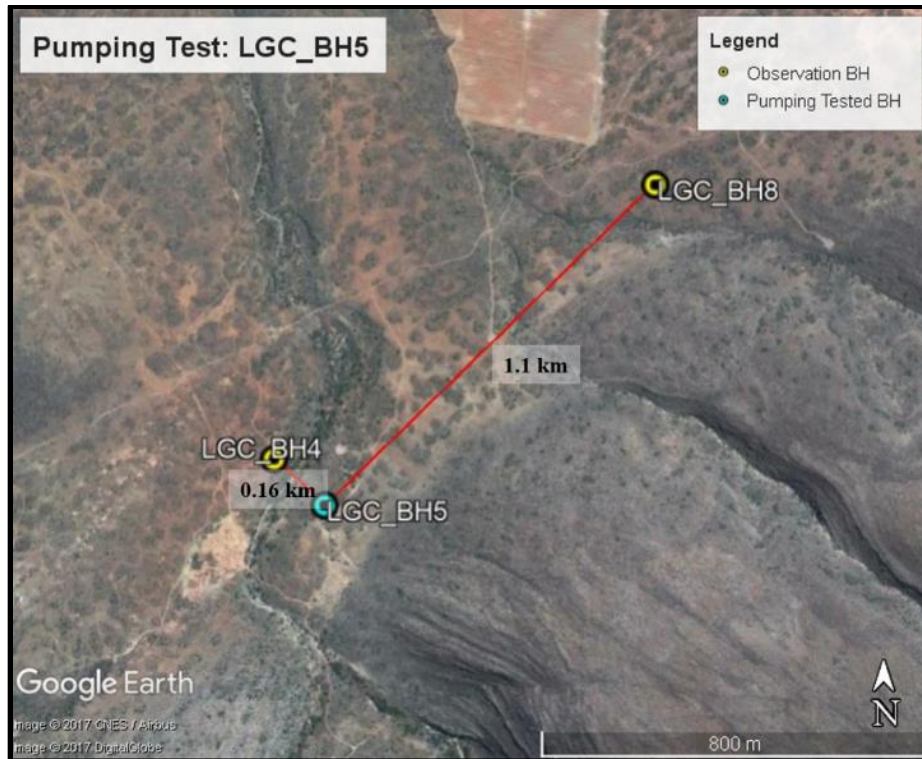


Figure 35: Pumping test at LGC_BH5 and distribution of observation boreholes.

5.2.6 Step Test: LGC_BH5

The Step Test was conducted on the 3 June 2016. The rest water level (RWL) was 8.51 mbgl and the test pump was installed at 95 mbgl in the borehole with a depth of 98.4 m. Water level was drawn down to 86.49 m below the RWL during the third step, conducted at a rate of 21.31 L/s after which the water level reached pump inlet after 4 minutes (**Figure 36**). The step test provided an initial T of 47 m²/day.

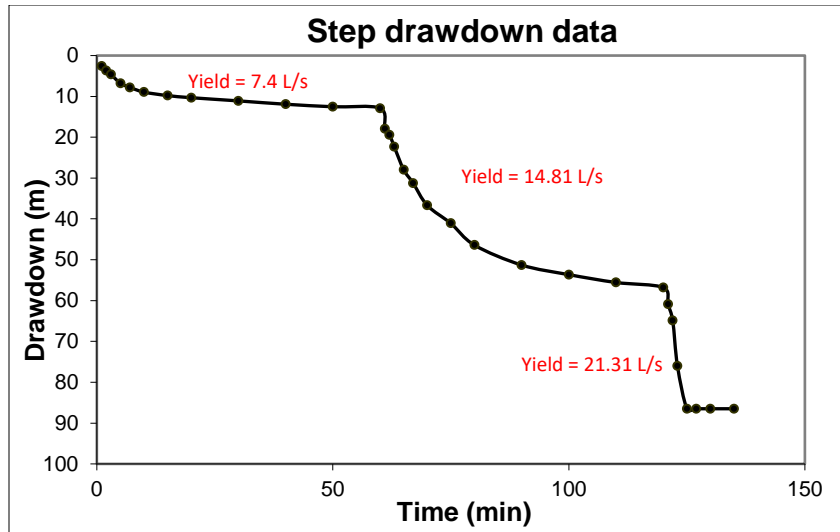


Figure 36: Step Test drawdown curve for LGC_BH5 borehole. Notice how the 3rd step fails at 21.3 L/s.

5.2.7 Constant Discharge Test: LGC_BH5

Based on the water level response to the Step Test and depth of water bearing fractures the CDT was conducted at a rate of 8 L/s. This rate was selected so as not to dewater the fractures, yet stress the aquifer sufficiently. A total drawdown of 24.26 m was recorded at completion of the CDT. The log-log plot of the drawdown with time for the 24 hour CDT is shown in **Figure 37**.

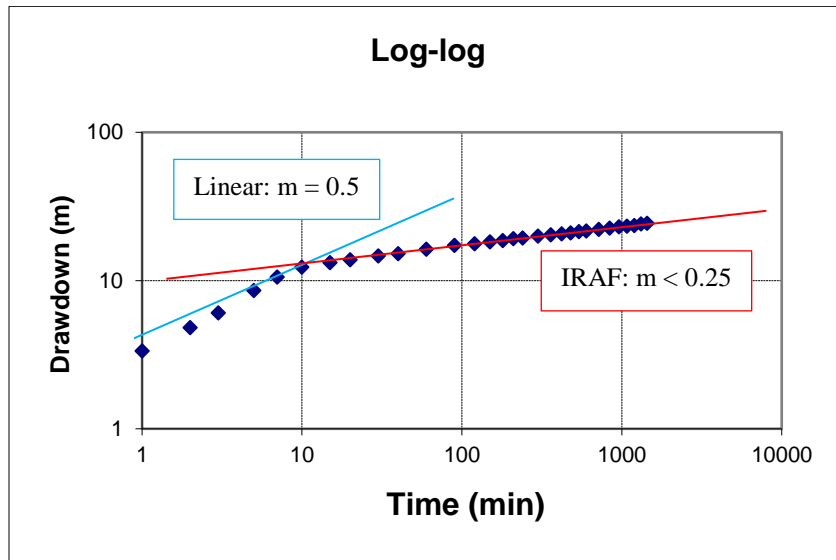


Figure 37: Log-log plot of drawdown of LGC_BH5 with diagnostic flow regimes.

There is a brief period of linear flow ($m = 0.5$) during the first 15 minutes of the CDT. Thereafter IRAF ($m < 0.25$) occurs until termination of test (1440 minutes). In the semi-log Cooper Jacob and Derivative Plot (**Figure 38**) the first derivative curve (green line) is near horizontal from 15 – 1440 minutes.

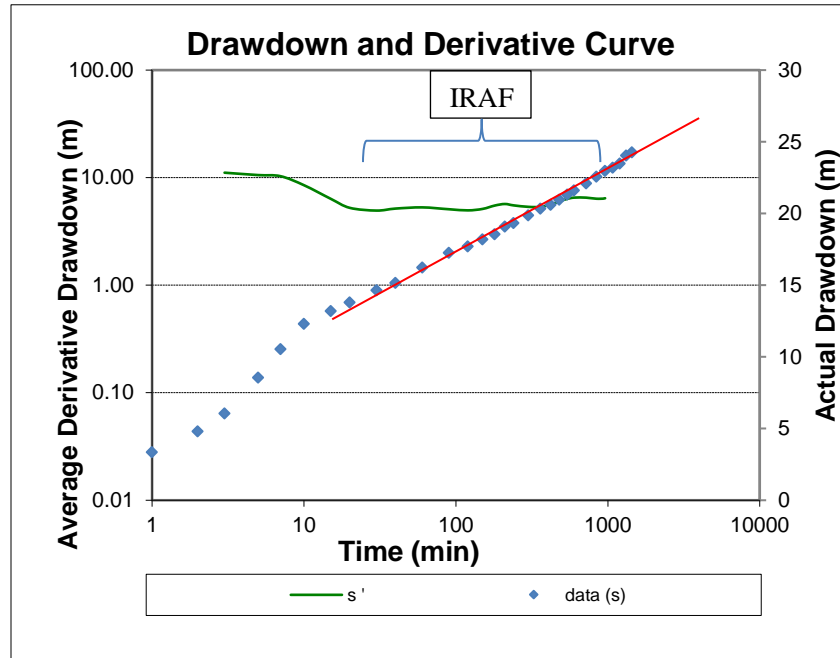


Figure 38: Derivate plot (primary axis) and drawdown plot (secondary axis) of LGC_BH5 with IRAF gradient fit marked with red line.

The Cooper-Jacob method was applied to time 15 – 1440 minutes, during IRAF to estimate Transmissivity (T). A T of $22.4 \text{ m}^2/\text{day}$ was estimated.

The residual drawdown is presented in **Figure 39** together with the fitted curve used to determine the T value using the Theis recovery method. A T of $24.6 \text{ m}^2/\text{day}$ was estimated using the recovery data. This correlates well with the T estimated using Cooper-Jacob for the drawdown of the IRAF flow regime.

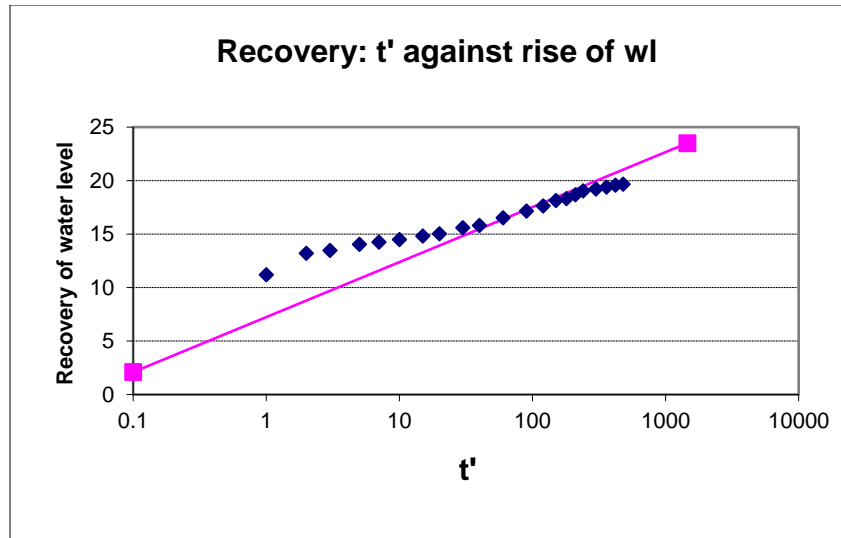


Figure 39: Recovery graph of LGC_BH5 applying Theis to determine Transmissivity.

5.2.7.1 Observation Boreholes and Storativity

LGC_BH4 and LGC_BH8, 163 m and 1100 m away respectively, were used as observation boreholes. A total drawdown of 1.09 m was measured in LGC_BH4. Applying the Theis Recovery solution a storativity of 1.5×10^{-3} is estimated.

5.2.8 LGC_BH8

LGC_BH8 was drilled to a depth of 100m, with a blow yield of 15 000 L/hr and a major water strikes at 64 m. The location of LGC_BH8 and observation boreholes is given in **Figure 40**.

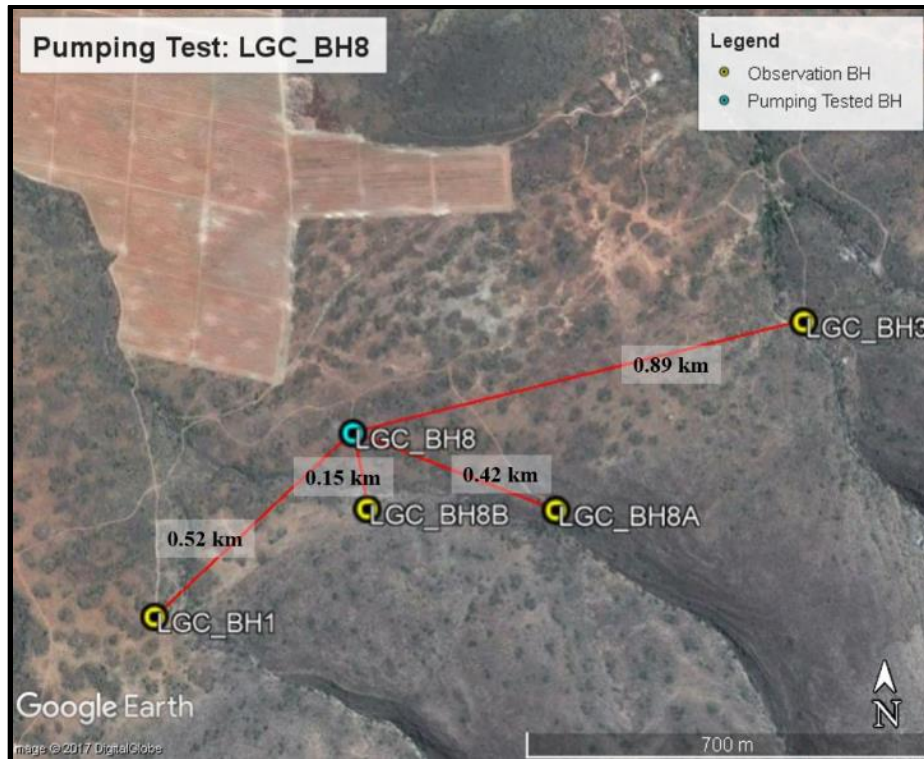


Figure 40: Pumping test at LGC_BH8 and distribution of observation boreholes.

5.2.8.1 Step Test: LGC_BH8

The Step Test was conducted on the 28 May 2016. The rest water level (RWL) was 11.49 mbgl and the test pump was installed at 95 mbgl in the borehole with a depth of 83.5 m. The water level was drawn down to 72.01 m below the RWL at the end of the fourth step, conducted at a rate of 10.4 L/s. During this final step the water level reached pump inlet after 10 minutes **Figure 41**. An initial T of 21 m²/day and the water level response during the Step Test were used as a guide for determining the rate of the CDT.

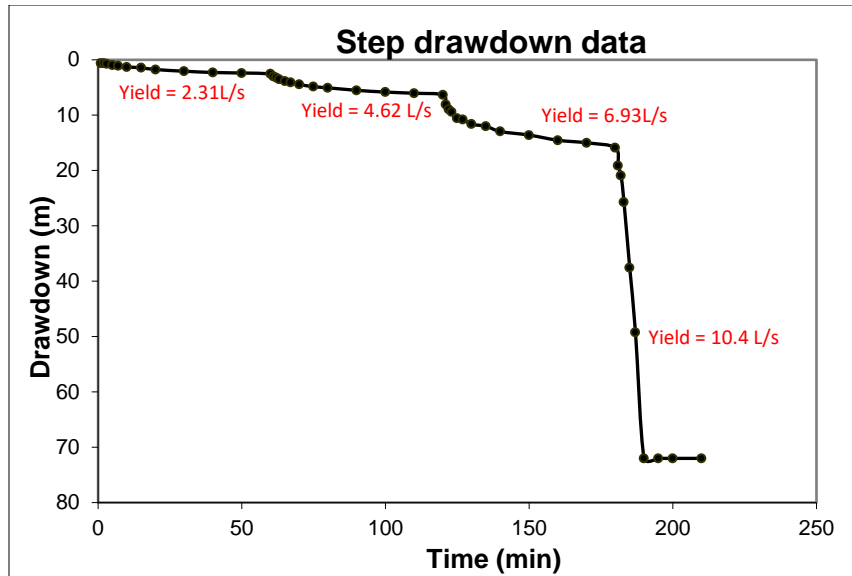


Figure 41: Step Test drawdown curve for LGC_BH8 borehole. Notice how the 4th step fails at 10.4 L/s.

5.2.8.2 Constant Discharge Test: LGC_BH8

Following the water level response to the Step Test, the CDT was conducted at a rate of 7 L/s as the rate of 10.4 L/s caused the water level to drop below the water bearing strike at 64 m. The test lasted the full 24 hours (1 440 minutes) and final drawdown was 49.94 m. The log-log plot of drawdown with time for the CDT is shown in **Figure 42**.

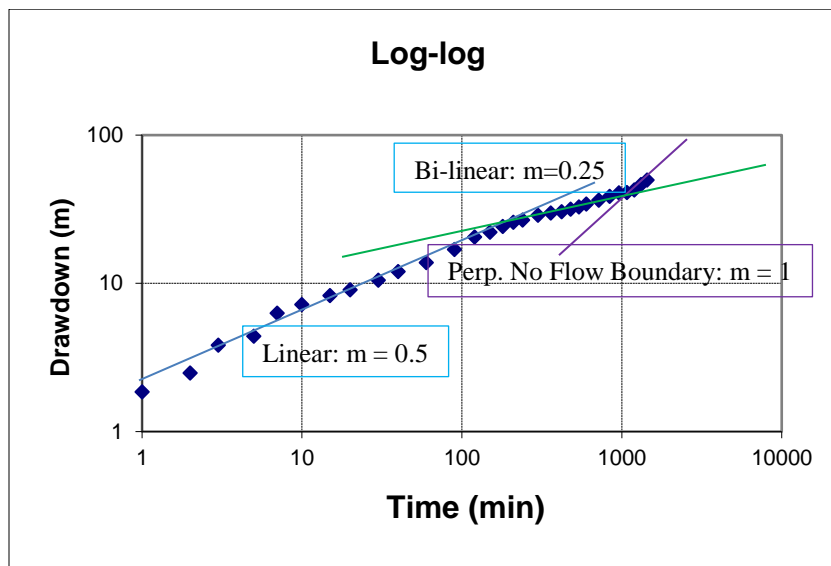


Figure 42: Log-log plot of drawdown of LGC_BH8 with diagnostic flow regimes.

Linear flow ($m = 0.5$) occurs from the start of the test to 180 minutes. Thereafter there is a period of bi-linear flow ($m = 0.25$) until 1080 minutes. From 1080 – 1440 minutes a quadrupling of slope occurs ($m = 1$) representing 2 perpendicular no-flow boundaries. The dewatering of two fractures is clearly shown in the Drawdown and Derivative Curve Plot (**Figure 43**), with the first derivative (green line) showing a rise and decrease of drawdown at 180 minutes, and a similar pattern at approximately 720 minutes.

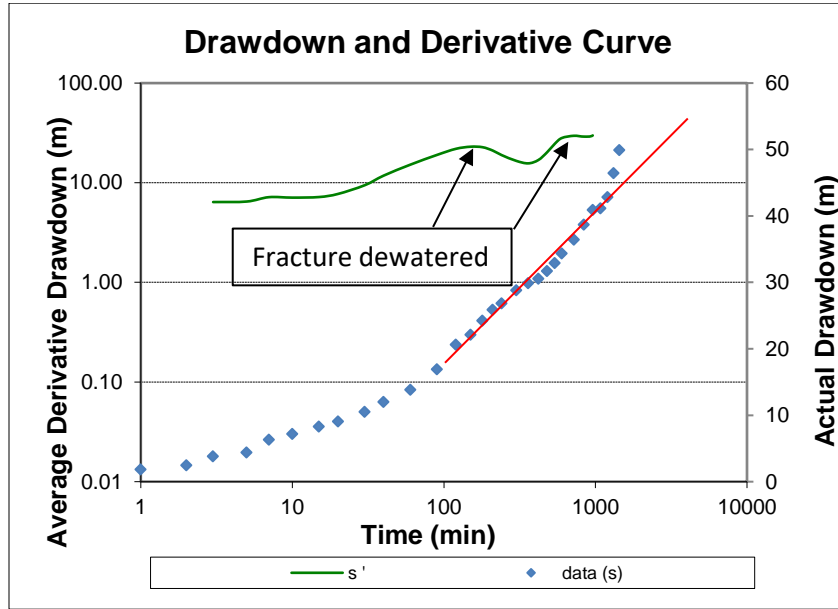


Figure 43: Derivate plot (primary axis) and drawdown plot (secondary axis) of LGC_BH8 with linear flow gradient fit marked with red line.

The Cooper-Jacob method was applied to time 180 – 1080 minutes, during bilinear flow to estimate Transmissivity. A transmissivity of $4.1 \text{ m}^2/\text{day}$ was estimated.

The residual drawdown is presented in **Figure 44** together with the fitted curve used to determine the T value using the Theis Recovery method. A transmissivity of $25.4 \text{ m}^2/\text{day}$ was estimated using the recovery data. This correlates poorly with the estimated T using Cooper-Jacob for the drawdown of the linear flow regime. It must be noted here that Cooper-Jacob is ideally only applied to fractured aquifers with homogenous acting flow media. The initial T estimated during the step test ($21 \text{ m}^2/\text{day}$) correlates with the T estimated using the Theis Recovery method ($25.4 \text{ m}^2/\text{day}$).

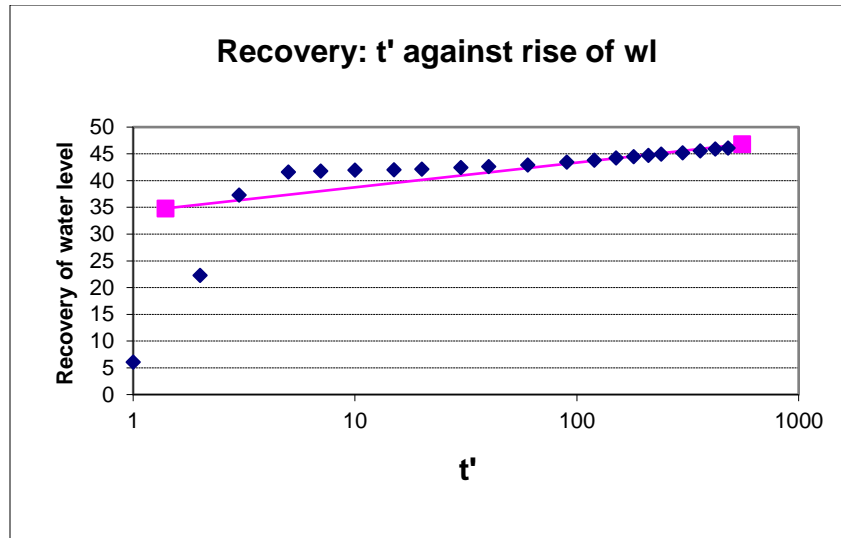


Figure 44: Recovery graph of LGC_BH8 applying Theis to determine Transmissivity.

5.2.8.1 Observation Boreholes and Storativity

LGC_BH1, LGC_BH8A, LGC_BH8B and LGC_BH3, were used as observation boreholes. The distances are 524 m, 150 m, 420 m and 890 m away respectively. A total drawdown of 0.94 m was measured in LGC_BH8B and 1.51 m in LGC_BH1. Applying the Theis solution a storativity of 0.9×10^{-4} is estimated.

5.2.9 Habata_2

Habata_2 was drilled to a depth of 120 m, with major water bearing fractures found at 66 m, 71 m, and 72 m within the Rietvlei Formation. The location of Habata_2 and the proximity of observation boreholes is given in **Figure 45**.

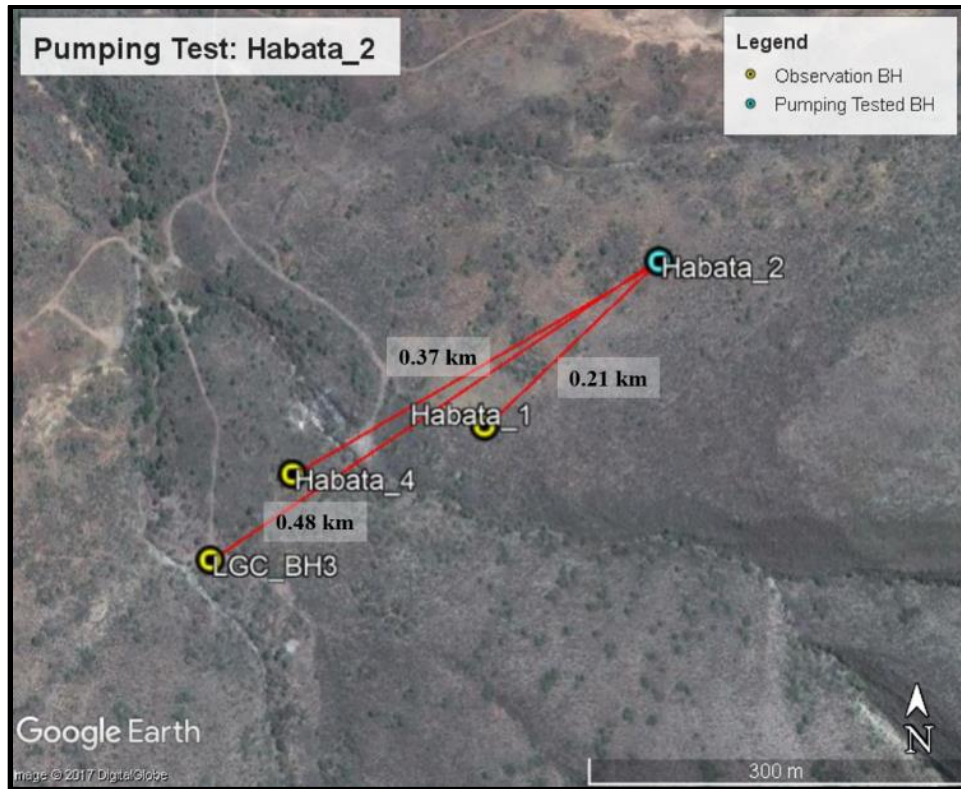


Figure 45: Pumping test at Habata_2 and distribution of observation boreholes.

5.2.9.1 Step Test: Habata_2

The Step Test commenced on the 19 June 2017. The rest water level (RWL) was 25.26 mbgl and the test pump was installed at 85.1 mbgl in the borehole with a depth measurement of 120 m. The water level was drawn down to 57.12 m below the RWL at the end of the fourth step, conducted at a rate of 7.4 L/s. The water level dropped gradually during the first 3 steps, however it dropped significantly faster during the fourth step (**Figure 46**). The water level response to the different abstraction rates provides a guide for determining an appropriate rate for the CDT. An initial T of $9 \text{ m}^2/\text{day}$ was estimated from the Step Test.

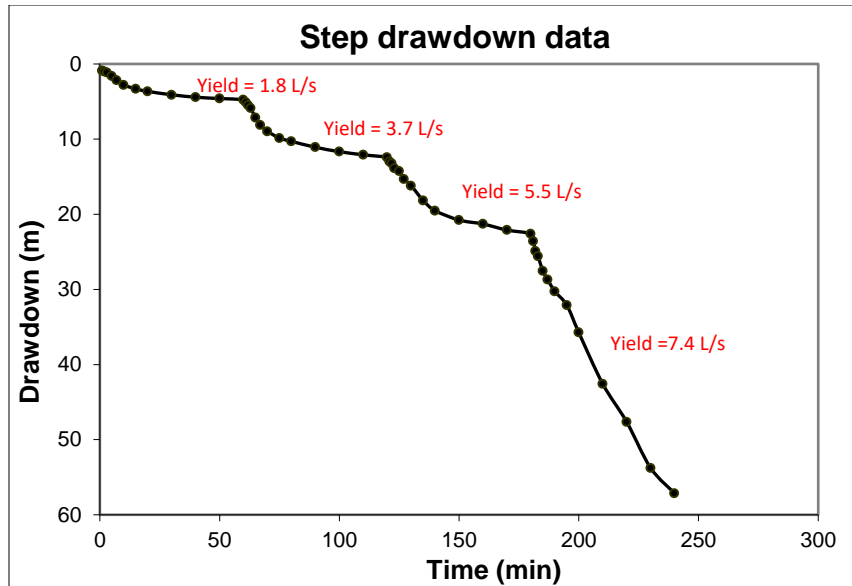


Figure 46: Step Test drawdown curve for Habata_2 borehole.

5.2.9.2 Constant Discharge Test: Habata_2

The CDT was conducted at a rate of 4.4 L/s and lasted the full 24 hours (1 440 minutes) with a drawdown of 22.05 mbgl. The log-log plot of the drawdown with time for the 24 hour CDT is shown in Figure 47.

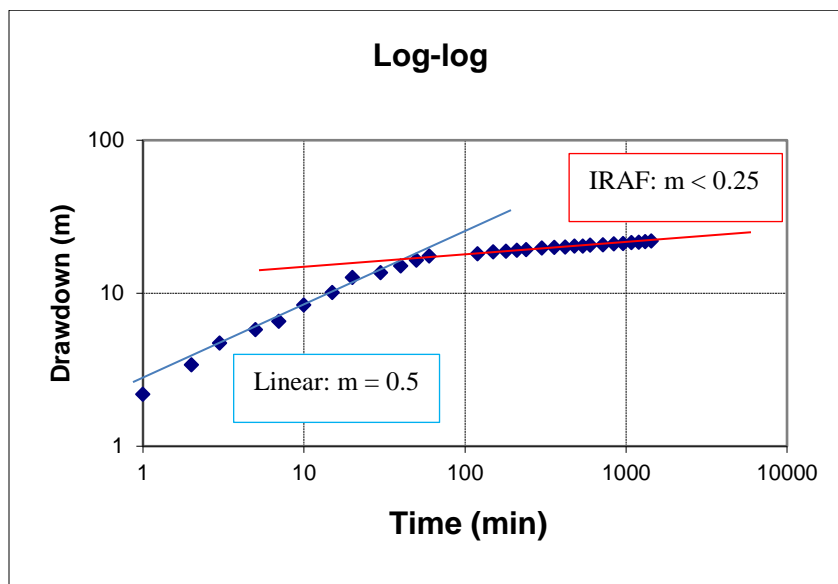


Figure 47: Log-log plot of drawdown of Habata_2 with diagnostic flow regimes.

Linear flow ($m = 0.5$) occurs from 0 – 50 minutes, after which IRAF ($m < 0.25$) occurs to the end of test, with possible boundary conditions occurring at later time (1200 minutes). In the semi-log

Cooper-Jacob and Derivative Plot (**Figure 48**) the first derivative curve (green line) is near horizontal from 120 – 1440 minutes.

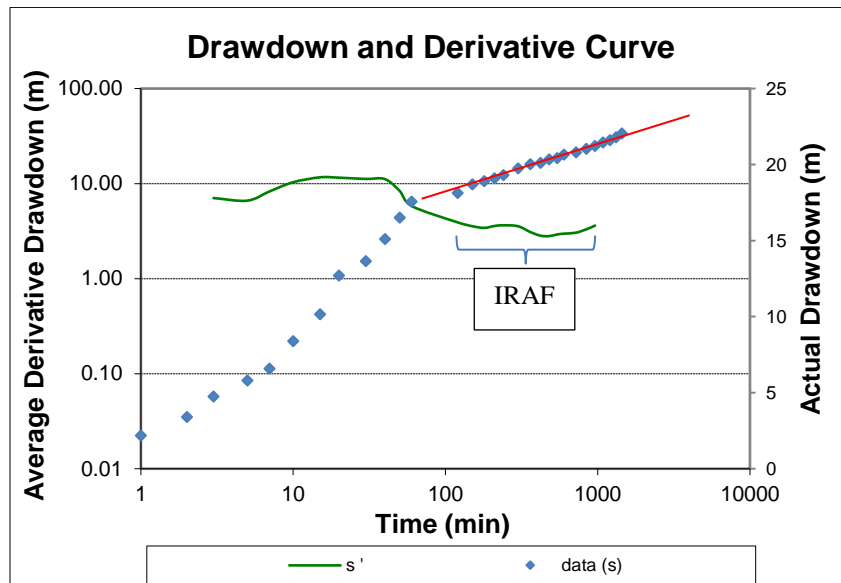


Figure 48: Derivate plot (primary axis) and drawdown plot (secondary axis) of LGC_BH2 with IRAF gradient fit marked with red line.

The Cooper-Jacob method was applied to time during which IRAF occurred (120 – 1440 minutes). A T of $20.8 \text{ m}^2/\text{day}$ was estimated.

The recovery is presented in **Figure 49** together with the fitted curve used to determine the T value using the Theis recovery method. A T of $22.6 \text{ m}^2/\text{day}$ was estimated using the recovery data. This correlates well with the transmissivity estimated using Cooper-Jacob for the drawdown of the IRAF flow regime.

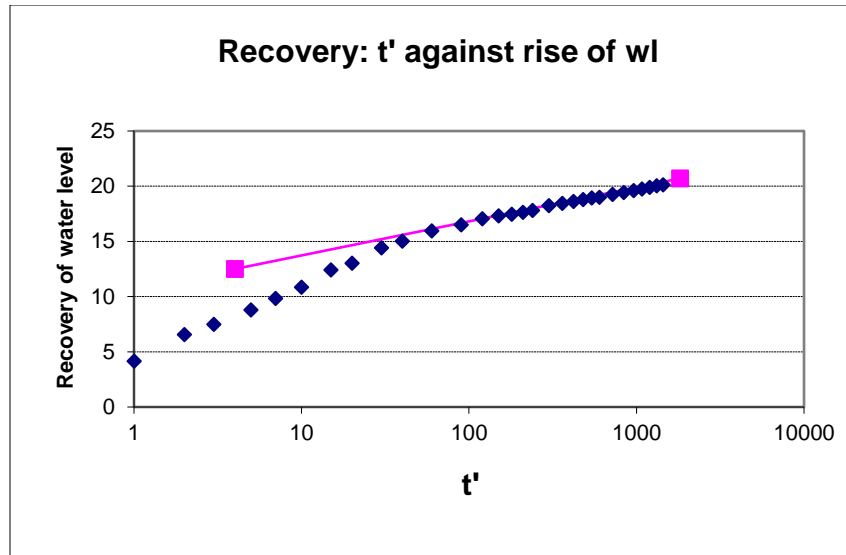


Figure 49: Recovery graph of Habata_2 applying Theis to determine Transmissivity.

5.2.9.1 Observation Boreholes and Storativity

LGC_BH3, Habata_4 and Habata_1, were used as observation boreholes. Distances from the test borehole are 480 m, 370 m and 210 m respectively. No drawdown was measured in any of these observation boreholes – storativity was not estimated.

5.2.10 Habata_4

Habata_4 was drilled to a depth of 96.8 m, with the main water bearing fractures found at 29 m, 30 m, 42 m, 74 m and 86 m within the Rietvlei Formation. A massive quartz vein drill chip (5 cm thick and 15 cm in length, **Figure 12**) was intersected at 74 m, similar to that found during drilling of LGC_BH3. Drilling terminated due to a high blow yield in excess of 80 000 L/hr. The location of Habata_4 and observation boreholes used during the pumping test is shown in **Figure 50**.



Figure 50: Pumping test at Habata_4 and distribution of observation boreholes.

5.2.10.1 Step Test: Habata_4

The Step Test commenced on the 27 June 2017. The rest water level (RWL) was 19.32 mbgl and the test pump was installed at 64 mbgl in the borehole with a depth measurement of 96.8 m. The Step Test involved three steps with a drawdown of 44.72 m (pump inlet) during the third step (**Figure 51**). An initial T of $39 \text{ m}^2/\text{day}$ was estimated from Step Test data. The water level response to the different abstraction rates as well as depth of water bearing fractures is then taken into account to determine the abstraction rate of the CDT.

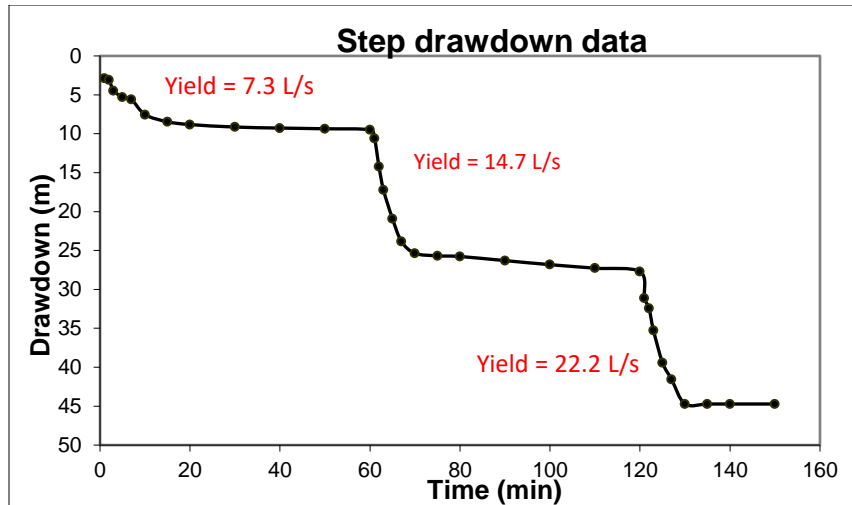


Figure 51: Step Test drawdown curve for Habata_4 borehole.

5.2.10.2 Constant Discharge Test: Habata_4

Based on the borehole response to the Step Test the CDT was conducted at a rate of 11 L/s. Water level was drawn down to 24.7 m below the rest water level after 24 hours. The log-log plot of the drawdown with time is shown in **Figure 52**.

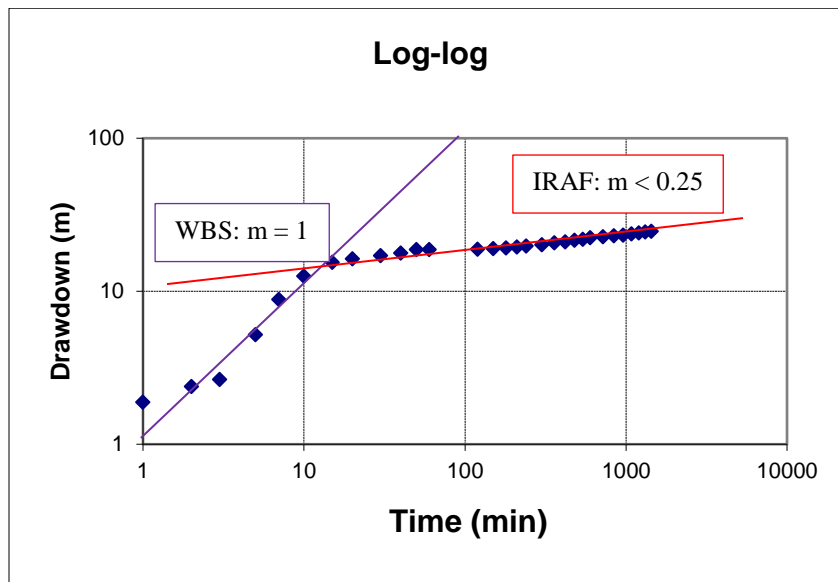


Figure 52: Log-log plot of drawdown of Habata_4 with diagnostic flow regimes.

Once well bore storage (WBS) had been abstracted (after 10 minutes), the rate of drawdown decreased to the end of test with a gradient of less than 0.25, indicating IRAF.

In the semi-log Cooper Jacob and Derivative Plot (**Figure 53**) the derivative curve clearly depicts a decrease in drawdown once WBS has been abstracted (after 10 minutes). Thereafter drawdown

decreases sharply from 40 - 120 minutes and increases sharply again to approximately 480 minutes. This indicates a possible recharge boundary. There is a subsequent increase in drawdown until 480 minutes, followed by a decrease and increase to late time. The Cooper-Jacob fit applied to late time gives an estimated T value of $27.7 \text{ m}^2/\text{day}$.

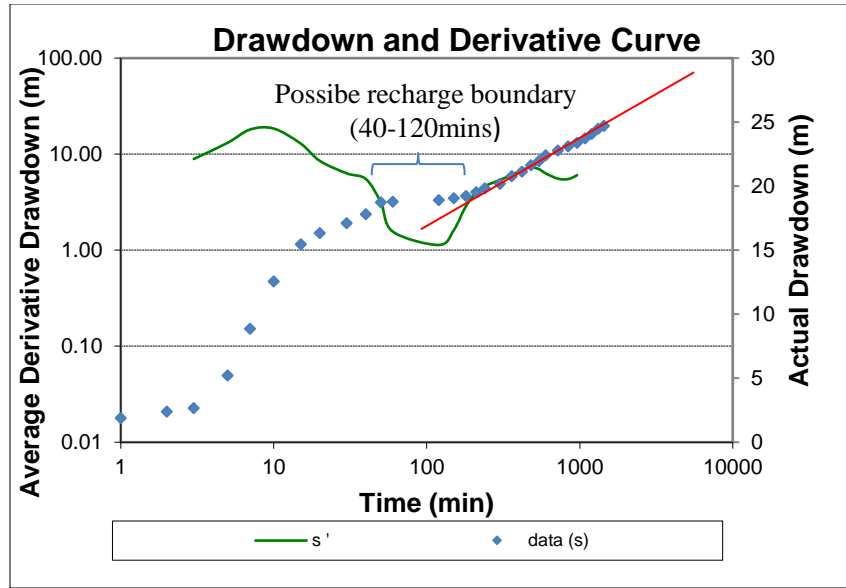


Figure 53: Derivate plot (primary axis) and drawdown plot (secondary axis) of Habata_4 with IRAF gradient fit marked with red line.

Recovery data is presented in **Figure 54** together with the fitted curve used to determine the T value using the Theis Recovery method. A transmissivity of $87.2 \text{ m}^2/\text{day}$ was estimated using the recovery data. This correlates poorly with the transmissivity value of $27.7 \text{ m}^2/\text{day}$ estimated using Cooper-Jacob for the drawdown of the late time IRAF. The T calculated from the residual drawdown is however deemed plausible as this represents natural groundwater inflow to the borehole.

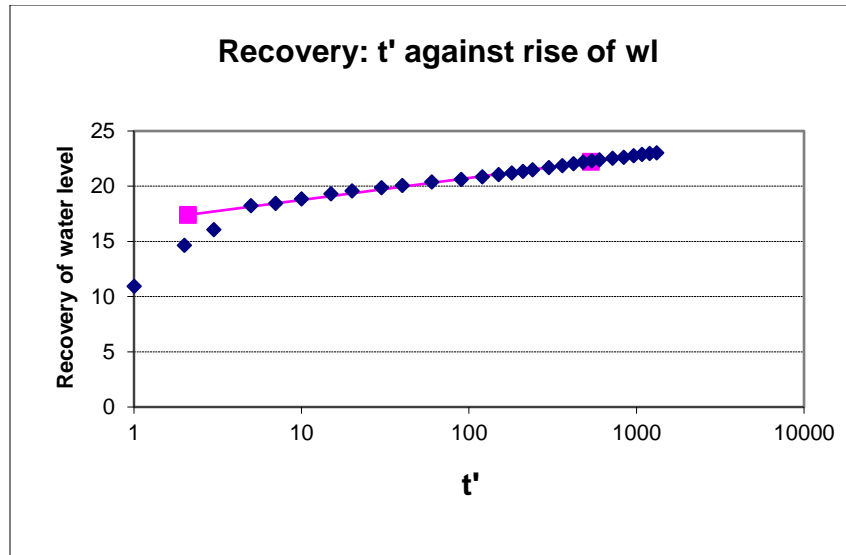


Figure 54: Recovery graph of Habata_4 applying Theis to determine Transmissivity.

5.2.10.1 Observation Boreholes and Storativity

LGC_BH1, LGC_BH3, LGC_BH2 and HBH1 were selected as observation boreholes. A drawdown of 0.09 m, 5.8 m, 1.41m and 0 m was measured in these boreholes respectively. Applying the Theis solution a storativity of 0.7×10^{-4} is estimated.

5.2.11 Habata_8

Habata_8 was drilled to a depth of 102 m, with minor water bearing fractures found at 61 m and the main water bearing fracture zone between 72 and 84 m within the sandstone of the Rietvlei Formation. The location of Habata_8 and observation boreholes included in the pumping test is given in **Figure 55**.

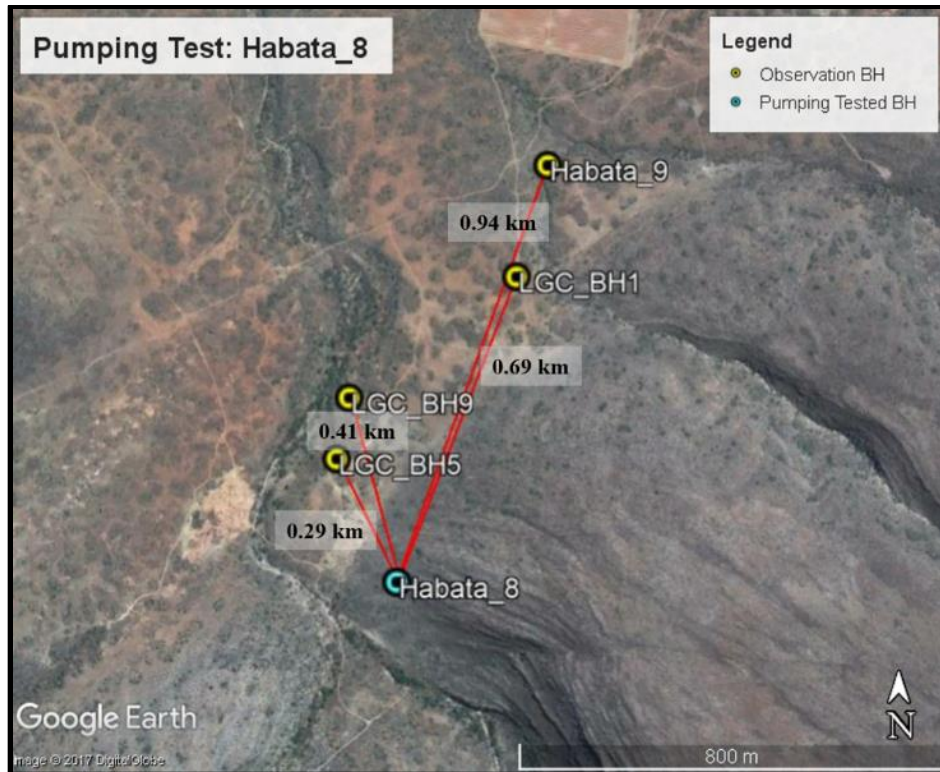


Figure 55: Pumping test at Habata_8 and distribution of observation boreholes.

5.2.12 Step Test: Habata_8

The Step Test commenced on the 1 July 2017. The rest water level (RWL) was 19.06 mbgl and the test pump was installed at 89 mbgl in the borehole with a depth measurement of 102 m. The water level was drawn down to 69.94 m below the RWL at the end of the fourth step – with water reaching pump inlet after the first 5 minutes of this final step (**Figure 56**). The water level dropped gradually during the first 3 steps, however it plummeted to pump inlet during the fourth step conducted at 13.65 L/s. An initial *T* estimate of 26 m²/day results.

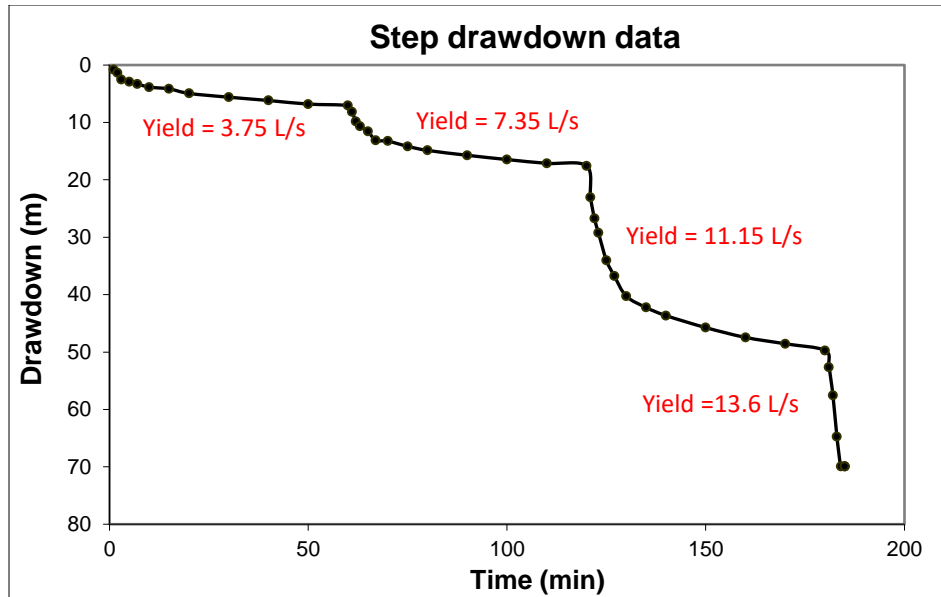


Figure 56: Step Test drawdown curve for Habata_8 borehole.

5.2.12.1 Constant Discharge Test: Habata_8

Based on the water level response to the different abstraction rates of the Step Test and positions of the water bearing fractures, the CDT was conducted at a rate of 7.32 L/s. Water level was drawn down to 33.36 m at the end of the 24 hour period. The log-log plot of the drawdown with time for the CDT is shown in **Figure 57**.

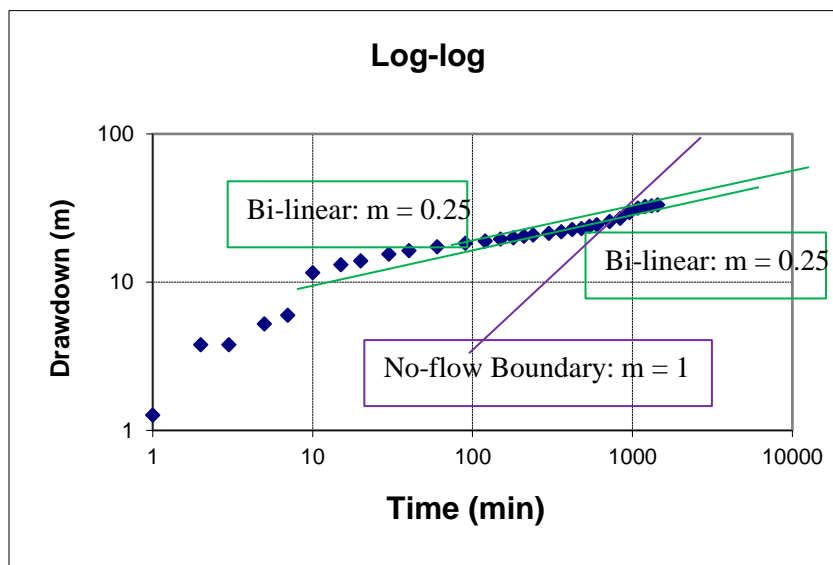


Figure 57: Log-log plot of drawdown of Habata_8 with diagnostic flow regimes.

The rate of drawdown for the first 10 minutes was erratic, and likely part of WBS. After 10 minutes, bi-linear flow took place until 600 minutes. There was then a doubling in slope and then a decrease in drawdown rate at approximately 1080 minutes, after which bi-linear flow occurred again.

In the semi-log Cooper Jacob and Derivative Plot (**Figure 58**) the derivative curve clearly depicts a doubling of slope in drawdown after a boundary is met at approximately 600 minutes. Transmissivity is estimated at 13.4 m²/day using this method with the curve matching line fitted to the middle time (10 – 600 mins) when RAF occurred.

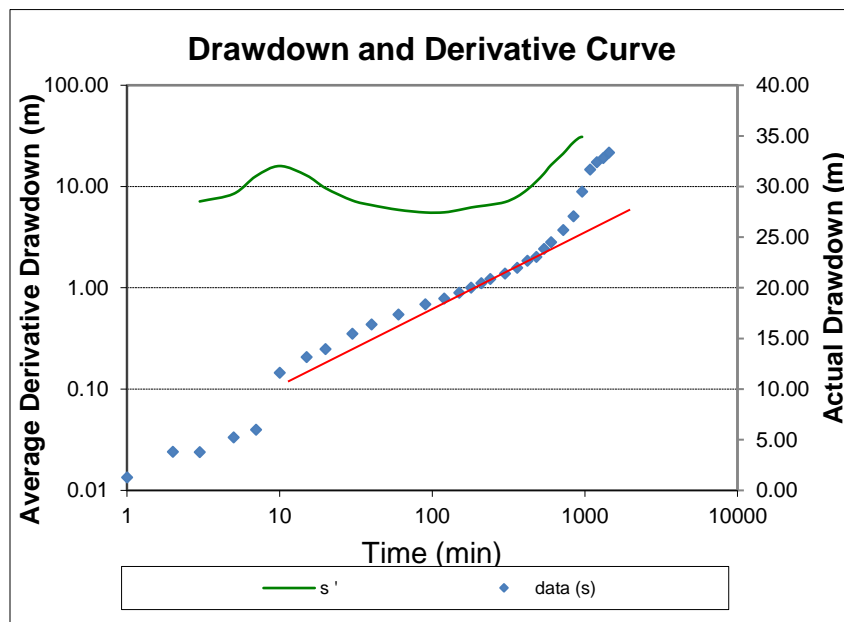


Figure 58: Derivate plot (primary axis) and drawdown plot (secondary axis) of Habata_8 with bi-linear gradient fit marked with red line.

Recovery is presented in **Figure 59** together with the fitted curve used to determine the T value using the Theis recovery method. A transmissivity of 11.1 m²/day was estimated which correlates well with the T estimated using Cooper-Jacob for the drawdown of the bi-linear flow regime.

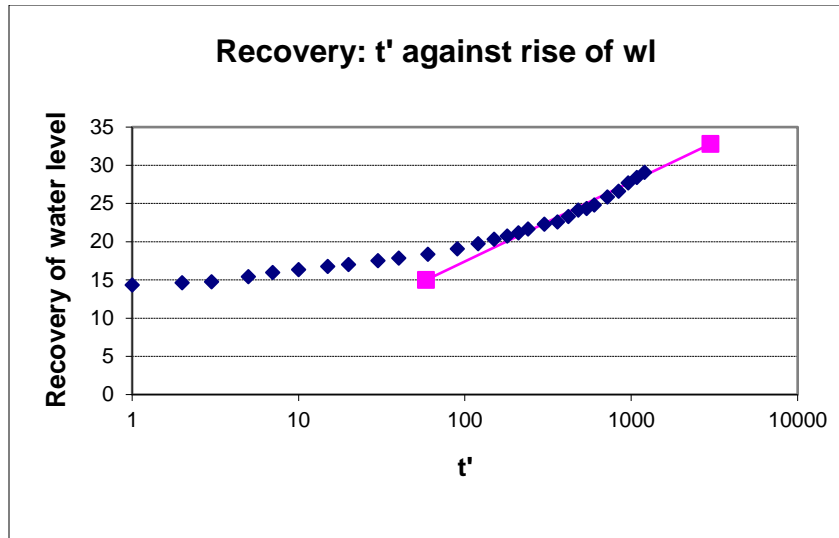


Figure 59: Recovery graph of Habata_8 applying Theis to determine Transmissivity.

5.2.12.1 Observation Boreholes and Storativity

LGC_BH5, LGC_BH9 and LGC_BH1 were selected as observation boreholes. No drawdown was measured in any of the observation boreholes, thus storativity was not estimated.

5.3 PUMPING TEST RESULTS SUMMARY

A summary of the field measurements is provided in **Table 6**. Again, it must be stated that drilling and pumping tests took place in phases - observation borehole selection was limited to boreholes completed by the time of testing. All boreholes recovered more than 75% in a minimum of eight hours, except for LGC_BH3 with 67% recovery. Drilling and pumping tests were conducted during dry season. Groundwater level monitoring of production boreholes will provide data on recharge during average rainfall seasons.

5.3.1 Connected Boreholes

Various boreholes showed degrees of connectivity, that is, drawdowns were measured in observation boreholes where abstraction was not taking place. **Table 11** provides a summary of the results of the pumping tests and observation borehole data. Drawdown was recorded in observation boreholes up to 1.48 km away from tested boreholes.

This provides evidence of extensive, well-connected fracture networks. Six of the nine boreholes drilled into the Rietvlei Formation also have radial acting flow as the dominant flow regime. The

Rietvlei aquifer has good potential for well field development, which if monitored and managed correctly, can provide an invaluable long term asset for the desired use. If boreholes are however treated independently without monitoring of water levels and application of necessary abstraction rate adjustments, such a well-connected fracture network can easily be dewatered resulting in dry boreholes and regional groundwater level lowering.

In cases where drawdowns in observation boreholes were not measured, one cannot conclude that there is no connectivity. The highly fractured system indicates that there could be connectivity if the tested boreholes were tested at higher yields over a longer period of time. This must be accounted for in well field management when selected boreholes are used for production.

Table 11: A summary of connectivity of boreholes and possible reasons for the link.

Pumping Borehole	Connected Borehole	Comments / Probable linkage
HBH1	None	Recharged solely by a fault within the northern limb of the Rietvlei Formation syncline.
LGC_BH1	LGC_BH8; LGC_BH9	Similar geology, borehole positions trend in a north east - south west direction, as does the quartz breccia.
LGC_BH2	LGC_BH3	Incurred a drawdown when LGC_BH3 was tested; but did not impact LGC_BH3 when tested – LGC_BH3 was pumped at a significantly higher rate, resulting in a greater extent of the cone of depression.
LGC_BH3	LGC_BH2; LGC_BH3A	Direct linkage, similar drill log, and location of LGC_BH3A correlates well with the primary fracture direction on surface (north west to south east).
LGC_BH5	LGC_BH4	Direct linkage, similar drill log (with LGC_BH4 having a thicker Gydo FM layer) and location of LGC_BH4 matches the primary fracture direction (north west to south east).
LGC_BH8	LGC_BH1; LGC_BH8B	Direct linkage, similar drill log and location of LGC_BH8B matches the primary fracture direction (north west to south east).
Habata_2	None	No boreholes along the primary or secondary fracture zone, no drawdown was measured in the observation boreholes. The CDT rate was the lowest (4.4 L/s) of the tests - if a higher rate over a longer time period was used drawdown is likely to have occurred in observation boreholes.
Habata_4	LGC_BH3; LGC_BH2; LGC_BH1	Same geology, close proximity of LGC_BH3 which was sited on a massive quartz breccia with a north east - south west strike and massive quartz vein intersected at 71 m in Habata_4 indicate same geological setting.
Habata_8	None	Various shades of red-brown coloured sandstone were intersected during drilling unlike observation boreholes; located on a different primary fracture.

5.3.2 Flow characteristics and aquifer Parameters

Radial flow was the prevailing flow regime of the tested boreholes, with bi-linear flow occurring in boreholes with no-flow boundaries. The Cooper-Jacob solution was fitted to these flow regimes, taking care not to fit at flow boundaries. The following points are important in characterisation of the Rietvlei Aquifer:

- The following boreholes showed similar flow characteristics, as depicted in the Cooper-Jacob semi-log plots. Radial acting flow occurred from middle to late time, with either linear or bilinear (or a combination of the two) occurring during early time. Transmissivity as estimated by the Cooper-Jacob solution ranges from 20.5 – 27.7 m²/day, with the exception of LGC_BH3 with a T of 54.8 m²/day.
 - HBH1 – 25.2 m²/day
 - LGC_BH1 – 20.5 m²/day
 - LGC_BH5 – 22.4 m²/day
 - Habata_2 – 20.8 m²/day
 - Habata_4 – 27.7 m²/day
 - LGC_BH3 – 54.8 m²/day
- The abovementioned boreholes cross the extent of the Rietvlei Formation of the plunging syncline found within the study site. An average transmissivity of 23.32 m²/day (excluding outliers such as LGC_BH3), with the dominant flow regime being radial acting, forms the basis of the fractured aquifer flow for the study area.
- LGC_BH3 and Habata_4 were drilled into similar formations and have very similar T (~83 m²/day) values indicated by Theis Recovery method. They were drilled 106 m apart. The dominant flow regime was radial acting flow during late time
- LGC_BH8 and LGC_BH2 have limited fracture networks with perpendicular flow boundaries present. Not all boreholes drilled into the fractured TMG rock will comprise of extensive, well-connected fracture networks.
- The average storativity value for the tested boreholes is 4.8×10^{-4} , which less than the conservative range of 0.01 to 1×10^{-3} for Peninsula and Nardouw Formations provided by literature. This indicates that the Rietvlei Formation has less storativity within the matrix than the fractures which have similar T ranges to that of TMG in literature.

A summary of the aquifer parameters from the pumping tests is provided in **Table 12**.

Table 12: Summary of Aquifer Parameters determined from Pumping Test Analysis.

BH ID	Dominant Flow Regime	Transmissivity (m ² /day) in FC Program		Storativity	Comments on flow characteristics
		Cooper-Jacob	Theis Recovery		
HBH1	Radial Flow	25.2	22	NMD	-Linear flow in the first 15 min, followed by bilinear flow from 15-40 min, then by IRAF to 150 minutes. Two flow boundaries are present at 180 and 420 minutes.
LGC_BH1	Radial Flow	20.5	25.3	1.4 x 10 ⁻⁴ – 3.6 x 10 ⁻⁴	-IRAF occurs from 15 – 540 min. For early time (0-15 min) a 0.5 gradient indicates bi-linear flow. Minor flow boundary at 720 mins.
LGC_BH2	Linear flow of limited fracture extent	41.3	38.7	NMD	-Bilinear flow at early time (0-180 min), then fracture dewatering to give a quadrupling of slope in semi log plot, representing two perpendicular no-flow boundaries. Near horizontal gradient of late time recovery in Theis plot also indicates dewatering.
LGC_BH3	Radial Flow	54.8	83.6	7.2 x 10 ⁻⁴	-Very large fracture, high yielding borehole (30 L/s), highly transmissive. Flow regime is bi-linear throughout the test.
LGC_BH5	Radial Flow	22.4	24.6	1.5 x 10 ⁻³	-IRAF occurs from 15 minutes to end of test. For early time (0-10 min) a 0.5 gradient indicates linear flow.
LGC_BH8	Bilinear - linear flow	4.1	25.4	0.9 x 10 ⁻⁴	-Initial slope of 0.5 from 0-90 m indicating linear flow. A doubling of the slope occurs at 90 min, indicating a no-flow boundary is met. A quadrupling of the slope at 420 min indicates another no-flow boundary is met.
Habata_2	Radial Flow	20.8	22.6	NMD	-Initial slope (0 – 120 m) of 0.5 indicating linear flow (fracture only) and then IRAF from 120 - end of test.
Habata_4	Radial Flow	27.7	87.2	0.7 x 10 ⁻⁴	-A slope of 1 occurs between 3-15 min indicating WBS. Thereafter m < 0.25 to end of test indicating IRAF. Flow boundaries are present, however not clearly defined as flow regime remains IRAF.
Habata_8	Bilinear Flow	15.7	17	NMD	-Good recovery. Bilinear flow from 0-480 min with a slope of 0.25 in semi-log graph. A doubling of the slope occurs after 480 mins indicating a no-flow boundary.

NMD = No measured drawdown in observation borehole; IRAF = Infinite radial acting flow; min = minute/s

5.4 ASSESSMENT OF HYDROGEOCHEMISTRY AND GROUNDWATER QUALITY FOR IRRIGATION

A statistical summary of the laboratory results is presented in **Table 13**. This provides a statistical spread of the chemical data used to interpret the hydrogeochemical processes taking place in the study area.

Table 13: Descriptive statistics of laboratory results for the nine boreholes.

	pH	EC (mS/m)	mg/L									
			TDS	Ca ²⁺	Mg ²⁺	Na ⁺	K ⁺	Cl ⁻	SO ₄ ²⁻	HCO ₃ ⁻	Mn	Fe
Mean	6.1	90.5	562.8	25.8	20.4	103.0	13.7	202.7	92.3	51.5	1.9	4.7
Standard Error	0.1	20.6	131.1	4.7	5.0	28.4	2.1	53.9	29.9	7.7	0.7	3.5
Median	6.2	90.6	541.0	29.5	21.4	93.0	15.5	239.0	61.0	52.4	1.4	0.3
Standard Deviation	0.4	61.8	393.2	14.1	15.1	85.2	6.2	161.6	89.6	23.1	2.0	10.5
Sample Variance	0.2	3819.8	154643.9	199.2	227.2	7251.8	38.9	26125.4	8035.5	535.8	4.2	110.7
Minimum	5.3	13.8	88.0	8.1	3.3	8.8	5.6	15.0	5.0	5.7	0.1	0.2
Maximum	6.7	207.4	1327.0	43.3	47.0	255.3	25.8	480.0	288.0	92.9	6.8	32.4

The groundwater chemistry results are given in **Table 14**. The results have been classified according to electrical conductivity (EC), in ascending order. The increase in abundance of major ions (Ca²⁺, Mg²⁺, Na⁺, K⁺, SO₄²⁻, Cl⁻, and HCO₃⁻) links directly to increasing EC.

Table 14: Groundwater chemistry results, classified according to electrical conductivity (represented by orange bar, in ascending order).

BH ID	pH	EC mS/m	TDS mg/l	Ca mg/l	Mg mg/l	Na mg/l	K mg/l	Cl mg/l	SO4 mg/l	HCO3 mg/l	Mn (mg/L)	Fe mg/l
HBH01	6.2	13.8	88	8.3	3.3	8.8	5.6	15	5	48	0.58	0.2
Habata_8	5.8	22.9	146	8.1	3.7	16.7	8.2	40	33	36	2.22	0.4
LGC_BH1	6.6	44.3	265	16.1	8.5	50.9	8.8	70.5	32	62.8	1.24	0.26
LGC_BH5	6.7	69	413	15.9	11.5	52.8	9.6	80.6	21	52.4	1.36	0.29
LGC_BH3	6.2	90.6	541	40.6	21.9	93	15.5	239	61	49.3	0.13	0.18
Habata_4	5.8	99.3	636	29.5	21.4	101.8	15.9	262	136	56	0.11	0.3
LGC_BH2	6.3	129.6	830	43.3	32.8	134.9	16.3	263	147	60	2.9	4.3
LGC_BH8	6.4	137.8	819	30	33.1	213.2	17.3	374.6	108	92.9	1.6	4.38
Habata_2	5.3	207.4	1327	40.8	47	255.3	25.8	480	288	5.74	6.76	32.4

5.4.1 Hydrochemical facies

A Piper diagram has been used to classify the groundwater types. The Piper diagram also indicates the hydrogeochemical processes potentially responsible for the evolution of groundwater quality within the Rietvlei Formation. The samples plotted on the Piper diagram (**Figure 60**) clearly show the different hydrochemical facies. The following points describe the classes of groundwater:

- **Type 1:** HBH1 is a Na – HCO₃⁻ type groundwater. This groundwater likely evolved from Ca/Mg- HCO₃⁻ and became sodium enriched through ion exchange along its flow path. The low salinity (EC = 13.8 mS/m) indicates fresher recharge in comparison to the rest of the groundwater samples.
- **Type 2:** The remaining samples are Na – Cl type groundwater. These samples plot close to a typical sea water sample as shown in **Figure 6**. This is typical of marine derived or ancient groundwater, however the salinities are low in comparison. Groundwater is likely undergoing salinisation along its south-west to north-east flow path. There are two distinct groups within Type 2:
 - **Type 2a:** Habata_8, LGC_BH1 and LGC_BH5 with EC values of 22.9 mS/m, 44.3 mS/m and 69 mS/m respectively
 - **Type 2b:** LGC_BH3, Habata_4, LGC_BH2, LGC_BH8, and Habata_2 with EC values of 90.6 mS/m, 99.3 mS/m, 129 mS/m, 137 mS/m, and 207 mS/m respectively.

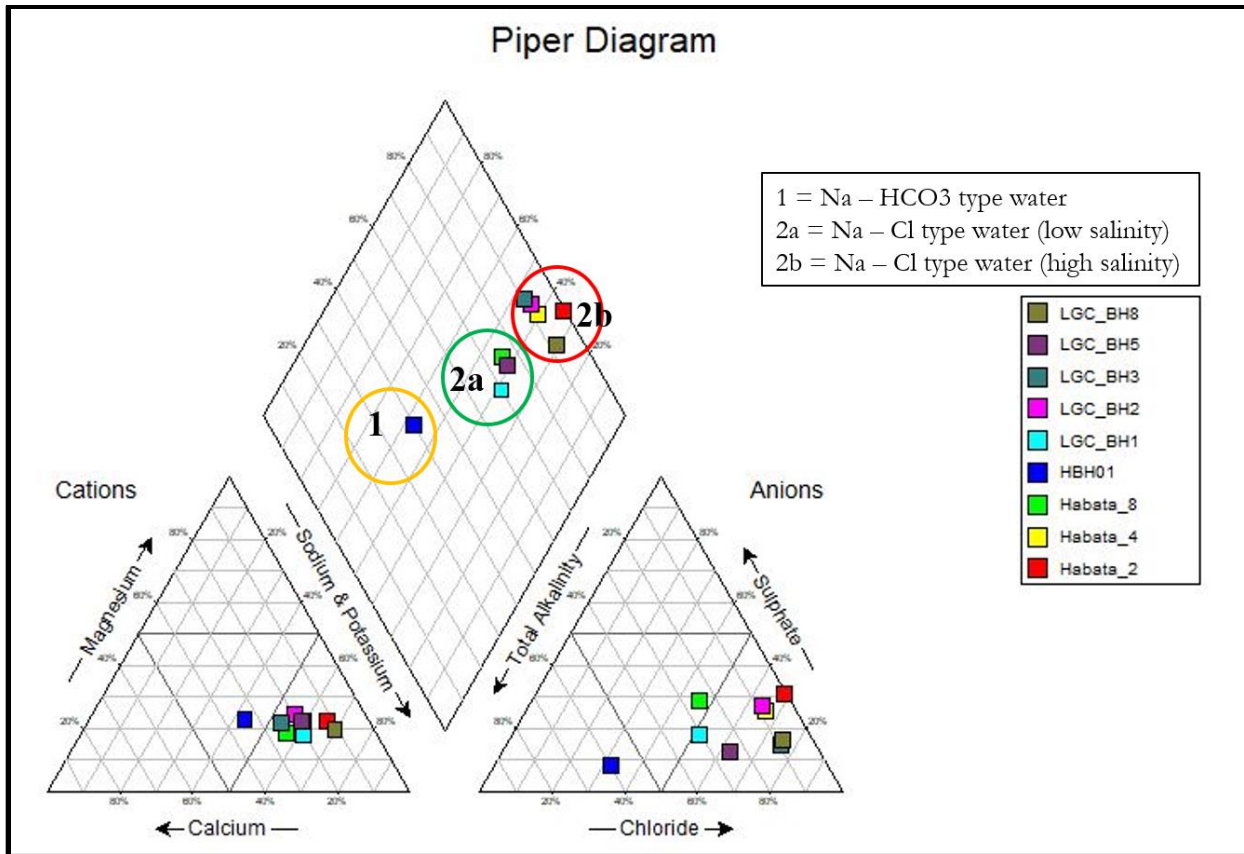


Figure 60: Piper diagram indicating groundwater types.

Stiff diagrams of the samples on the same scale axes are presented in **Figure 61**. The same scale axis allows a direct comparison of the salinity of the groundwater types to be made. It is clear here that the shape of Habata_2, Habata_4, LGC_BH2, LGC_BH3 and to a lesser extent LGC_BH5 have a similar signature – corresponding with Type 2 groundwaters classed according to the Piper diagram.

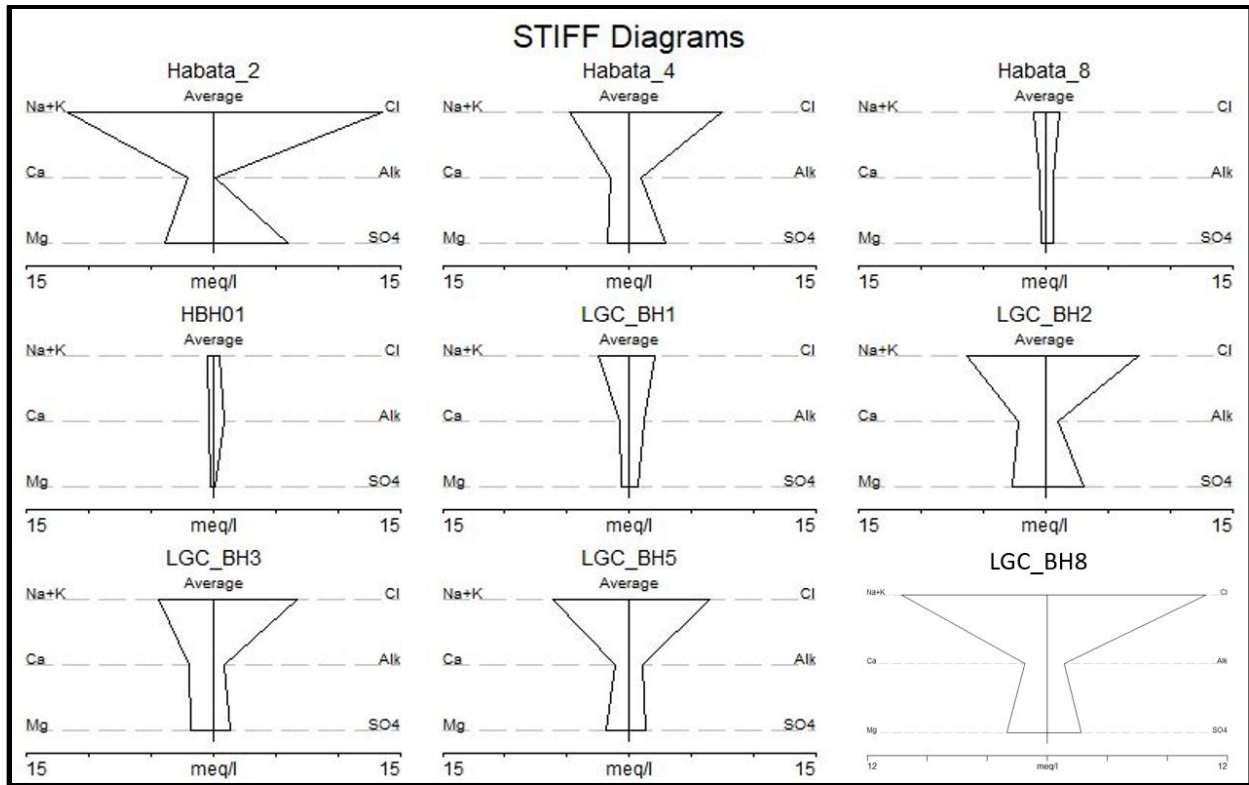


Figure 61: Stiff diagrams of the sampled boreholes, normalised to the same axis to gain a perspective on the relative salinity.

The stiff diagrams have been plotted on a geological map (**Figure 62**). It now becomes apparent that there is a correlation between groundwater type and spatial distribution of groundwater. Boreholes in close proximity to the Bokkeveld Formation have higher salinities. Salinity also increases with increasing distance from the mountainous areas to the south west of the site where recharge occurs.

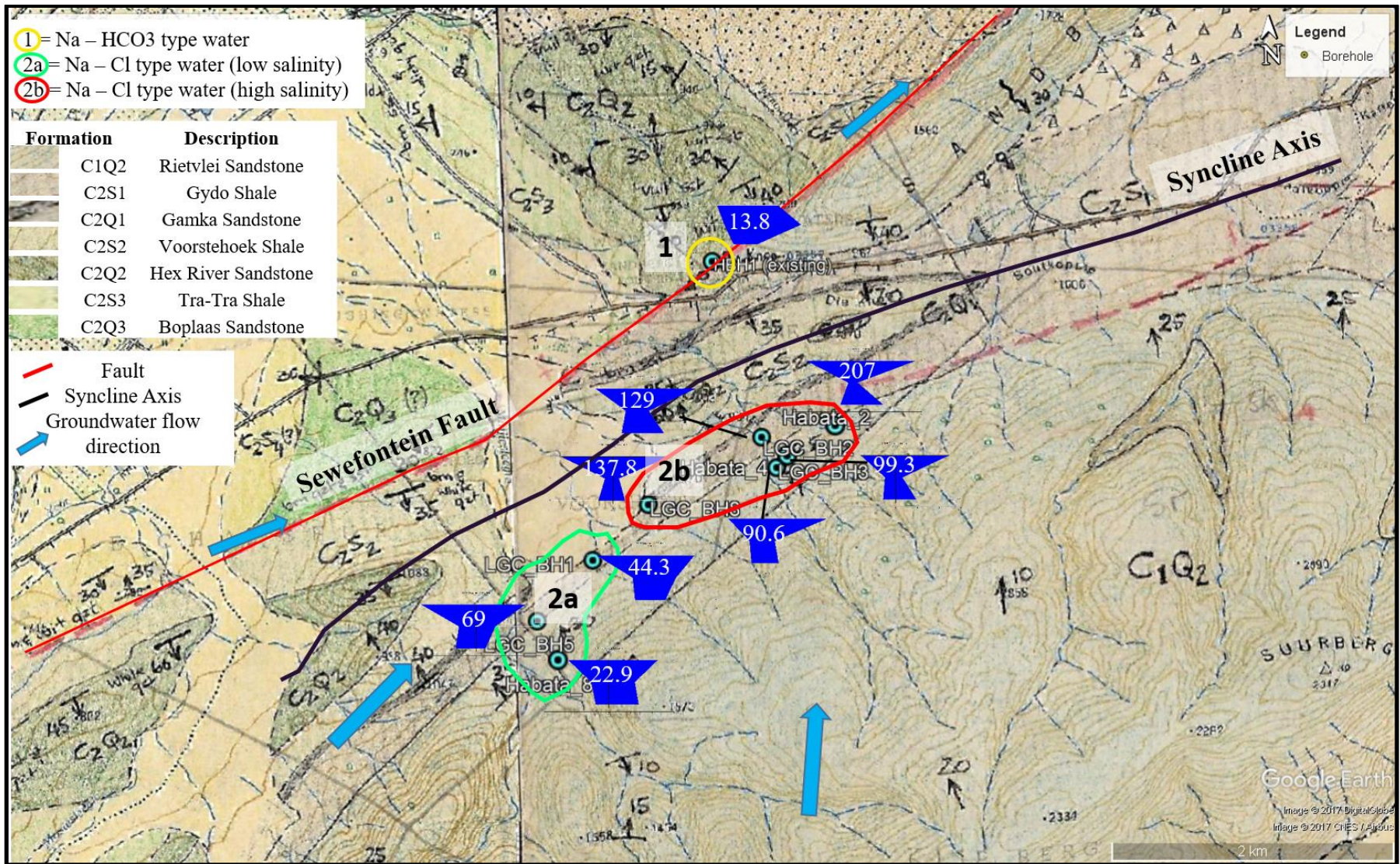


Figure 62: Geological map with stiff diagrams and groundwater types (marked with colour polygons), as well as groundwater flow direction. Salinity as a measure of EC (mS/m) is plotted on the respective stiff diagram.

5.4.2 Hydrogeochemical processes

5.4.2.1 Correlation analysis

Pearson's correlation matrices were used to determine the relationships between different chemical parameters (**Table 15**). Correlations of low negative (>-0.5) and low positive (<0.5) are considered to have minor significance and have thus been removed. It can clearly be seen that all major elements are strongly correlated with each other. This suggests that groundwater sampled from the boreholes in the Rietvlei Formation are undergoing similar hydrogeochemical processes. Manganese (Mn), iron (Fe) and sulphate (SO_4) on the other hand have negative correlations with pH indicating an inverse relationship. Fe, Mn and SO_4 are more readily soluble in the slightly acidic groundwaters typical of TMG sandstones.

Table 15: Pearson's correlation matrix of pH, EC (mS/m), TDS and major ions (mg/L).

	pH	EC mS/ m	TDS mg/l	Ca mg/l	Mg mg/l	Na mg/l	K mg/l	Cl mg/l	SO ₄ mg/l	HCO ₃ mg/l	Mn (mg/L)	Fe mg/l
pH	1											
EC mS/m		1										
TDS mg/l		0.99	1									
Ca mg/l		0.84	0.83	1								
Mg mg/l		0.99	0.98	0.87	1							
Na mg/l		0.96	0.95	0.76	0.96	1						
K mg/l	0.57	0.97	0.97	0.85	0.97	0.94	1					
Cl mg/l	0.3	0.97	0.96	0.84	0.97	0.97	0.97	1				
SO ₄ mg/l	0.69	0.92	0.94	0.74	0.91	0.87	0.94	0.90	1			
HCO ₃ mg/l	0.72									1		
Mn (mg/L)	0.59	0.69	0.71		0.66	0.65	0.66	0.57	0.78	-	1	
Fe mg/l	0.68	0.78	0.80		0.75	0.76	0.79	0.72	0.87	-	0.928	1

Correlational analysis work hand in hand with stoichiometric analysis and bivariate (X-Y) plots to try and identify or explain the main hydrogeochemical processes responsible for the evolution of the groundwater chemistry. A comparison of various major ions was conducted to provide possible processes responsible for groundwater chemistry, specifically ion-exchange.

5.4.2.2 Sodium against Chloride

A plot of sodium against chloride (meq/L) from water samples provides a linear relationship. If meteoric water is the source of Na^+ in groundwater, then the sample will plot on the 1:1 evaporation line (Gomo et al. 2013). A deviation from 1:1 line indicates that processes other than concentration or dilution are responsible for the sodium/chloride concentration (Neal and Kirchner 2000). When sodium concentrations are low, ion exchange reactions buffer the sodium concentration relative to chloride by releasing sodium into the groundwater from cation exchange sites. When sodium concentration is high in groundwater, adsorption onto ion exchange sites takes place. The concentration of chlorine relative to sodium thus provides an indication of which process took place (Neal and Kirchner 2000).

Figure 63 provides the relationship of chloride vs sodium in meq/L. The samples from HBH1 (Type 1), LGC_BH1, LGC_BH5, and Habata 8 (Type 2a), plot very close to the 1:1 line. The remaining samples (Type 2b) plot below the line. This indicates that groundwater from these boreholes has undergone sodium adsorption.

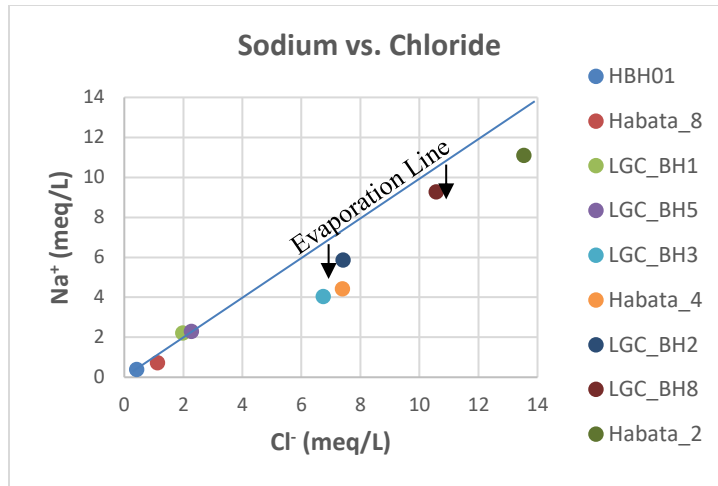


Figure 63: Bivariate plot of Na⁺ against Cl⁻ for the study site. Arrows are used to indicate the ion-exchange processes when samples deviate from the 1:1 line.

5.4.2.3 Calcium and magnesium against Sulphate and Bicarbonate ions

According to Guler et al (2002) a plot of Ca²⁺ + Mg²⁺ against SO₄²⁻ + HCO₃⁻ will result in a straight line of 1:1 if dissolution of dolomite (or gypsum) and calcite are the dominant reactions in groundwater. Samples plot below the 1:1 line (**Figure 64**) indicating that ion exchange is taking place (Fisher and Mulican 1997). The shift of sample plots indicates a decrease of Ca²⁺ + Mg²⁺ cations as they exit the groundwater to occupy open cation exchange sites (Gomo et al. 2013).

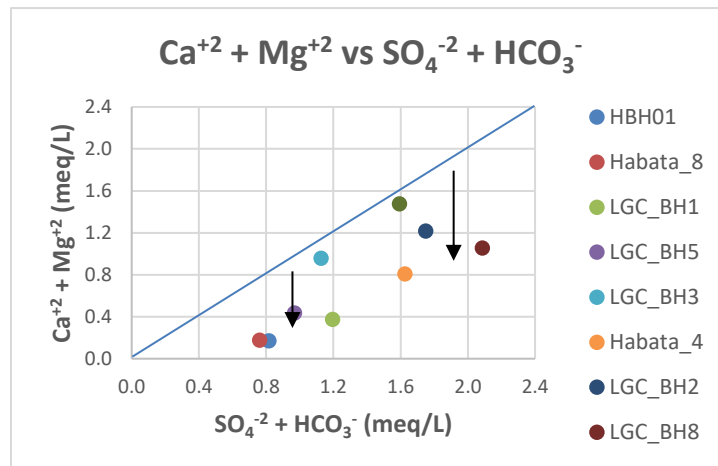


Figure 64: Bivariate plot of Ca²⁺ + Mg²⁺ against SO₄²⁻ + HCO₃⁻. Arrows emphasise the ion-exchange resulting in samples plotting off the 1:1 line.

5.4.2.4 Analysis of saturation indices

Analysis of the saturation indices of the most common mineral phases (as provided in the Phreeqc data base) indicate that groundwater is under saturated with respect to carbonate (calcite, dolomite and aragonite) and sulphate (gypsum and anhydrite) minerals – that is dissolution of these minerals will take preference over precipitation when the groundwater comes into contact with the host rock. Notably Halite (NaCl) is undersaturated, and if present, will dissolve in the aquifer. Manganese based minerals are also undersaturated, specifically Hausmannite and Manganite. The Rietvlei aquifer is greatly oversaturated with iron mineral phases Goethite, Hematite and Fe(OH)₃, they will thus precipitate (typically under oxidizing conditions). The SI indices for the common minerals within the study area are given in **Table 16**.

Table 16: Saturation Indices for the 9 borehole samples

BH ID	pH	SI _{Goethite}	SI _{Hematite}	SI _{Hausmannite}	SI _{Manganite}	SI _{Halite}
HBH01	6.2	5.02	12.06	-18.68	-7.82	-8.4
LGC_BH1	6.6	6.26	14.52	-14.7	-6.36	-6.99
LGC_BH2	6.3	6.5	15.01	-16.26	-6.98	-6.04
LGC_BH3	6.2	4.87	11.74	-20.97	-8.59	-6.23
LGC_BH5	6.7	6.6	15.22	-13.75	-6.01	-6.92
LGC_BH8	6.4	6.8	15.61	-16.25	-6.95	-5.69
Habata_2	5.3	4.34	10.69	-23.29	-9.66	-5.52
Habata_4	5.8	3.86	9.73	-24.48	-9.89	-6.15
Habata_8	5.8	4.1	10.21	-20.21	-8.47	-7.71

5.4.3 Assessment of irrigation groundwater quality

The classifications used for the assessment of groundwater quality for irrigation relate to the irrigation water – it must be borne in mind that soil and plant properties also need to be taken into consideration to determine overall suitability and long term effects. The classifications and results are discussed briefly below, with the collective results summarized in **Table 22** at the end of the section.

5.4.3.1 SAR and EC

According to Richards (1954), groundwater with SAR values less than 10 are excellent, 10 – 18 is good, 18 – 26 is fair, and greater than 26 is unsuitable for irrigation. All sampled boreholes have SAR values less 10, with a range of 0.7 – 6.4, and are thus considered excellent for irrigation. A combination of the salinity as a measure of EC, and SAR have been plotted on a Wilcox Diagram (**Figure 65**). The diagram shows that the groundwater ranges from low salinity and low sodium (classed as C1S1) for HBH1 and Habata_8, to high salinity and medium sodium (classed as C3S2) for LGC_BH8 and Habata_2. These can be used in almost all soil types with minimum potential sodium exchange (Kumar et al, 2007) – ideally, the soils irrigated with the C3S2 type water will be well drained (Mohan et al, 2000).

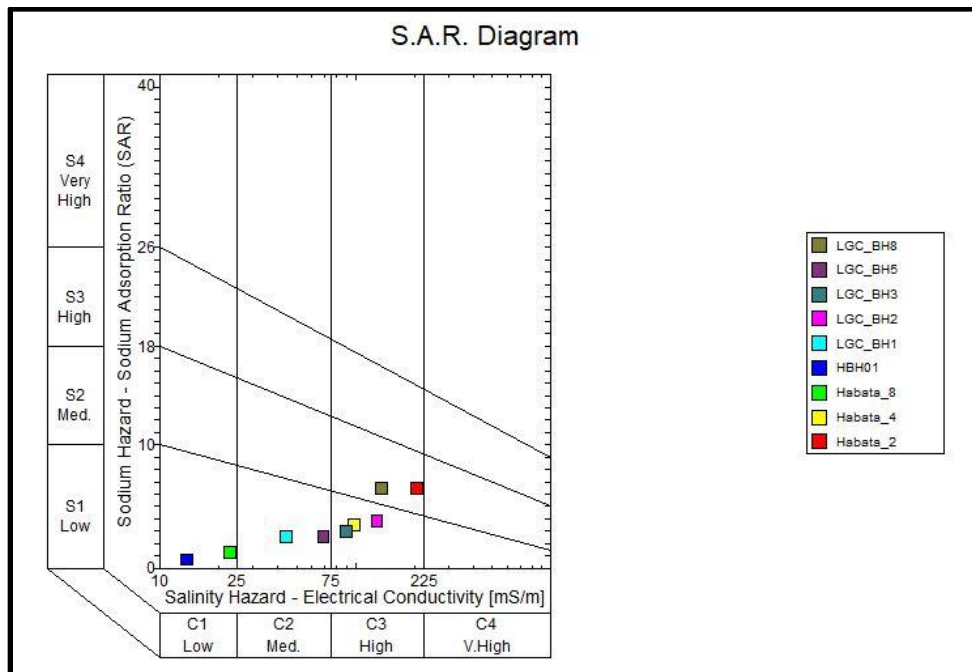


Figure 65: Wilcox diagram of groundwater for irrigation.

5.4.3.2 Total Hardness (TH)

Hardness provides an indication of mixing ability of irrigation water. 33% of groundwater samples have a TH of <75 and are thus considered soft, 11% are within the 75 – 150 classification and are considered moderately hard, while the remaining 56% have a hardness value of 150 – 300 and are thus considered hard. LGC_BH8, LGC_BH2 and Habata_2 should initially be avoided for irrigation, and the method of irrigation should be designed to minimise scaling and the resultant blockage of outlets. TH values are provided in **Table 17**.

Table 17: Total hardness values of groundwater samples in ascending order from left to right.

BH ID	HBH 1	Habata_8	LGC_B H1	LGC_B H5	Habata_4	LGC_B H3	LGC_B H8	LGC_B H2	Habata_2
TH	34.3	35.4	75.1	87.0	161.6	191.4	211.0	243.0	295.1

5.4.3.3 Sodium Percentage

The sodium percentage varies from 7.9% to 31.6% with 56% of the boreholes being in the excellent category, and 44% being classed as good for irrigation. Sodium percentages are provided in **Table 18**.

Table 18: Sodium percentages of groundwater samples in ascending order from left to right.

BH ID	HBH0 1	Habata_8	LGC_B H5	LGC_B H3	LGC_B H1	Habata_4	LGC_B H2	Habata_2	LGC_B H8
Na %	7.9	9.7	18.6	19.0	19.5	20.5	23.3	27.5	31.6

5.4.3.4 Kelly's Ratio (KR)

Kelly's Ratio is also a sodium based classification. Only HBH1 had a KR value less than 1 and are thus considered suitable for irrigation. Habata_8 has a KR value of 1 and is thus considered acceptable, whereas the rest of the boreholes had KR values ranging from 1.1 – 2.2, and are therefore considered unsuitable according to Kelly's Ratio (1963). Mixing of groundwater is recommended, while avoiding Habata_2 and LGC_BH8 is also advised. Again, well drained soils

are better suited to avoid negative effects of elevated sodium levels. Kelly's ratio values are provided in **Table 19**.

Table 19: Kelly's ratio values for groundwater samples in ascending order from left to right.

BH ID	HBH 1	Habata _8	LGC_B H3	LGC_B H2	LGC_B H5	Habata _4	LGC_B H1	Habata _2	LGC_B H8
Kelly's Ratio	0.6	1.0	1.1	1.2	1.3	1.4	1.5	1.9	2.2

5.4.3.5 Magnesium Hazard (MH)

Magnesium Hazard classification depends on the alkali earth ions Ca^{2+} and Mg^{2+} which are generally at equilibrium in most groundwater (Hem 1985, cited in Houatmia 2016). Elevated Mg^{2+} can promote soil alkalinity which lowers crop yields (Kumar et al., 2007). Water with MH values less than 50 are considered suitable and MH values above 50 are considered unsuitable for irrigation. 44% of the groundwater samples had MH values less than 50. The remaining 56% are considered unsuitable for irrigation according to the Magnesium hazard rating (**Table 20**).

Table 20: Magnesium hazard rating for groundwater samples in ascending order from left to right.

BH ID	HBH 01	Habata _8	LGC_B H1	LGC_B H3	LGC_B H5	Habata _4	LGC_B H2	LGC_B H8	Habata _2
Mg Hazard	40	43	47	47	54	54	56	65	65

5.4.3.6 Permeability Index (PI)

The PI is used to determine soil permeability affected by long-term irrigation. PI values for this study range from 62.8 - 118.9. No groundwater samples fall within the safe category (<25) while 44% are considered to have a moderate PI classification, and the remaining 56% are classed as unsafe. The PI for the groundwater samples is provided in **Table 21**. Regular soil sampling (at least annually) should be conducted and analysed to determine if soil is losing permeability.

Table 21: Permeability index rating of groundwater samples in ascending order from left to right.

BH ID	LGC_B H3	LGC_B H2	Habata _2	Habata _4	LGC_B H8	LGC_B H5	LGC_B H1	Habata _8	HBH0 1
PI	62.8	64.0	66.4	70.3	77.9	79.9	86.9	104.2	118.9

5.5 SUMMARY

There are two processes taking place that determine groundwater quality within the study area; 1) mineralization along the flow path and 2) ion exchange. Distance from the recharge source allows more time for these processes to progress, and thus result in groundwaters of higher salinity. The low pH is also a parameter that dissolves iron and manganese from the Rietvlei Formation which were elevated in groundwater samples. Two distinct groups - Type 1 and Type 2 - the latter of which comprises two subgroups are present.

Type 1

HBH1 is a Na – HCO₃⁻ type groundwater. This groundwater likely evolved from Ca/Mg- HCO₃⁻ and became sodium enriched through ion exchange along its flow path. The low salinity (EC = 13.8 mS/m) indicates fresher recharge in comparison to the rest of the groundwater samples.

Type 2a

Boreholes LGC_BH1, LGC_5 and Habata_8 are Na-Cl type waters, with relatively low salinity. They are located in the south western corner of the study area (closer to the recharge source) and are drilled further away from the Bokkeveld Formation. These boreholes also ranked favourably for irrigation classifications.

Type 2b

Boreholes LGC_BH2, LGC_BH3, LGC_BH8, Habata_2 and Habata_4 also classify as Na-Cl water type, however have an elevated salinity in comparison to Type 2a. Group 2b is further from the recharge source, and thus undergoes more ion exchange and mineral dissolution as the groundwater flow path is longer.

Classification of groundwater for irrigation according to the different methods is summarized in **Table 22**. Overall, the potential for using as groundwater is considered good. Boreholes which yield the best quality groundwater water in order from most suitable to least suitable are as follows:

1. HBH1 (Group 1)
2. Habata_8 (Group 2a)
3. LGC_BH1 (Group 2a)
4. LGC_BH5 (Group 2a)
5. LGC_BH3 (Group 2b)
6. Habata_4 (Group 2b)
7. LGC_BH8 (Group 2b)
8. Habata_2 (Group 2b)

Recommendations for the initial stages of irrigation with groundwater are as follows:

- Soils should be sampled and tested annually to determine if irrigation water is lowering permeability of soil.
- Habata_4, LGC_BH8 and Habata_2 did perform less favourably in the irrigation classifications. They are also lower yielding boreholes, and are thus considered suitable for aquifer monitoring and not as primary production boreholes.
- Leaching should be applied on a regular basis, where the best quality available irrigation water is used to flush out the accumulated salts from the root zone. The volume used during flushing must be in excess of the volume of water required by the crop.
- Gypsum should be applied to maintain, or increase calcium and magnesium content in soil, promoting a granular and permeable texture.
- Mixing of better quality groundwater with poorer quality groundwater can also be applied to reach volume demands in peak season. The mixing ratios should be modelled to obtain the best possible quality, and samples should be sent to an accredited laboratory to determine irrigation suitability.

Table 22: Classification of groundwater suitability for irrigation.

Parameter	Range	Classification	Borehole ID
EC (mS/m)	<25	Excellent	HBH1; Habata_8
	25-75	Good	LGC_BH1; LGC_BH5
	75-200	Permissible	LGC_BH2; LGC_BH3; LGC_BH8; Habata_4
	200-300	Doubtful	Habata_2
Na%	<20	Excellent	HBH1; LGC_BH1; Habata_8; LGC_BH3; LGC_BH5
	20-40	Good	LGC_BH2; LGC_BH8; Habata_4
	40-60	Permissible	0
	60-80	Doubtful	0
	>80	Unsuitable	0
MH	<50	Suitable	HBH1; LGC_BH1; Habata_8; LGC_BH3;
	>50	Unsuitable	LGC_BH2; LGC_BH5; LGC_BH8; Habata_2; Habata_4
TH	<75	Soft	HBH1; LGC_BH1; Habata_8
	75-150	Moderately Hard	LGC_BH5
	150-300	Hard	LGC_BH2; LGC_BH3; LGC_BH8; Habata_2; Habata_4
	>300	Very Hard	0
SAR	<10	Excellent	HBH1; LGC_BH1; LGC_BH2; LGC_BH3; LGC_BH5; LGC_BH8; Habata_2; Habata_4; Habata_8
	10-18	Good	0
	18-26	Fair	0
	>26	Unsuitable	0
KR	<1	Suitable	HBH1
	>1	Unsuitable	LGC_BH1; LGC_BH2; LGC_BH3; LGC_BH5; LGC_BH8; Habata_2; Habata_4; Habata_8
PI	<25	Safe	0
	25-75	Moderate	LGC_BH2; LGC_BH3; Habata_2; Habata_4;
	>75	Unsafe	HBH1; LGC_BH1; LGC_BH5; LGC_BH8; Habata_8

CHAPTER 6: CONCLUSION AND RECOMMENDATIONS

6.1 CONCLUSIONS

The Rietvlei Formation is not the most favourable target when other units of the TMG are available for groundwater development. In this study area the Rietvlei Formation has undergone extensive folding and fracturing, resulting in well-connected fracture networks. Pumping test data indicate that connectivity can occur over as much as 1.48 km, and the dominant flow regime is radial acting flow. The aquifer has potential to be developed as a well field, and with long term monitoring, can be managed in a sustainable manner. Groundwater quality varies throughout the site, with the best quality groundwater sourced from an already existing borehole, located in the Sewefontein Fault. The boreholes drilled in the Klipberg Mountain have quality which improves away from the synclinal axis, towards the mountainous areas from which recharge occurs. NaCl enriched groundwater is attributed to ion exchange and mineralization occurring within longer flow paths. Increasing ion exchange occurs closer to the hinge of the syncline, where fracture networks cross cut arenaceous TMG and the argillaceous BVG. The main findings are briefly presented in the following subsections.

6.1.1 Groundwater Exploration

Conducting geophysics over the rugged terrain of the TMG is challenging and can prove costly. The value of a good conceptual understanding of the hydrogeological setting cannot be over emphasised. Geophysics can be used during the initial phases of an exploration project – after selection of areas of interest – to correlate targets for geological survey. Satellite imagery and geological field mapping save on time and allow significantly larger areas to be covered. Borehole logs should be compared to expected conditions and drill targets should be revised if necessary. Drill logs provide actual subsurface conditions and the conceptual model should be updated accordingly.

Boreholes drilled closer to the synclinal axis intersected massive water bearing fractures with drill chips of up to 14 cm in comparison with fractures in distal boreholes (~6 cm drill chips). Transmissivity is higher and water quality poorer in the boreholes closer to the synclinal axis. This indicates that fracture networks closer to the synclinal hinge are more extensive, and likely cross cut the TMG and adjacent BVG. The argillaceous, fractured Gydo Formation, likely contributes salinity to the slightly acidic Rietvlei groundwater.

6.1.2 Groundwater Flow Characteristics and Aquifer Parameters

The Rietvlei Formation is often overlooked when older TMG Formations are present. The folding and faulting post deposition in most cases causes fractures to propagate through the various TMG Formations. Large scale, well connected fracture networks develop, in this case with connected boreholes up to 1.48 km apart. The 24 hour Pumping Tests, recovery test data and observation boreholes provided a large sample set for analysing the Rietvlei aquifer characteristics. The high transmissivity (23.32 m²/day) of the Rietvlei aquifer indicates that it has the potential to be used as a wellfield. The relatively low storativity (4.8 x 10⁻⁴) highlights the necessity of careful planning and management to ensure longevity of the resource. It is expected that higher pumping rates over longer time periods will result in drawdown occurring at greater distances from the pumped borehole.

A limitation when interpreting pumping tests is that the analytical solutions are all applicable to confined aquifers (Van Tonder et al. 2002). This is not the case for TMG aquifers which are semi-confined to unconfined.

6.1.3 Hydrogeochemical Processes and Groundwater Quality

There are two processes taking place that determine groundwater quality within the study area; 1) mineralization along the flow path and 2) ion exchange. Distance from the recharge source allows more time for these processes to progress, and thus result in groundwaters of higher salinity. The acidic groundwater dissolves iron and manganese from the Rietvlei Formation which were elevated in groundwater samples. Two distinct groups are present.

The groundwater quality of the only existing borehole, HBH1, is unique in comparison to boreholes drilled into the Klipberg Mountain. It was drilled into the Sewefontein Fault. Included as an observation borehole in most of the pumping tests, HBH1 showed no connectivity to boreholes drilled into the syncline. This was confirmed with analysis of the groundwater signature using simple graphical methods namely Piper and Stiff diagrams. Groundwater within the fault is Na - HCO₃⁻ type water (Type 1), while that of the Rietvlei Formation is Na-Cl type water (Type 2), and is more saline than HBH1.

Further value is added to the graphical methods used to classify water types when overlain on geological maps. In this case the salinity of groundwater increases towards the fold axis of the plunging syncline, where the greatest amount of fracturing has occurred. The notable increase in salinity according to geological formation indicates two subgroups of Type 2 water, based on salinity.

Groundwater suitability for irrigation can be classified according to various parameters. According to some classifications, all boreholes included in this study provide suitable irrigation water, while

other classifications deem all boreholes unsuitable. There are however other variables involved in determining the final crop yield, specifically soil properties and crop tolerance to saline water. The good quality groundwater of the Rietvlei Formation (average salinity of 90 mS/m) and high blow yields (15000 L/hr to > 80 000 L/hr) do however support Greef (1990) and Kirchner's (1997) recommendations that the Rietvlei Sandstones be investigated for potential groundwater supply.

6.2 RECOMMENDATIONS

During exploration in the fractured and folded Rietvlei Formation, different sources should be targeted, especially as connectivity is possible. When drilling, careful thought must be applied to 1) ensuring groundwater of sufficient volumes is intersected, and 2) the quality of the groundwater will be suitable for the purpose. A high yielding borehole of poor quality can require substantial investment to reach a quality suitable for the desired purpose, and should be avoided when possible.

Potential for well field development is high in well connected fracture systems, and careful planning must be applied to ensure long term success of such a wellfield. The following recommendations are made:

- Drilling should take place away from the fold axis when argillaceous rock types are adjacent to the Rietvlei Formation, as this will potentially result in poorer quality groundwater. When the Rietvlei formation is overlain by an impermeable layer, such as the Gydo Formation, artesian conditions can result, which should also be avoided.
- A baseline study of soil properties should be conducted before groundwater irrigation takes place. Follow up soil sampling and analysis will determine if groundwater is lowering the permeability of soil and thus impacting crop yields. Once soils become sodic, rehabilitation is costly and time intensive.
- Long term monitoring of groundwater levels in production boreholes, as well as back-up boreholes should be conducted to enable sustainable management of wellfields within well connected fractured aquifers.
- A numerical groundwater flow model should be developed to model the impact of using groundwater for irrigation from the Rietvlei Sandstone of the study site.

REFERENCES

- ABEM, 2010, Instruction Manual: Terrameter SAS 4000/1000, Sweden.
- Appelo, C.A.J., Postma, D., 2005. *Geochemistry, groundwater and pollution*. (2nd ed.) Amsterdam, The Netherlands: Taylor & Francis.
- Aref, F, Roosta, R., 2016. Assessment of groundwater quality and hydrochemical characteristics in Farashband Plain, Iran. *Arab Journal of Geoscience* 2016 9:752
- Barenblatt, G.E., Zheltov, I.P. & I.N. Kochina 1960. Basic concepts in the theory of seepage of homogeneous liquids in fissured rocks.- *J. of Applied Mathematics* 24(5):1286-1303.
- Barker, J.A., 1988. A Generalized Radial Flow Model for Hydraulic Tests in Fractured Rock. *Water Resources, Res.*, Vol. 24, No. 10, pp. 1796 – 1804.
- Bäumle, R., 2003. *Geohydraulic Characterisation of Fractured Rock Flow Regimes: Regional Studies in Granite (Lindau, Black Forest, Germany) and Dolomite (Tsumeb Aquifers, Northern Namibia)*, Doctorate Thesis, Karlsruhe University.
- Bear, J., and Bachmat, Y., 1987. On the Concept and Size of Representative Elementary Volume (REV). In: *Advances in Transport Phenomena in a Porous Media*, pp 3 – 20, Vol. 128. Dordrecht.
- Cinco, H., and Samaniego, F., (1981), *Transient Pressure Analysis for fractured wells*, *Journal of Petroleum Technology*, September 1981 edn.
- Cooper, H.H. and C.E. Jacob, 1946. A generalized graphical method for evaluating formation constants and summarizing well field history, *Am. Geophys. Union Trans.*, vol. 27, pp. 526-534.
- Cape Farm Mapper, viewed 18 January 2018, <https://gis.elsenburg.com/apps/cfm/>
- De Beer CH 2001. The stratigraphy, lithology and structure of the Table Mountain Group. A synthesis of the hydrogeology of the Table Mountain Group: formation of a research strategy. WRC, Pretoria, South Africa, pp 9–18.
- Domenico, P., Schwartz F., (1998) *Physical and chemical hydrogeology*, 2nd edn. Wiley, New York.
- Doneen, L.D. (1964) *Notes on Water Quality in Agriculture* published as a Water Science and Engineering Paper 4001, Department of Water Science And Engineering, University of California.
- Driscoll, F.G., (1986), *Groundwater and Wells* (2nd edn.), Johnson Filtration Systems, Inc., St. Paul, Minnesota.
- Fipps, G., (1998), *Irrigation Water Quality Standards and Salinity Management Strategies*, Texas A&M AgriLife Extension Service, Texas.
- Fisher RS, Mulican WF III (1997) Hydrochemical evolution of sodium-sulfate and sodium-chloride groundwater beneath the northern Chihuahuan desert, Trans-Pecos, Texas, USA. *Hydrogeology J*, 10:455–474
- Greef, G.J., 1990. Detailed Geohydrological Investigation in the Poesjesnels River Catchment in the Breede River Valley with Special Reference to Mineralization. Report No. 120/1/90, Water Research Commission, Pretoria.
- Ferris, J.G., Knowless, D.B., Brown, R.H., and Stallman, R.W., (1962), *Theory of Aquifer Tests*, U.S. Geological Survey, Water Supply Paper 1536E, pp 174.

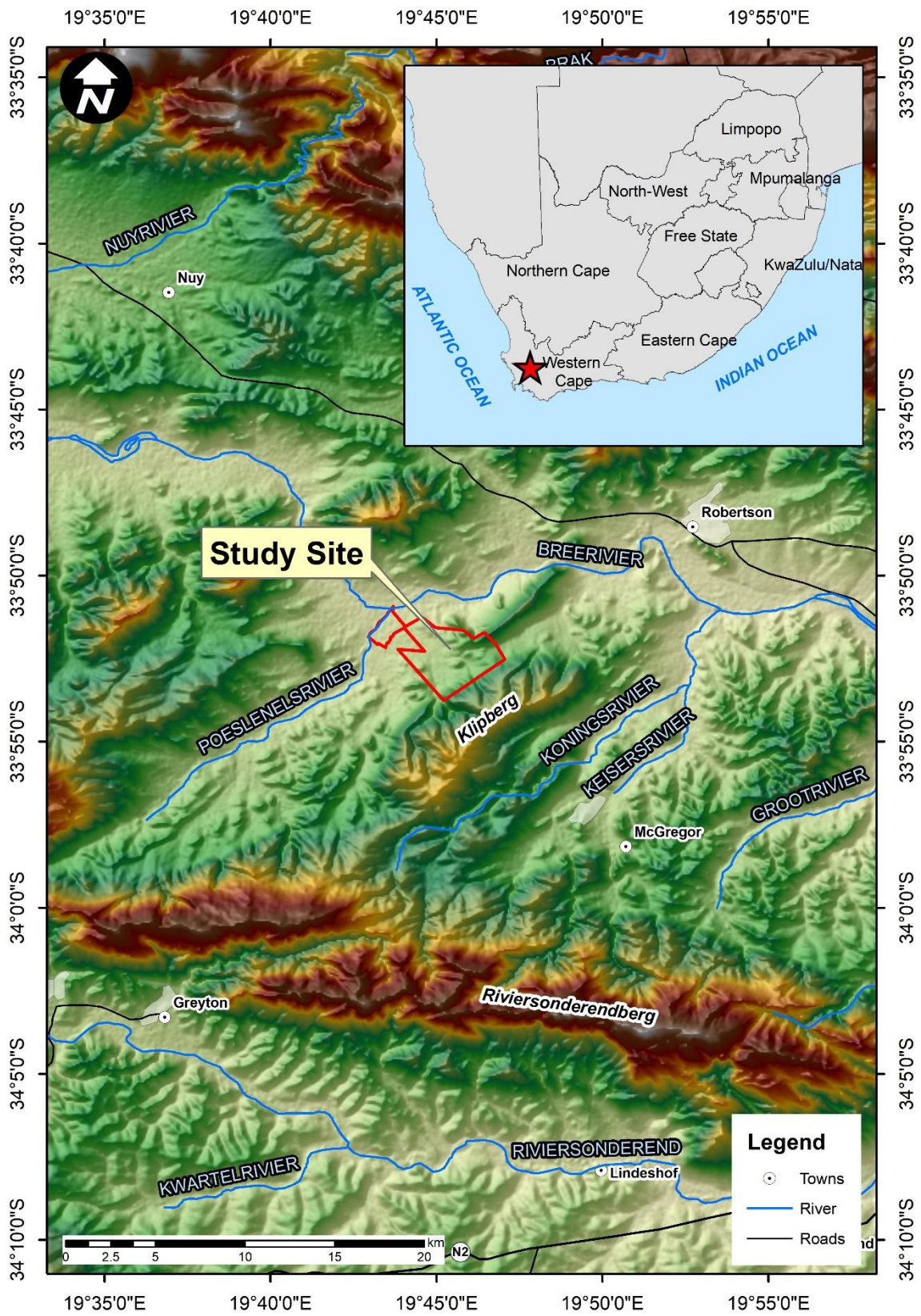
- Fraser, L., and Stemmet, Q., (2002), Geophysical Techniques Appropriate for Exploration of Table Mountain Group Aquifers, In: A synthesis of the hydrogeology of the Table Mountain Group – formation of a research strategy (eds K. Pieterse and R Parsons), pp 33-44. Report No. TT 158/01, Water Research Commission, Pretoria.
- Fipps, G., (1996), Irrigation Water Quality Standards and Salinity Management, Agrilife Extension, doc B-1667 4-03, Texas.
- Gomo, M., Van Tonder, G., and Steyl, G., (2013), Investigation of the hydrogeochemical processes in an alluvial channel aquifer located in a typical Karoo Basin of Southern Africa. *Environmental Earth Science*, vol 70: pg 227-238.
- Greef, G.J., (1990), Detailed Geohydrological Investigation in the Poesjesnels River Catchment in the Breede River Valley with Special Reference to Mineralization, Water Research Commission rep. nr. 120/1/90, Stellenbosch.
- Gringarten, A.C., and Ramey, H.J., (1973), The Use of Source and Green's Functions in Solving Unsteady – Flow Problems in Reservoirs. *SPE Journal*, 1973, vol. 255, pp.285 – 296.
- Guler, C., Thyne, G.D., McCray, J.E., Turner, A.K., (2002) Evaluation of graphical and multivariate statistical methods for classification of water chemistry data, *Hydrogeology J* 10:455–474. Gringarten, A.C., H.J. Ramey Jr. and R. Raghavan, 1974. Unsteady-State Pressure Distributions Created by a
- Halford, K., Weight, W., and Schreiber, R., (2006), Interpretation of Transmissivity Estimates from Single-Well Pumping Aquifer Tests, *Groundwater*, Vol. 44, No. 3, pg 467-471. Kirchner, J., Moolman, J.H., Du Plessis, H.M., and Reynders, A.G., 1997. Causes and Management of Salinity in the Breede River Valley, South Africa, *Hydrogeology Journal*, Vol. 5, no. 1.
- Houatmia, F., Azouzi, R., Charef, A., and Bedir, M., (2016), Assessment of groundwater quality for irrigation and drinking purposes and identification of hydrogeochemical mechanisms evolution in Northeastern Tunisia, *Environmental Earth Sciences*, (2016) 75:746.
- Kelly W.P., (1963), Use of Saline Irrigation Water, *Soil Science*, 95(4): 55-60.
- Kirsch, R. (ed), 2009, *Groundwater Geophysics: A Tool for Hydrogeology*, Springer Books, Heidelberg.
- Kotze, J.C., (2000), *Hydrogeology of the Table Mountain Sandstone Aquifer – Klein Karoo*. PHD Thesis submitted to Institute of Groundwater Studies, University of Orange Free State, Bloemfontein.
- Kumar, V., Amarender, B., Dhakater, R., Sankaran, S., Kumar, R., 2014, Assessment of groundwater quality for drinking and irrigation use in shallow hard rock aquifer of Pudunagaram, Palakkad District Kerala, *Applied Water Science Journal*, (2016) 6:149-167.
- Kumar, M., Kumari, K., Ramanathan, AL., Saxena R., (2007), A comparative evaluation of groundwater suitability for irrigation and drinking purposes in two intensively cultivated districts of Punjab, India. *Environmental Geology*, 53(3): 533-574.
- Kruseman, G.P., and De Ridder, N.A., 2000. *Analysis and Evaluation of Pumping Test Data*, 2nd edn, Veenman Drukkers, Netherlands.
- Lin, L., Lin, H., and Xu, Y. 2014. Characterisation of Fracture Network and Groundwater Preferential Flow Path in the Table Mountain Group (TMG) Sandstones, South Africa. *Water SA* Vol. 40 No.2.
- Lin, L. 2007. *Hydraulic Properties of the Table Mountain Group (TMG) Aquifers*, Dissertation for Doctor of Philosophy, University of the Western Cape.

- Lukas, E., (n.d.), Windows Interpretation System for Hydrogeologists, version 3.02.189, Bloemfontein, South Africa.
- Maclear, L.G.A., (1996), The Geohydrology of the Swartkops River Basin – Uitenhage Region, Eastern Cape, Unpublished M.Sc. Dissertation, UCT.
- Maclear, L.G.A., (2001), The Uitenhage Artesian Basin, In: A synthesis of the hydrogeology of the Table Mountain Group – formation of a research strategy (eds K. Pietersen and R Parsons), pp 33-44. Report No. TT 158/01, Water Research Commission, Pretoria.
- McNeill, J., 1980, Electromagnetic Terrain Conductivity Measurement as Low Induction Numbers, Technical Note TN-6, Geonics Limited, Canada.
- Meyer, P.S., (1999), An Explanation of the 1: 500 000 General Hydrogeological Map Oudsshoorn 3320, DWAF, Pretoria.
- Meyer, P.S., (2001), An Explanation of the 1:500 000 General Hydrogeological Map of Cape Town 3317, DWAF, Pretoria.
- Mohan, R., Singh, A.K., Tripathi, J.K., Chowdary, G.C., (2000), Hydrochemistry and quality assessment of groundwater in Naini Industrial area, Allahabad District, Uttar Pradesh. Journal of Geology Society, India, 55: 77-89.
- Neal, C., and Kirchner, J., (2000), Sodium and chloride levels in rainfall, mist, streamwater, and groundwater at the Plynlimon catchments, mid-Wales: inferences in hydrological and chemical controls, Hydrology and Earth System Sciences, 4(2): 295-310.
- Parkhurst DL, Appelo CAJ (1999) PHREEQC for windows version 3.3.12.12704. A hydrogeochemical Transport model. US Geological.
- Parsons, R., (2001), Development of Groundwater Resources for the Arabella Country Estate, In: A synthesis of the hydrogeology of the Table Mountain Group – formation of a research strategy (eds K. Pietersen and R Parsons), pp 33-44. Report No. TT 158/01, Water Research Commission, Pretoria.
- Pietersen, K., and Parsons, R. 2002. A synthesis of the hydrogeology of the Table Mountain Group – formulation of a research strategy. Report No. TT 158/01, Water Research Commission, Pretoria.
- Piper, M., (1944), A graphic procedure in the geochemical interpretation of water-analyses, EOS Trans. AGU, 25(6), 914-928.
- Richards LA (ed) (1954) Diagnosis and improvement of saline and alkali soils. In: USDA Handbook no. 60, Washington, pp 160.
- Rosewarne, P., (1979), Groundwater Conditions of the Lower Groothoek Area, Hex River Valley, DWAF Report, Gh. 3186.
- Rowearne, P., (1989), Case Study: St Francis-on-Sea: In: A synthesis of the hydrogeology of the Table Mountain Group – formation of a research strategy (eds K. Pietersen and R Parsons), pp 33-44. Report No. TT 158/01, Water Research Commission, Pretoria.
- Rosewarne, P., 2002a. Hydrogeological Characteristics of the Table Mountain Group Aquifers. In: A synthesis of the hydrogeology of the Table Mountain Group – formation of a research strategy (eds K. Pietersen and R Parsons), pp 33-44. Report No. TT 158/01, Water Research Commission, Pretoria.

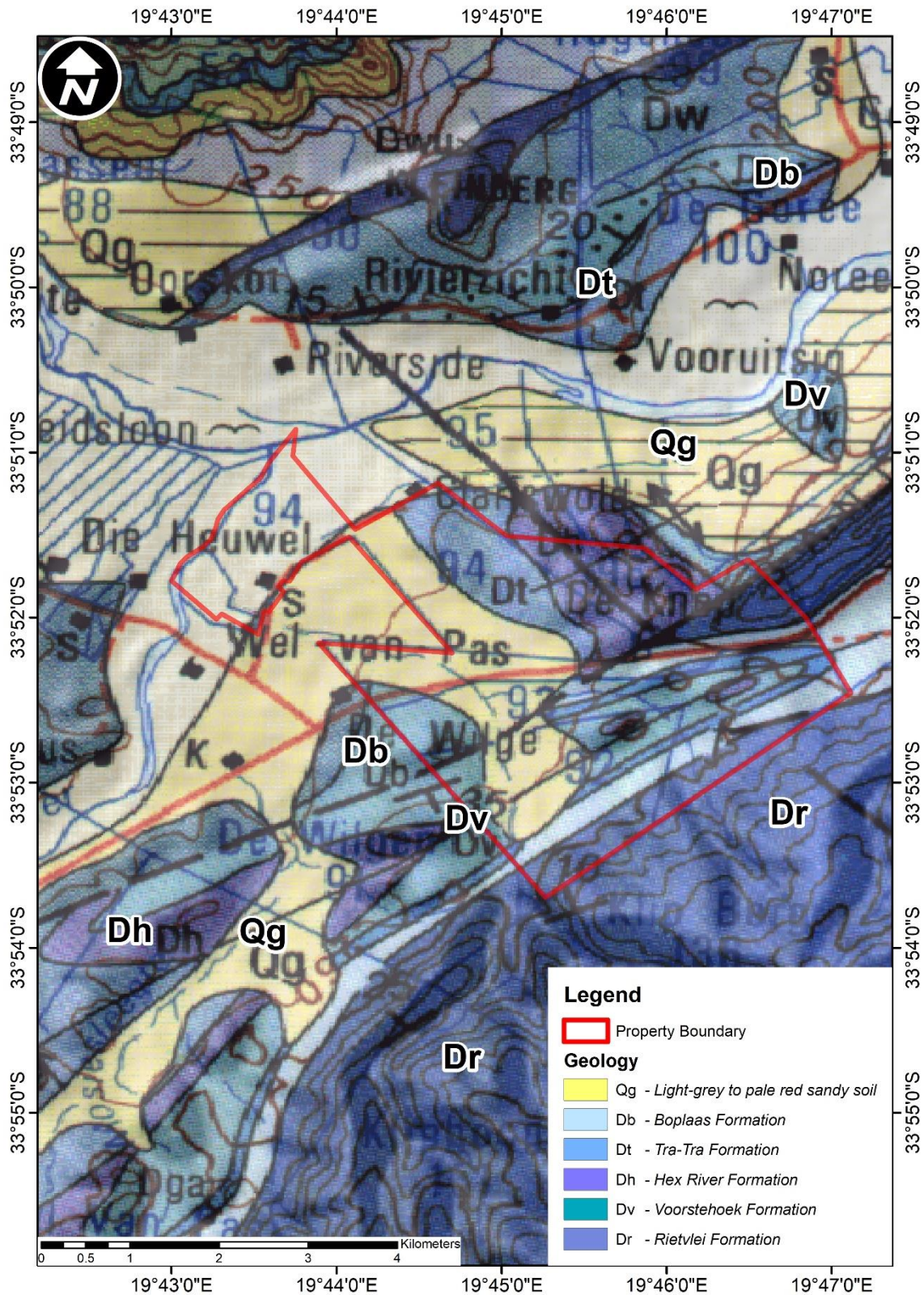
- Rosewarne, P 2002b. Case study: Hex River valley. In: A synthesis of the hydrogeology of the Table Mountain Group – formation of a research strategy (eds K. Pietersen and R Parsons), pp 178-182. Report No. TT 158/01, Water Research Commission, Pretoria.
- Telford W. M., Geldart L. P. and Sheriff R. E. (1990). Applied Geophysics: Second Edition. Cambridge University Press.
- Thamm, A.G. & Johnson, M.R. 2006. The Cape Supergroup. In: Johnson, M.R., Anhaeusser, C.R., & Thomas, R.J. (Eds.), The Geology of South Africa, Council for Geoscience South Africa, pp443-460.
- Theis, C.V. 1935. The relation between the lowering of the piezometric surface and the rate and duration of discharge of a well using groundwater storage.- American Geophysical Union Trans. 16: 519-524.
- Theron, J.N 1972. The stratigraphy and sedimentation of the Bokkeveld Group. D.Sc. thesis (unpublished.), University of Stellenbosch.
- Theron, J.N., Looek, J.C. 1988. Devonian deltas of the Cape Supergroup, South Africa. In: McMillan, M.J., Embry, A.F, Glass, D.J. (Eds.), Devonian of the World, vol. 1, Memoir 14. Canadian Society of Petroleum Geologists, pp. 729–740.
- Thomas, C., 1997, 1:250 000 Geological Series, 3319 Worcester; Geological Survey of South Africa. – Pretoria: Council for Geoscience.
- Woodford A.C., 2002. Interpretation and Applicability of Pumping Tests in the Table Mountain Group Aquifers, In: A synthesis of the hydrogeology of the Table Mountain Group – formation of a research strategy (eds K. Pietersen and R Parsons), pp 71 - 84. Report No. TT 158/01, Water Research Commission, Pretoria.
- South African National Standard (2003), Development, maintenance and management of groundwater resources, Part-4: Test-pumping of water boreholes, SANS 10299-4:2003, edn 1.1., Published by Standards South Africa.
- Szabolcs, I. and Darab, C. (1964), The influence of irrigation water of high sodium carbonate content of soils, Proceedings of 8th ISSS, Trans vol. II , 802-812
- Theis, C.V., 1935. The relation between the lowering of the piezometric surface and the rate and duration of discharge of a well using groundwater storage, Am. Geophys. Union Trans., vol. 16, pp. 519-524.
- Todd DK (1980) Groundwater hydrology. Wiley, New York, p. 535.
- Van Tonder, G., Bardenhgen, I., Rieman, K., Van Bosch, J., Dzanga, P., Xu, Y., (2002), Manual on Pumping test Analysis in Fractured Rock Aquifers. Report No 1116/1/02, Water Research Commission, Pretoria.
- Umvoto and SRK (2000), Reconnaissance Investigation into the Development and Utilization of Artesian Groundwater, Using the E10 Catchment as a Pilot Study Area: CAGE Project
- Van Tonder G.J., J.F. Botha, W.-H. Chiang, H. Kunstmannb, Y. Xu (2001). Estimation of the sustainable yields of boreholes in fractured rock formations. Journal of Hydrology 241, 70–90.
- Weaver, J., (1999), Hydrogeology of the Table Mountain Group. A Case Study at Botrivier, In: A synthesis of the hydrogeology of the Table Mountain Group – formation of a research strategy (eds K. Pietersen and R Parsons), pp 33-44. Report No. TT 158/01, Water Research Commission, Pretoria.

Willman, M., Carrera J, Sanchez-Vila, E., and Vazquez-Sune, E., (2007), On the Meaning of the Transmissivity Values Obtained from Recovery Tests. *Hydrogeology Journal* (2007) 15: 833-842.

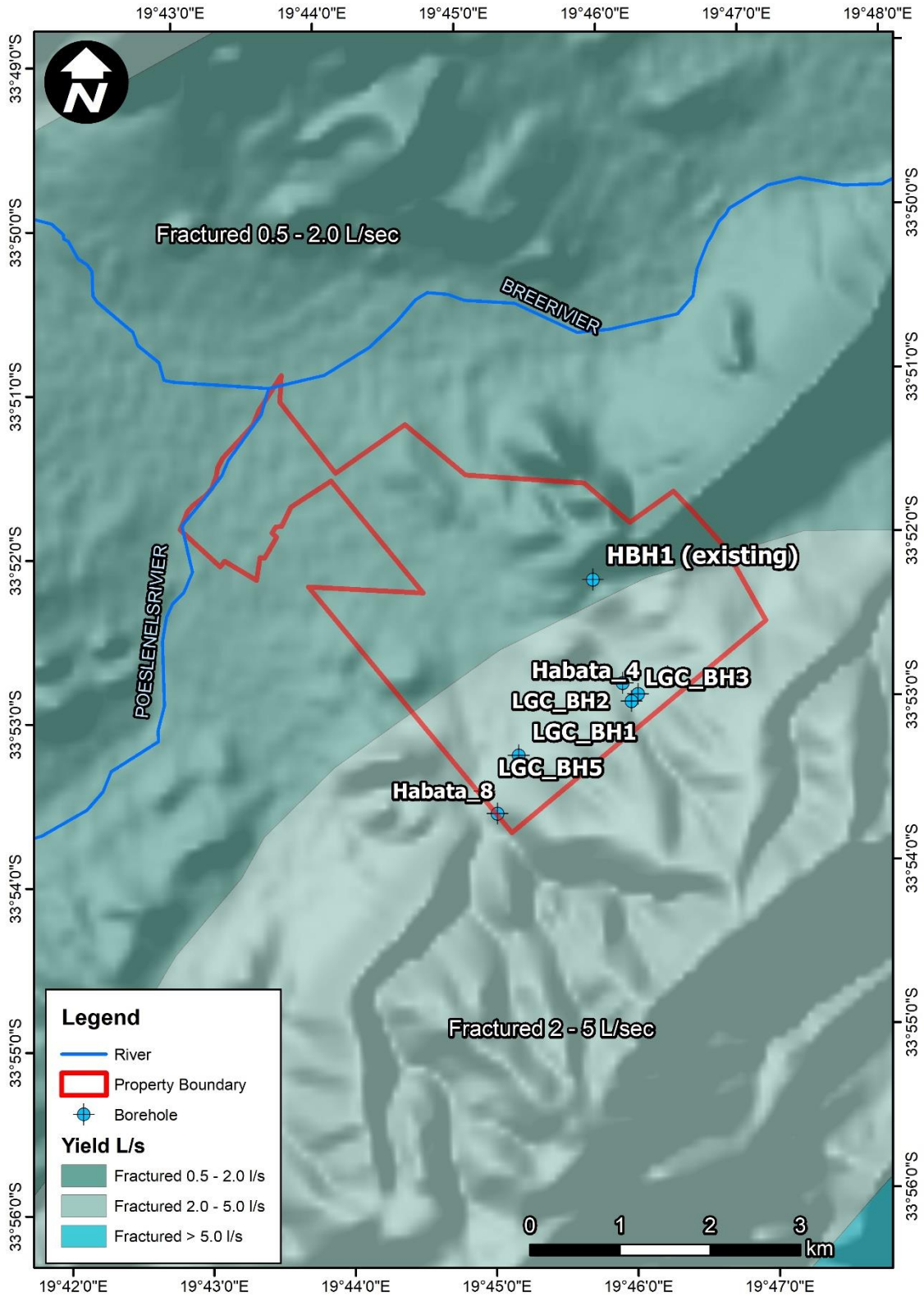
APPENDIX A (MAPS)



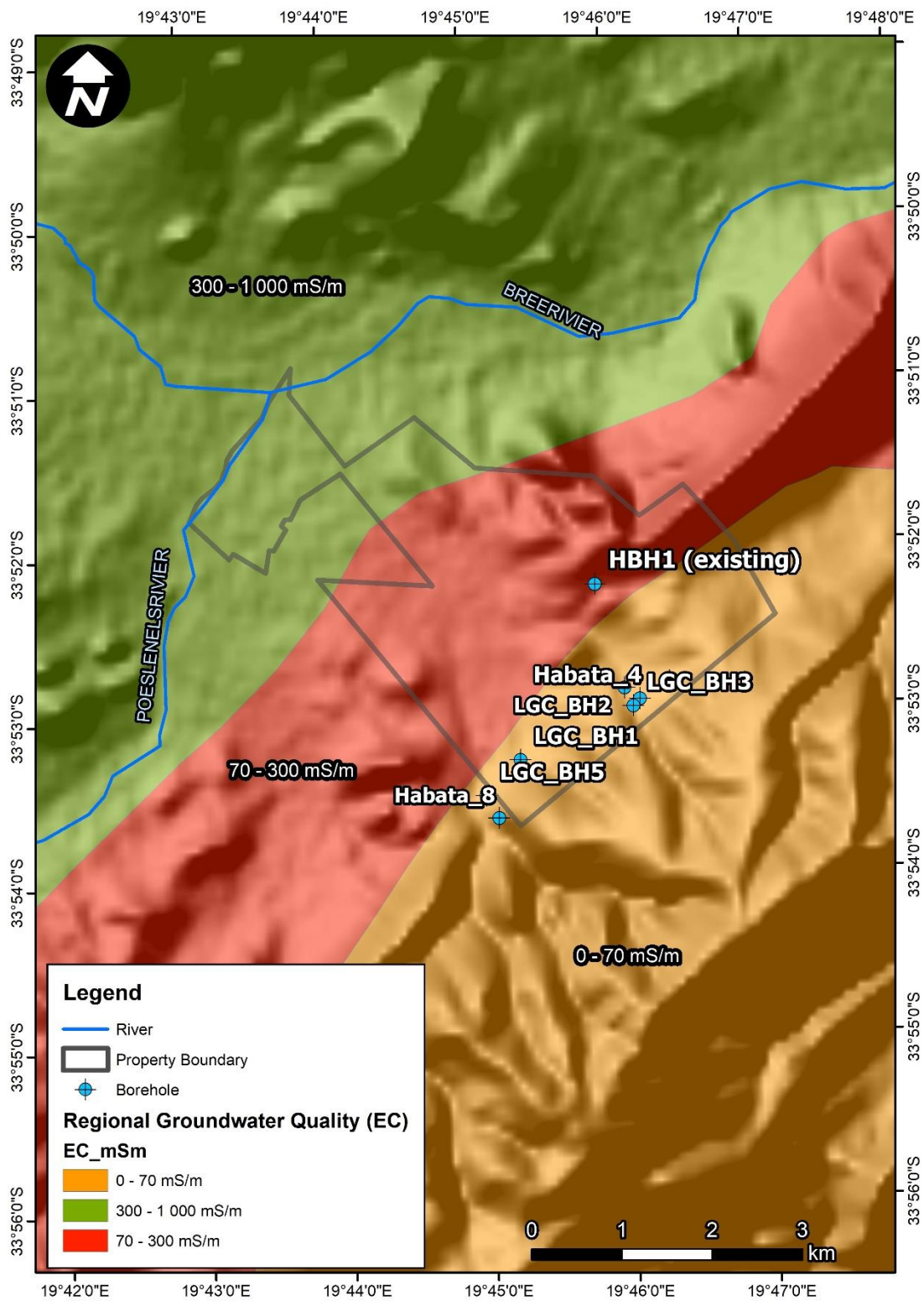
Map 1: Location of the study area, also referred to as Habata Agri.



Map 2: Regional geological setting of the study area overlain on a DEM to gain topographical perspective (adapted from 1:250 000, Worcester Map, CGS)



Map 3: Aquifer type and average yield overlain on a DEM (DWAf 2001).



Map 4: Groundwater quality classed according to electrical conductivity.

APPENDIX B (DRILL LOGS)

Log of Borehole No. : HBH1

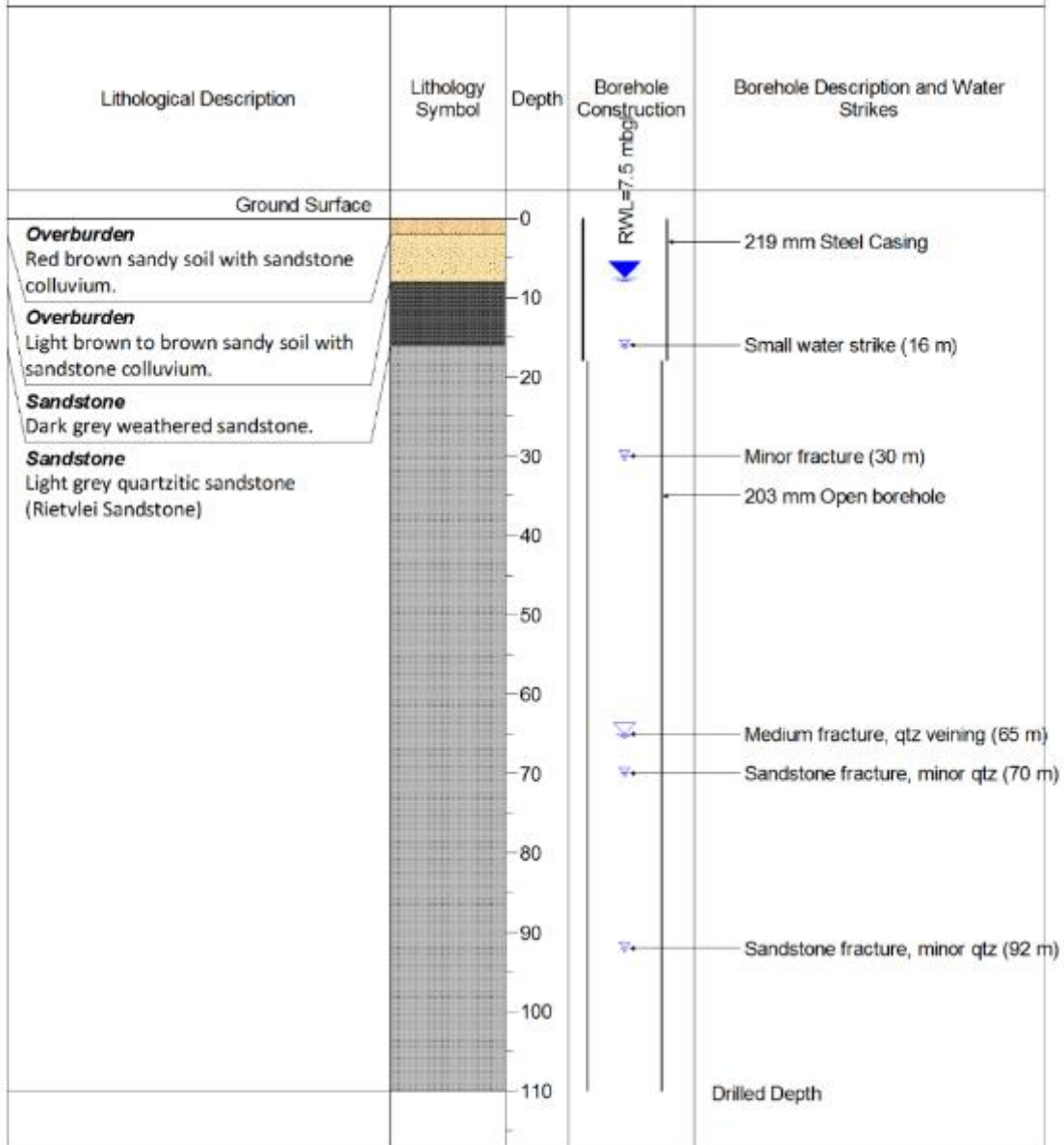
Location: Le Grand Chasseur **Latitude:** -33.8706
Date: Unknown **Longitude:** 19.764150
Client: Hannes Joubert **Ground Elevation:** 284 mamsl

Lithological Description	Lithology Symbol	Depth	Borehole Construction	Borehole Description and Water Strikes
Ground Surface		0		
Overburden Light brown to red clayey sand		0		219 mm Steel Casing
Fault Zone Bokkeveld Formation and downthrown Rietvlei sandstone. Psilemolane (manganese hydroxide at shallow depths of Fault contact)		10	RWL = 10.38 m bgl ▼	203 mm Open borehole
		20		
		30		
		40		
		50		Current depth

Drilled By: Unknown **Remarks:** Airlift Yield = Unknown (Old Boreole)
Drill Method: Unknown
Logged By: Neville Paxton

Log of Borehole No. : LGC_BH1

Location: Le Grand Chasseur **Latitude:** -33.888204°
Date: 29 March 2016 **Longitude:** 19.754686°
Client: Hannes Joubert **Ground Elevation:** 276 mamsl



Drilled By: MD Drilling

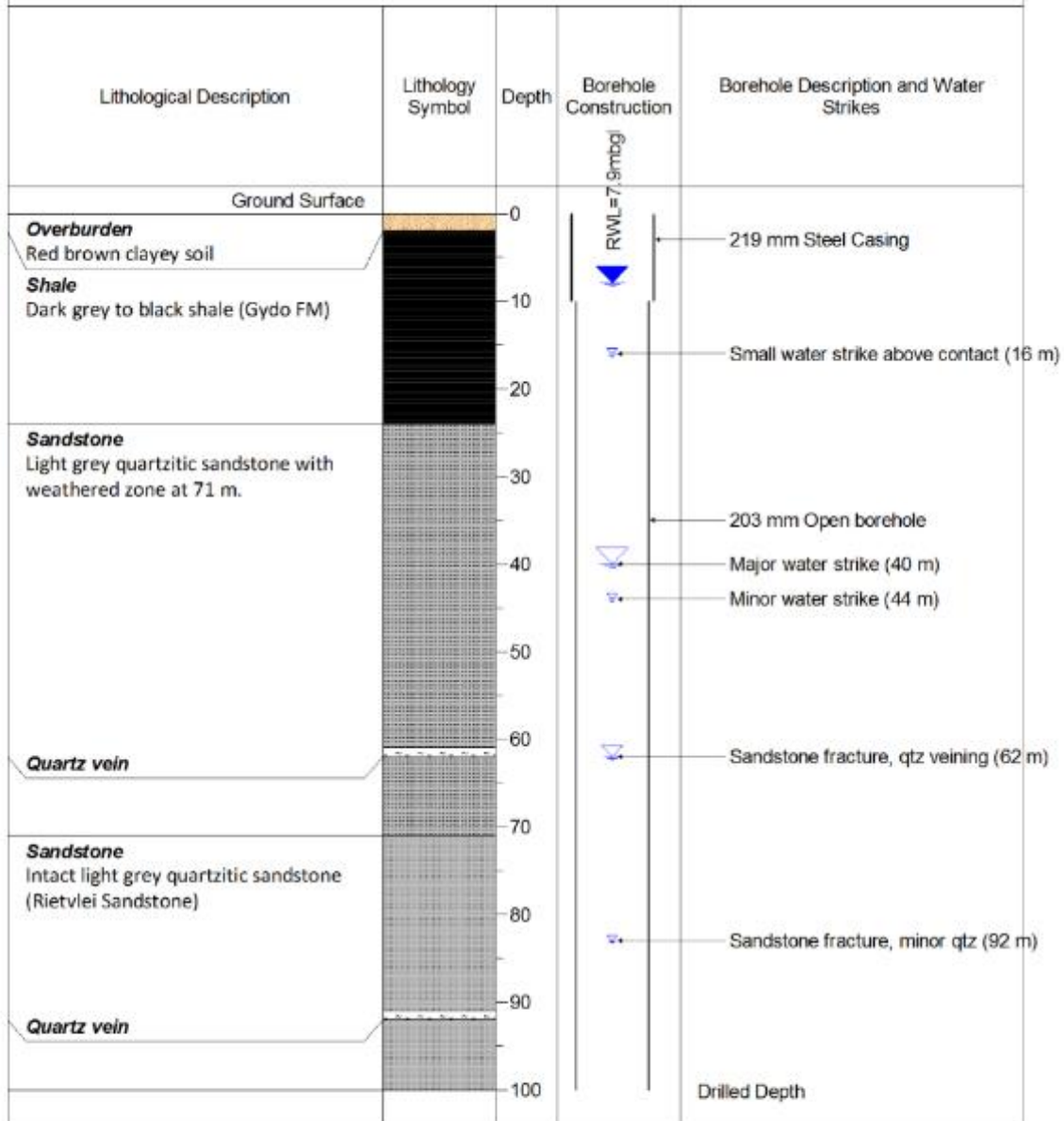
Remarks: Airlift Yield = 36 000 L/Hr

Drill Method: Air Percussion

Logged By: Neville Paxton

Log of Borehole No. : LGC_BH2

Location: Le Grand Chasseur **Latitude:** -33.881231°
Date: 29 March 2016 **Longitude:** 19.767218°
Client: Hannes Joubert **Ground Elevation:** 288 mamsl



Drilled By: MD Drilling

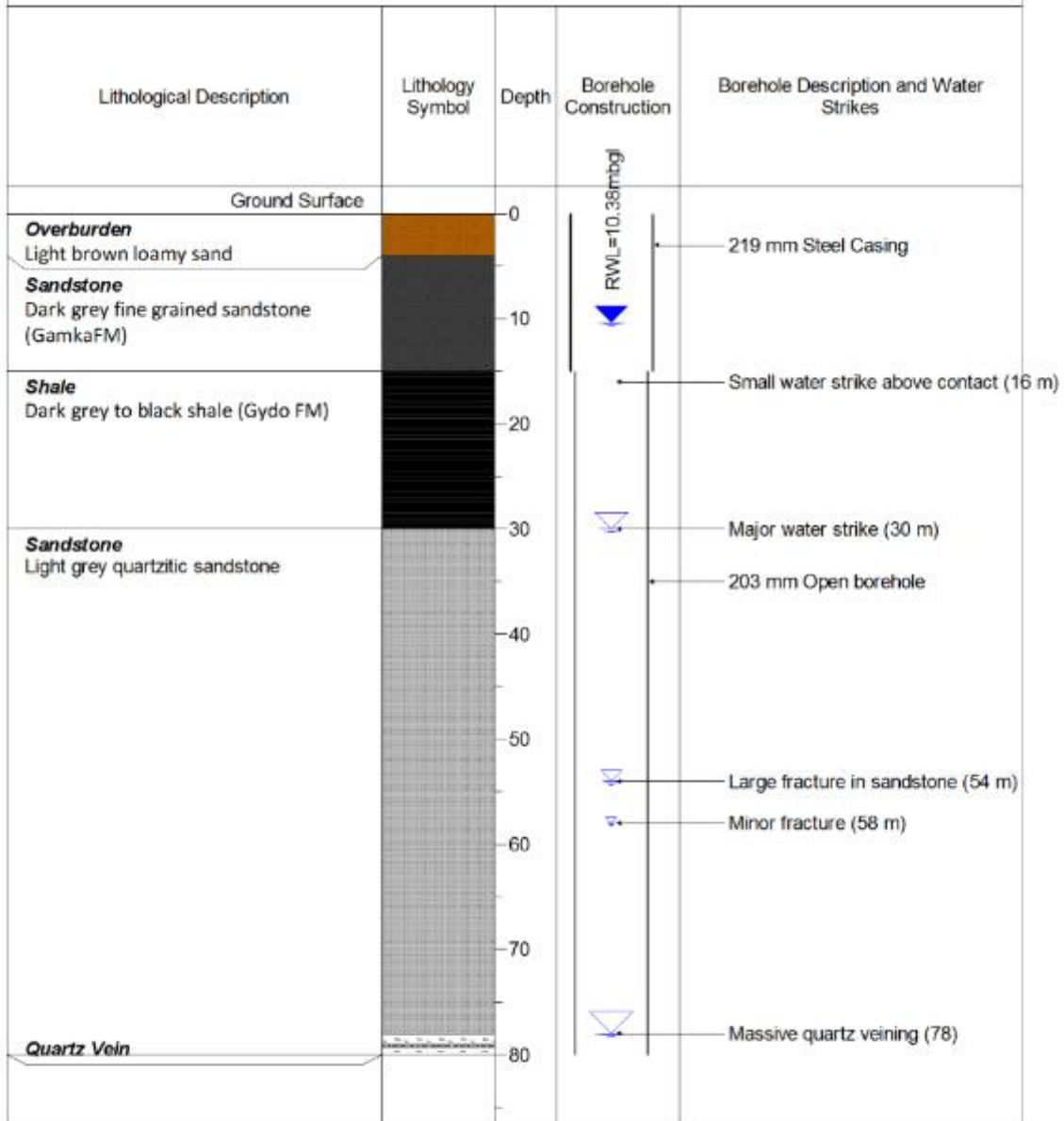
Remarks: Airlift Yield = 40 000 L/Hr

Drill Method: Air Percussion

Logged By: Neville Paxton

Log of Borehole No. : LGC_BH3

Location: Le Grand Chasseur **Latitude:** -33.883079°
Date: 30 March 2016 **Longitude:** 19.76206
Client: Hannes Joubert **Ground Elevation:** 304 mamsl



Drilled By: MD Drilling

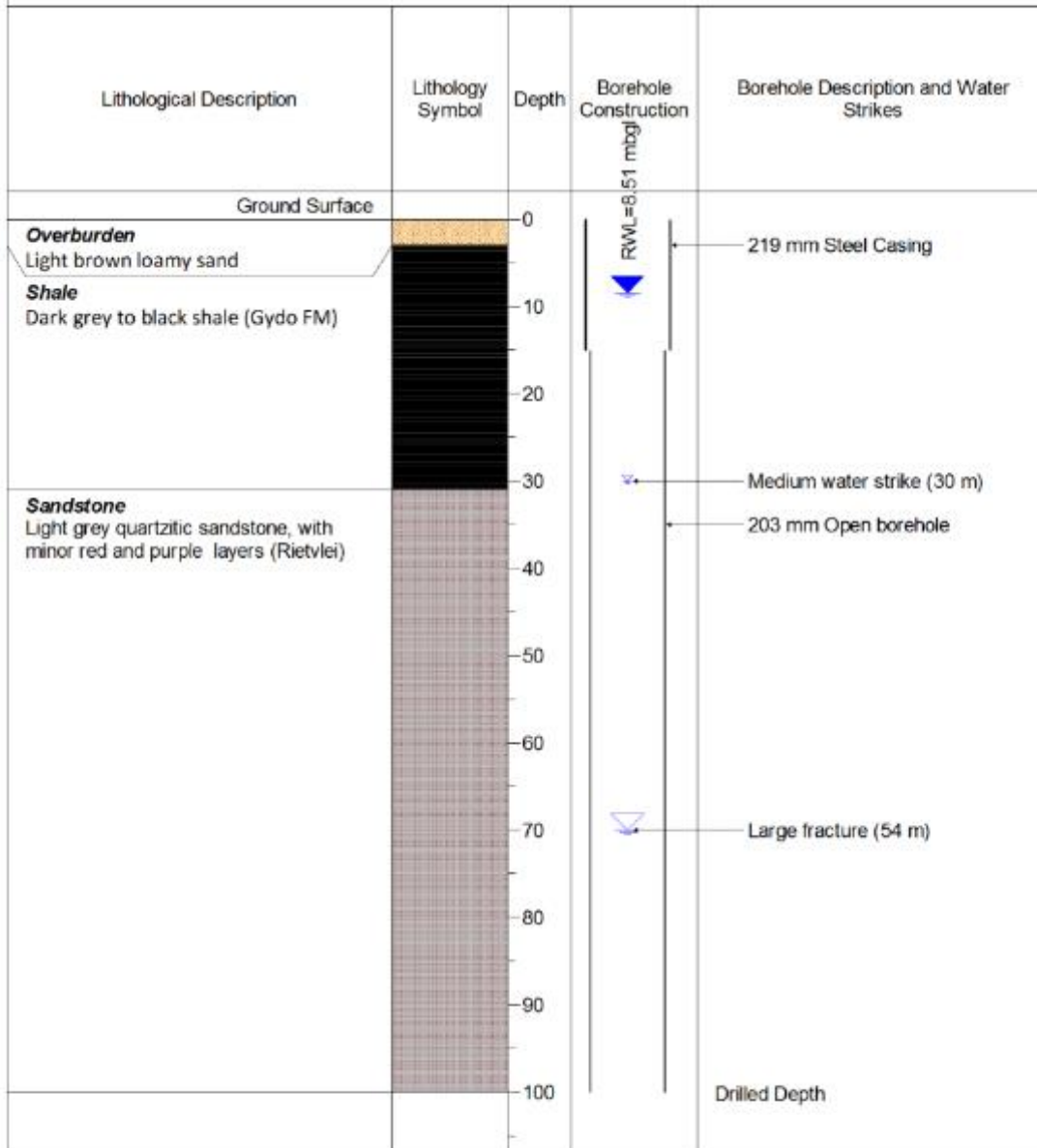
Remarks: Airlift Yield = 80 000 L/Hr

Drill Method: Air Percussion

Logged By: Neville Paxton

Log of Borehole No. : LGC_BH5

Location: Le Grand Chasseur **Latitude:** -33.891720
Date: 15 April 2016 **Longitude:** 19.750500
Client: Hannes Joubert **Ground Elevation:** 274 mamsl



Drilled By: MD Drilling

Remarks: Airlift Yield = 70 000 L/Hr

Drill Method: Air Percussion

Logged By: Neville Paxton

Log of Borehole No. : LGC_BH8

Location: Le Grand Chasseur **Latitude:** -33.8850
Date: 06 April 2016 **Longitude:** 19.758860
Client: Hannes Joubert **Ground Elevation:** 278 mamsl

Lithological Description	Lithology Symbol	Depth	Borehole Construction	Borehole Description and Water Strikes
Ground Surface		0		
Overburden Light brown to red clayey sand		0 - 10		219 mm Steel Casing
Shale Dark grey to black shale (Gydo FM)		10 - 30		
Sandstone Light grey quartzitic sandstone, with minor quartz veining throughout (Rietvlei)		30 - 120		203 mm Open borehole
			RWL = 11.49 m bgl	
				Medium water strike (64 m)
				Drilled Depth

Drilled By: MD Drilling

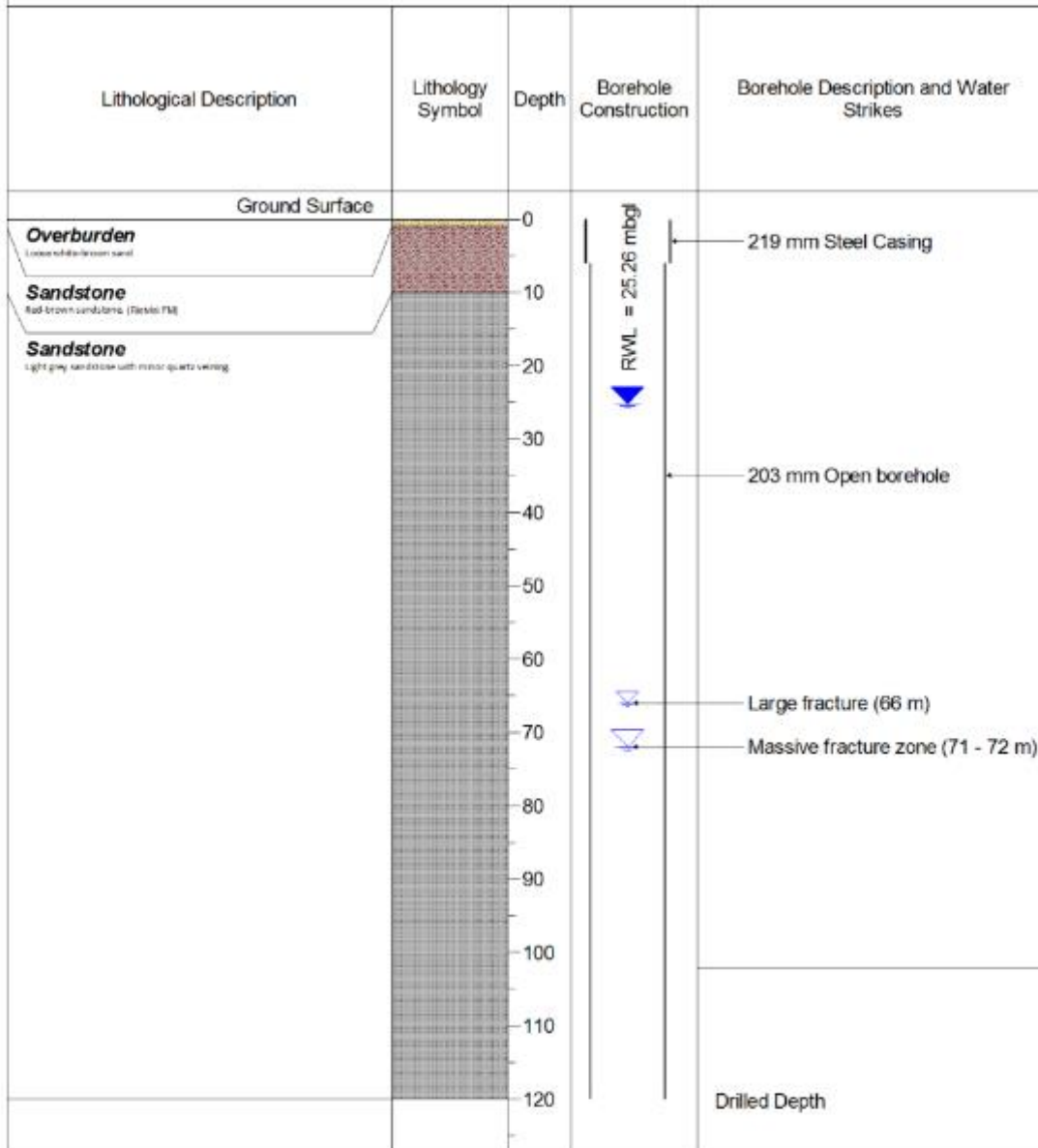
Remarks: Airlift Yield = 15 000 L/Hr

Drill Method: Air Percussion

Logged By: Neville Paxton

Log of Borehole No. : Habata_2

Location: Le Grand Chasseur **Latitude:** -33.880694°
Date: **Longitude:** 19.772528°
Client: Hannes Joubert **Ground Elevation:** 313 mamsl



Drilled By: MD Drilling

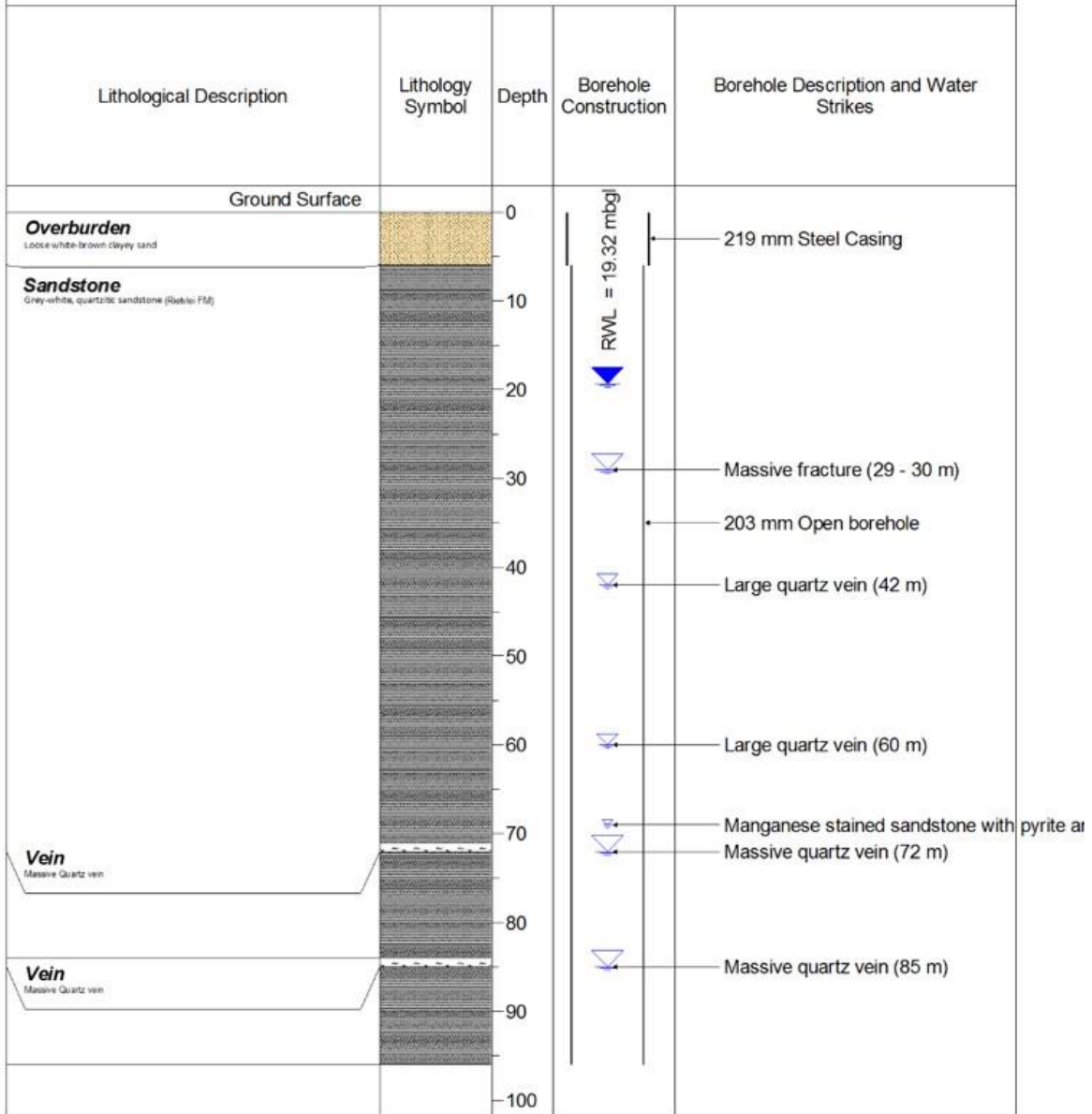
Remarks: Airlift Yield = 20 000 L/Hr, drilled to 120 m

Drill Method: Air Percussion

Logged By: Neville Paxton

Log of Borehole No. : Habata_4

Location: Le Grand Chasseur **Latitude:** -33.88239
Date: **Longitude:** 19.769
Client: Hannes Joubert **Ground Elevation:** 304 mamsl



Drilled By: MD Drilling

Remarks: Airlift Yield = 80 000 L/Hr

Drill Method: Air Percussion

Logged By: Neville Paxton

Log of Borehole No. : Habata_8

Location: Le Grand Chasseur **Latitude:** -33.894040
Date: **Longitude:** 19.751930
Client: Hannes Joubert **Ground Elevation:** 301 mamsl

Lithological Description	Lithology Symbol	Depth	Borehole Construction	Borehole Description and Water Strikes	
Ground Surface					
Overburden White-brown sand	█	0	219 mm Steel Casing		
Sandstone Light grey sandstone		10			
		20			
		30			
Sandstone Highly varied colour, red, white, brown, purple sandstone (Rietvlei FM)	█	40	203 mm Open borehole		
		50			
		60			
		70			
		80			
		90			
		100			
					110
					120
					130

RWL = 19.06 mboj

▼

▼

▼

Drilled By: MD Drilling **Remarks:** Airlift Yield = 40 000 L/Hr
Drill Method: Air Percussion
Logged By: Neville Paxton

APPENDIX C (PUMPING TEST RESULTS)

FORM 5 F

CONSTANT DISCHARGE TEST & RECOVERY

BOREHOLE TEST RECORD SHEET

PROJ NO: P1628	MAP REFERENCE: 33.8706	PROVINCE: WC
BOREHOLE NO: HBH1 (BH09)	19.76415	DISTRICT: ROBERSTON
ALT BH NO: 0		SITE NAME: LEGRAND
ALT BH NO: 0		
BOREHOLE DEPTH: 51.90	DATUM LEVEL ABOVE CASING (m): 0.45	EXISTING PUMP: 0
WATER LEVEL (mbdl): 10.91	CASING HEIGHT: (magl): 0.51	CONTRACTOR: AB PUMPS
DEPTH OF PUMP (m): 46.00	DIAMPUMP INLET(mm): 200	PUMP TYPE: BP50

CONSTANT DISCHARGE TEST & RECOVERY

TEST STARTED				TEST COMPLETED			
DATE: 11/06/2016	TIME: 07H30	DATE: 11/06/2016	TIME: 07H30	TYPE OF PUMP:	BP50		

			OBSERVATION HOLE 1	OBSERVATION HOLE 2	OBSERVATION HOLE 3
			NR: BH03	NR: BH10	NR:

DISCHARGE BOREHOLE			Distance(m); 1.4	Distance(m); 1.3	Distance(m);
---------------------------	--	--	------------------	------------------	--------------

TIME (MIN)	DRAW DOWN (M)	YIELD (L/S)	TIME (MIN)	RECOVERY (M)	TIME (min)	Drawdown (m)	Recovery (m)	TIME (min)	Drawdown (m)	Recovery	TIME (min)	Drawdown (m)
1	3.68		1	10.50	1	0.00		1	0.00		1	
2	4.23		2	8.53	2			2			2	
3	5.06	3.47	3	8.25	3			3			3	
5	5.80	5.05	5	7.51	5			5			5	
7	7.70		7	7.31	7			7			7	
10	9.12	5.04	10	7.25	10			10			10	
15	11.53		15	7.13	15			15			15	
20	11.97	5.05	20	7.00	20			20			20	
30	12.45		30	6.81	30			30			30	
40	12.70	5.03	40	6.63	40			40			40	
60	13.14		60	6.40	60			60			60	
90	13.65	5.04	90	6.17	90			90			90	
120	14.08		120	5.92	120			120			120	
150	14.32	5.02	150	5.75	150			150			150	
180	14.46		180	5.58	180			180			180	
210	14.60	5.01	210	5.40	210			210			210	
240	15.00		240	5.25	240	0.00		240	0.00		240	
300	15.38	5.05	300	4.98	300			300			300	
360	15.53		360	4.73	360			360			360	
420	15.75	5.03	420	4.50	420			420			420	
480	16.10		480	4.28	480	0.00		480	0.00		480	
540	16.20	5.01	540		540			540			540	
600	16.45		600		600			600			600	
720	17.04	5.02	720		720	0.00		720	0.00		720	
840	17.29		840		840			840			840	
960	17.61	5.04	960		960	0.00		960	0.00		960	
1080	17.95		1080		1080			1080			1080	
1200	18.17	5.03	1200		1200	0.00		1200	0.00		1200	
1320	18.32	5.03	1320		1320			1320			1320	
1440	18.46		1440		1440	0.00		1440	0.00		1440	
1560			1560		1560			1560			1560	
1680			1680		1680			1680			1680	
1800			1800		1800			1800			1800	
1920			1920		1920			1920			1920	
2040			2040		2040			2040			2040	
2160			2160		2160			2160			2160	
2280			2280		2280			2280			2280	
2400			2400		2400			2400			2400	
2520			2520		2520			2520			2520	
2640			2640		2640			2640			2640	
2760			2760		2760			2760			2760	
2880			2880		2880			2880			2880	
3000			3000		3000			3000			3000	
3120			3120		3120			3120			3120	
3240			3240		3240			3240			3240	
3360			3360		3360			3360			3360	
3480			3480		3480			3480			3480	
3600			3600		3600			3600			3600	
3720			3720		3720			3720			3720	
3840			3840		3840			3840			3840	
3960			3960		3960			3960			3960	
4080			4080		4080			4080			4080	
4200			4200		4200			4200			4200	
4320			4320		4320			4320			4320	

Total time pumped(min):	1440	W/L	11.83	W/L	44.85	W/L
Average yield (l/s):	5.03					

FORM 5 F														
CONSTANT DISCHARGE TEST & RECOVERY														
BOREHOLE TEST RECORD SHEET														
PROJ NO:	P1628		MAP REFERENCE: 33.8882				PROVINCE:		WESTERN CAPE					
BOREHOLE NO:	BH 01		19.75469				DISTRICT:		ROBERTSON					
ALT BH NO:	LGC BH01						SITE NAME:		LE GRAND					
ALT BH NO:	0													
BOREHOLE DEPTH:	99.40		DATUM LEVEL ABOVE CASING (m): 0.45				EXISTING PUMP:		0					
WATER LEVEL (mbdl):	10.71		CASING HEIGHT: (magl): 0.42				CONTRACTOR:		AB PUMPS					
DEPTH OF PUMP (m):	95.00		DIAM PUMP INLET(mm): 200				PUMP TYPE:		GW 9602					
CONSTANT DISCHARGE TEST & RECOVERY														
TEST STARTED					TEST COMPLETED									
DATE:	31/05/2016		TIME:	14H00		DATE:			TIME:			TYPE OF PUMP:	GW 9602	
					OBSERVATION HOLE 1			OBSERVATION HOLE 2			OBSERVATION HOLE 3			
					NR: LGC BH08			NR: LGC BH09			NR:			
					Distance(m); 300			Distance(m); 420			Distance(m);			
TIME	DRAW	YIELD	TIME	RECOVERY	TIME	Drawdown	Recovery	TIME	Drawdown	Recovery	TIME	Drawdown		
(MIN)	DOWN (M)	(L/S)	MIN	(M)	(min)	m	(m)	(min)	(m)		(min)	(m)		
1	7.53		1	21.45	1		0.00	1	0.00	0.77	1			
2	9.94		2	16.76	2			2			2			
3	11.57	12.94	3	15.81	3			3			3			
5	13.80	14.04	5	15.25	5			5			5			
7	15.35		7	14.85	7			7			7			
10	17.20	14.05	10	14.40	10			10			10			
15	18.90		15	14.11	15			15			15			
20	20.01	14.04	20	13.78	20			20			20			
30	21.10		30	13.16	30			30			30			
40	21.96	14.03	40	12.70	40			40			40			
60	23.14		60	12.05	60	0.04		60	0.00	0.77	60			
90	24.61	14.06	90	11.13	90			90			90			
120	25.42		120	10.57	120	0.10		120	0.00	0.77	120			
150	26.15	14.04	150	9.85	150			150			150			
180	26.95		180	9.38	180	0.12		180	0.00	0.73	180			
210	27.60	14.02	210	8.95	210			210			210			
240	28.22		240	8.45	240	0.25	0.00	240	0.00	0.69	240			
300	29.16	14.05	300	7.70	300	0.39		300			300			
360	30.07		360	7.03	360	0.48		360	0.05	0.66	360			
420	30.64	14.05	420	6.27	420	0.70		420	0.13	0.64	420			
480	31.58		480	5.35	480	0.85	0.00	480	0.19	0.61	480			
540	31.99	14.03	540		540	0.92		540	0.24		540			
600	32.36		600		600	1.02		600	0.30		600			
720	33.64	14.05	720		720	1.20	0.00	720	0.39		720			
840	34.55		840		840	1.37		840	0.45		840			
960	35.17	14.02	960		960	1.54	0.00	960	0.49		960			
1080	35.75		1080		1080	1.63		1080	0.54		1080			
1200	36.09		1200		1200	1.79	0.00	1200	0.60		1200			
1320	56.65		1320		1320	1.97		1320	0.69		1320			
1440	37.53		1440		1440	2.17	0.00	1440	0.77		1440			
1560			1560		1560			1560			1560			
1680			1680		1680			1680			1680			
1800			1800		1800			1800			1800			
1920			1920		1920			1920			1920			
2040			2040		2040			2040			2040			
2160			2160		2160			2160			2160			
2280			2280		2280			2280			2280			
2400			2400		2400			2400			2400			
2520			2520		2520			2520			2520			
2640			2640		2640			2640			2640			
2760			2760		2760			2760			2760			
2880			2880		2880			2880			2880			
3000			3000		3000			3000			3000			
3120			3120		3120			3120			3120			
3240			3240		3240			3240			3240			
3360			3360		3360			3360			3360			
3480			3480		3480			3480			3480			
3600			3600		3600			3600			3600			
3720			3720		3720			3720			3720			
3840			3840		3840			3840			3840			
3960			3960		3960			3960			3960			
4080			4080		4080			4080			4080			
4200			4200		4200			4200			4200			
4320			4320		4320			4320			4320			
Total time pumped(min):				1440		W/L	7.97		W/L	1.82		W/L		
Average yield (l/s):				14.05										

FORM 5 F														
CONSTANT DISCHARGE TEST & RECOVERY														
BOREHOLE TEST RECORD SHEET														
PROJ NO:	P1628		MAP REFERENCE:		33.88123		PROVINCE:		WC					
BOREHOLE NO:	LGC- BH02				19.76722		DISTRICT:		ROBERTSON					
ALT BH NO:	0						SITE NAME:		LE GRAND					
ALT BH NO:	0													
BOREHOLE DEPTH:	97.12		DATUM LEVEL ABOVE CASING (m):		0.52		EXISTING PUMP:		0					
WATER LEVEL (mbdl):	12.08		CASING HEIGHT: (magl):		0.15		CONTRACTOR:		AB PUMPS					
DEPTH OF PUMP (m):	89.00		DIAM PUMP INLET(mm):		200		PUMP TYPE:		GW 9602					
CONSTANT DISCHARGE TEST & RECOVERY														
TEST STARTED				TEST COMPLETED										
DATE:	22/05/2016		TIME:	7H30		DATE:	22/05/2016		TIME:	07H30		TYPE OF PUMP:	GW 9602	
				OBSERVATION HOLE 1			OBSERVATION HOLE 2			OBSERVATION HOLE 3				
				NR: BH03			NR:			NR:				
DISCHARGE BOREHOLE				Distance(m): 200			Distance(m):			Distance(m):				
TIME (MIN)	DRAW DOWN (M)	YIELD (L/S)	TIME (MIN)	RECOVERY (M)	TIME (min)	Drawdown (m)	Recovery (m)	TIME (min)	Drawdown (m)	Recovery	TIME (min)	Drawdown (m)		
1	2.71		1	44.82	1	0.00		1			1			
2	3.25		2	34.66	2			2			2			
3	3.82	11.90	3	25.47	3			3			3			
5	4.67	12.04	5	14.54	5			5			5			
7	5.68		7	14.35	7			7			7			
10	6.07	12.04	10	14.33	10			10			10			
15	6.76		15	14.21	15			15			15			
20	7.45	12.04	20	14.10	20			20			20			
30	8.73		30	13.62	30			30			30			
40	9.08	12.05	40	13.39	40			40			40			
60	9.57		60	13.00	60	0.00		60			60			
90	9.93	12.03	90	12.56	90			90			90			
120	10.40		120	12.17	120	0.00		120			120			
150	10.90	12.00	150	11.85	150			150			150			
180	11.45		180	11.75	180	0.00		180			180			
210	12.08	12.02	210	11.50	210			210			210			
240	13.48		240	11.25	240	0.00		240			240			
300	15.97	12.03	300	10.70	300	0.00		300			300			
360	19.09		360	10.27	360	0.00		360			360			
420	22.73	12.03	420	9.88	420	0.00		420			420			
480	26.84		480	9.51	480	0.00		480			480			
540	30.15	12.02	540		540	0.00		540			540			
600	33.97		600		600	0.00		600			600			
720	39.42	12.01	720		720	0.00		720			720			
840	46.28		840		840	0.00		840			840			
960	52.38	12.01	960		960	0.00		960			960			
1080	57.70		1080		1080	0.00		1080			1080			
1200	64.45	12.00	1200		1200	0.00		1200			1200			
1320	69.11	12.00	1320		1320	0.00		1320			1320			
1440	76.13		1440		1440	0.00		1440			1440			
1560			1560		1560			1560			1560			
1680			1680		1680			1680			1680			
1800			1800		1800			1800			1800			
1920			1920		1920			1920			1920			
2040			2040		2040			2040			2040			
2160			2160		2160			2160			2160			
2280			2280		2280			2280			2280			
2400			2400		2400			2400			2400			
2520			2520		2520			2520			2520			
2640			2640		2640			2640			2640			
2760			2760		2760			2760			2760			
2880			2880		2880			2880			2880			
3000			3000		3000			3000			3000			
3120			3120		3120			3120			3120			
3240			3240		3240			3240			3240			
3360			3360		3360			3360			3360			
3480			3480		3480			3480			3480			
3600			3600		3600			3600			3600			
3720			3720		3720			3720			3720			
3840			3840		3840			3840			3840			
3960			3960		3960			3960			3960			
4080			4080		4080			4080			4080			
4200			4200		4200			4200			4200			
4320			4320		4320			4320			4320			
Total time pumped(min):				1440		W/L	14.01		W/L			W/L		
Average yield (l/s):				12.00										

FORM 5 F														
CONSTANT DISCHARGE TEST & RECOVERY														
BOREHOLE TEST RECORD SHEET														
PROJ NO:	P1628		MAP REFERENCE:	33.88308		PROVINCE:	WESTERN CAPE							
BOREHOLE NO:	LGC BH 3 RIVER QUARTZ			19.76821		DISTRICT:	ROBERTSON							
ALT BH NO:	0					SITE NAME:	LE GRAND							
ALT BH NO:	0													
BOREHOLE DEPTH:	71.00		DATUM LEVEL ABOVE CASING (m):	0.50		EXISTING PUMP:	0							
WATER LEVEL (mbdl):	13.59		CASING HEIGHT: (magl):	0.19		CONTRACTOR:	AB PUMPS							
DEPTH OF PUMP (m):	65.00		DIAM PUMP INLET(mm):	200		PUMP TYPE:	GW 9602							
CONSTANT DISCHARGE TEST & RECOVERY														
TEST STARTED					TEST COMPLETED									
DATE:	19/05/2016		TIME:	15H15		DATE:	20/05/2016		TIME:	23H15		TYPE OF PUMP:	GW 9602	
					OBSERVATION HOLE 1			OBSERVATION HOLE 2			OBSERVATION HOLE 3			
					NR: BH02 OLD PIPE			NR: BH3A			NR:			
					Distance(m); 200			Distance(m); 120			Distance(m);			
TIME (MIN)	DRAW DOWN (M)	YIELD (L/S)	TIME (MIN)	RECOVERY (M)	TIME (min)	Drawdown (m)	Recovery (m)	TIME (min)	Drawdown (m)	Recovery (m)	TIME (min)	Drawdown (m)		
1	2.43	20.12	1	14.03	1		3.84	1		19.26	1			
2	3.05	27.74	2	13.45	2		3.84	2		19.26	2			
3	3.68	30.01	3	13.19	3		3.84	3		19.26	3			
5	3.99		5	12.68	5		3.84	5		19.23	5			
7	4.44		7	12.51	7		3.84	7		19.20	7			
10	4.88		10	12.30	10		3.83	10		19.17	10			
15	5.48	20.00	15	11.78	15		3.83	15		19.07	15			
20	5.88		20	11.62	20		3.83	20		18.85	20			
30	6.51	30.02	30	11.14	30		3.83	30		18.60	30			
40	6.97		40	10.85	40		3.82	40		18.22	40			
60	7.58	30.01	60	10.24	60	0.68	3.82	60		17.50	60			
90	8.41		90	9.49	90		3.75	90		16.47	90			
120	9.03	30.00	120	8.90	120	0.82	3.66	120		15.79	120			
150	9.58		150	8.41	150		3.56	150		15.31	150			
180	9.99	30.04	180	7.94	180	0.99	3.48	180		14.87	180			
210	10.47		210	7.60	210		3.41	210		14.35	210			
240	10.83	30.02	240	7.09	240	1.20	3.37	240		13.92	240			
300	11.21		300	6.84	300	1.38	3.29	300		13.44	300			
360	11.92	30.05	360	6.29	360	1.51	3.20	360		12.73	360			
420	12.33		420	5.92	420	1.85	3.14	420		12.15	420			
480	12.74	30.00	480	5.63	480	2.11	3.02	480		11.65	480			
540	13.12		540		540	2.29		540			540			
600	13.89	30.01	600		600	2.43		600			600			
720	14.32		720		720	2.76		720			720			
840	15.21	30.01	840		840	3.01		840			840			
960	15.77		960		960	3.15		960			960			
1080	16.12	30.02	1080		1080	3.32		1080	18.45		1080			
1200	16.54		1200		1200	3.50		1200	18.77		1200			
1320	16.82	30.00	1320		1320	3.65		1320	18.95		1320			
1440	17.26		1440		1440	3.84		1440	19.26		1440			
1560			1560		1560			1560			1560			
1680			1680		1680			1680			1680			
1800			1800		1800			1800			1800			
1920			1920		1920			1920			1920			
2040			2040		2040			2040			2040			
2160			2160		2160			2160			2160			
2280			2280		2280			2280			2280			
2400			2400		2400			2400			2400			
2520			2520		2520			2520			2520			
2640			2640		2640			2640			2640			
2760			2760		2760			2760			2760			
2880			2880		2880			2880			2880			
3000			3000		3000			3000			3000			
3120			3120		3120			3120			3120			
3240			3240		3240			3240			3240			
3360			3360		3360			3360			3360			
3480			3480		3480			3480			3480			
3600			3600		3600			3600			3600			
3720			3720		3720			3720			3720			
3840			3840		3840			3840			3840			
3960			3960		3960			3960			3960			
4080			4080		4080			4080			4080			
4200			4200		4200			4200			4200			
4320			4320		4320			4320			4320			
Total time pumped(min):				1440		W/L	12.17		W/L	12.17		W/L		
Average yield (l/s):				30.00										

FORM 5 F												
CONSTANT DISCHARGE TEST & RECOVERY												
BOREHOLE TEST RECORD SHEET												
PROJ NO: P1628			MAP REFERENCE: 33.89172			PROVINCE: WC			DISTRICT: ROBERTSON			
BOREHOLE NO: LGC BH05			19.7505			SITE NAME: LEGRAND						
ALT BH NO: 0												
ALT BH NO: 0												
BOREHOLE DEPTH: 98.40			DATUM LEVEL ABOVE CASING (m): 0.42			EXISTING PUMP: 0						
WATER LEVEL (m bdl): 12.53			CASING HEIGHT: (magl): 0.25			CONTRACTOR: AB PUMPS						
DEPTH OF PUMP (m): 95.00			DIAM PUMP INLET(mm): 200			PUMP TYPE: GW9602						
CONSTANT DISCHARGE TEST & RECOVERY												
TEST STARTED						TEST COMPLETED						
DATE: 03/06/2016		TIME: 13H00				DATE: 04/06/2016		TIME: 08H00		TYPE OF PUMP: GW9602		
OBSERVATION HOLE 1						OBSERVATION HOLE 2			OBSERVATION HOLE 3			
NR: LGC-BH04						NR:			NR:			
DISCHARGE BOREHOLE					Distance(m): 174M			Distance(m):				
TIME (MIN)	DRAW DOWN (M)	YIELD (L/S)	TIME (MIN)	RECOVERY (M)	TIME (min)	Drawdown (m)	Recovery (m)	TIME (min)	Drawdown (m)	Recovery (m)	TIME (min)	Drawdown (m)
1	3.35		1	13.07	1	0.00	1.08	1			1	
2	4.80	7.64	2	11.06	2		1.08	2			2	
3	6.05	8.03	3	10.80	3		1.08	3			3	
5	8.55		5	10.23	5		1.07	5			5	
7	10.55	8.01	7	10.02	7		1.07	7			7	
10	12.30		10	9.78	10		1.07	10			10	
15	13.20	8.03	15	9.43	15		1.06	15			15	
20	13.80		20	9.22	20		1.04	20			20	
30	14.65	8.04	30	8.67	30		1.04	30			30	
40	15.15		40	8.46	40		1.04	40			40	
60	16.24	8.02	60	7.74	60	0.08	1.03	60			60	
90	17.25		90	7.10	90		1.01	90			90	
120	17.70	8.01	120	6.64	120	0.11	0.98	120			120	
150	18.20		150	6.12	150		0.97	150			150	
180	18.55	8.03	180	5.94	180	0.14	0.95	180			180	
210	19.10		210	5.57	210		0.92	210			210	
240	19.33	8.02	240	5.21	240	0.16	0.91	240			240	
300	19.87		300	5.04	300	0.20	0.87	300			300	
360	20.33	8.01	360	4.88	360	0.22	0.84	360			360	
420	20.60		420	4.70	420	0.29	0.83	420			420	
480	20.97	8.03	480	4.59	480	0.38	0.81	480			480	
540	21.32		540		540	0.44		540			540	
600	21.61	8.03	600		600	0.55		600			600	
720	22.10		720		720	0.61		720			720	
840	22.58	8.02	840		840	0.68		840			840	
960	22.97		960		960	0.73		960			960	
1080	23.20	8.00	1080		1080	0.88		1080			1080	
1200	23.49		1200		1200	0.92		1200			1200	
1320	24.04	8.05	1320		1320	0.94		1320			1320	
1440	24.26		1440		1440	1.09		1440			1440	
1560			1560		1560			1560			1560	
1680			1680		1680			1680			1680	
1800			1800		1800			1800			1800	
1920			1920		1920			1920			1920	
2040			2040		2040			2040			2040	
2160			2160		2160			2160			2160	
2280			2280		2280			2280			2280	
2400			2400		2400			2400			2400	
2520			2520		2520			2520			2520	
2640			2640		2640			2640			2640	
2760			2760		2760			2760			2760	
2880			2880		2880			2880			2880	
3000			3000		3000			3000			3000	
3120			3120		3120			3120			3120	
3240			3240		3240			3240			3240	
3360			3360		3360			3360			3360	
3480			3480		3480			3480			3480	
3600			3600		3600			3600			3600	
3720			3720		3720			3720			3720	
3840			3840		3840			3840			3840	
3960			3960		3960			3960			3960	
4080			4080		4080			4080			4080	
4200			4200		4200			4200			4200	
4320			4320		4320			4320			4320	
Total time pumped(min):				1440		W/L	5.54		W/L	13.68		W/L
Average yield (l/s):				8.03								

FORM 5 F																
CONSTANT DISCHARGE TEST & RECOVERY																
BOREHOLE TEST RECORD SHEET																
PROJ NO: P1628		MAP REFERENCE: 33.885				PROVINCE: WC										
BOREHOLE NO: LGC BH08		19.75886				DISTRICT: ROBERTSON										
ALT BH NO: 0						SITE NAME: LE GRAND FARM										
BOREHOLE DEPTH: 90.50		DATUM LEVEL ABOVE CASING (m): 0.53				EXISTING PUMP: 0										
WATER LEVEL (mbdl): 13.09		CASING HEIGHT: (magl): 0.15				CONTRACTOR: AB PUMPS										
DEPTH OF PUMP (m): 83.50		DIAM PUMP INLET(mm): 200				PUMP TYPE: BP50										
CONSTANT DISCHARGE TEST & RECOVERY																
TEST STARTED				TEST COMPLETED												
DATE: 28/05/2016		TIME: 14H00		DATE:		TIME:		TYPE OF PUMP:				BP50				
DISCHARGE BOREHOLE				OBSERVATION HOLE 1			OBSERVATION HOLE 2			OBSERVATION HOLE 3			OBSERVATION HOLE 4			
NR: LG BH08B				NR: LG BH08A			NR: LG BH03			NR: LG BH01						
Distance(m): 200				Distance(m): 400			Distance(m): 900			Distance(m): 500						
TIME (MIN)	DRAW DOWN (M)	YIELD (L/S)	MIN	RECOVERY (M)	TIME (min)	Drawdown (m)	Recovery (m)	TIME (min)	Drawdown (m)	Recovery (m)	TIME (min)	Drawdown (m)	Recovery (m)	TIME (min)	Drawdown (m)	Recovery (m)
1	1.86		1	43.85	1		0.92	1			1			1		1.51
2	2.49	5.84	2	27.68	2		0.92	2			2			2		1.51
3	3.83	7.00	3	12.62	3		0.91	3			3			3		1.51
5	4.40		5	8.33	5		0.90	5			5			5		1.51
7	6.32		7	8.17	7		0.89	7			7			7		1.51
10	7.21		10	8.00	10		0.89	10			10			10		1.51
15	8.29	7.04	15	7.93	15		0.89	15			15			15		1.51
20	9.06		20	7.82	20		0.89	20			20			20		1.51
30	10.52	7.03	30	7.50	30		0.89	30			30			30		1.51
40	12.01		40	7.31	40		0.89	40	0.00		40	0.00		40		1.51
60	13.85	7.01	60	7.02	60	0.00	0.89	60			60			60		1.51
90	16.93		90	6.51	90		0.89	90	0.00		90	0.00		90	0.13	1.51
120	20.62	7.02	120	6.10	120	0.00	0.89	120			120			120		1.51
150	22.14		150	5.72	150		0.89	150	0.00		150	0.00		150	0.24	1.51
180	24.23	7.00	180	5.44	180	0.00	0.89	180			180			180		1.51
210	25.87		210	5.20	210		0.89	210	0.00		210	0.00		210	0.36	1.51
240	26.84	7.03	240	4.98	240	0.00	0.89	240			240			240		1.51
300	28.83		300	4.73	300	0.00	0.89	300			300			300	0.39	1.51
360	29.90	7.04	360	4.41	360	0.00	0.89	360			360			360		1.51
420	30.56		420	4.01	420	0.00	0.89	420	0.00		420	0.00		420		1.51
480	31.73	7.01	480	3.84	480	0.00	0.89	480			480			480	0.78	1.51
540	32.91		540		540	0.00		540			540			540		
600	34.38	7.00	600		600	0.00		600			600			600		
720	36.43		720		720	0.00		720	0.00		720	0.00		720	1.09	
840	38.67	7.02	840		840	0.00		840			840			840		
960	40.89		960		960	0.00		960	0.00		960	0.00		960	1.23	
1080	41.16	7.06	1080		1080	0.00		1080			1080			1080		
1200	42.83		1200		1200	0.00		1200	0.00		1200	0.00		1200	1.37	
1320	46.45	7.03	1320		1320	0.00		1320			1320			1320		
1440	49.94		1440		1440	0.00		1440	0.00		1440	0.00		1440	1.51	
1560			1560		1560			1560			1560			1560		
1680			1680		1680			1680			1680			1680		
1800			1800		1800			1800			1800			1800		
1920			1920		1920			1920			1920			1920		
2040			2040		2040			2040			2040			2040		
2160			2160		2160			2160			2160			2160		
2280			2280		2280			2280			2280			2280		
2400			2400		2400			2400			2400			2400		
2520			2520		2520			2520			2520			2520		
2640			2640		2640			2640			2640			2640		
2760			2760		2760			2760			2760			2760		
2880			2880		2880			2880			2880			2880		
3000			3000		3000			3000			3000			3000		
3120			3120		3120			3120			3120			3120		
3240			3240		3240			3240			3240			3240		
3360			3360		3360			3360			3360			3360		
3480			3480		3480			3480			3480			3480		
3600			3600		3600			3600			3600			3600		
3720			3720		3720			3720			3720			3720		
3840			3840		3840			3840			3840			3840		
3960			3960		3960			3960			3960			3960		
4080			4080		4080			4080			4080			4080		
4200			4200		4200			4200			4200			4200		
4320			4320		4320			4320			4320			4320		
Total time pumped(min):				1440	W/L		6.7	W/L		15.33	W/L		12.71	W/L		5.25
Average yield (l/s):				7.02												

FORM 5 F													
CONSTANT DISCHARGE TEST & RECOVERY													
BOREHOLE TEST RECORD SHEET													
PROJ NO:	P1815		MAP REFERENCE:		S33.880713			PROVINCE:		WESTERN CAPE			
BOREHOLE NO:	HABATA BH2				E19.77258			DISTRICT:		ROBERTSON			
ALT BH NO:	0							SITE NAME:		HABATA			
ALT BH NO:	#REF!												
BOREHOLE DEPTH:	120.02		DATUM LEVEL ABOVE CASING (m):		0.26			EXISTING PUMP:		NEW BOREHOLE			
WATER LEVEL (mbdl):	25.92		CASING HEIGHT: (magl):		0.30			CONTRACTOR:		AB PUMPS			
DEPTH OF PUMP (m):	85.10		DIAM PUMP INLET(mm):		180			PUMP TYPE:		BP50			
CONSTANT DISCHARGE TEST & RECOVERY													
TEST STARTED				TEST COMPLETED									
DATE:	20/06/2017		TIME:	08H30		DATE:			TIME:			TYPE OF PUMP:	BP50
				OBSERVATION HOLE 1			OBSERVATION HOLE 2			OBSERVATION HOLE 3			
				NR: HBB01			NR: LGC BH3			NR: HABATA-4			
				Distance(m): 1400			Distance(m): 476			Distanc376			
TIME	DRAW	YIELD	TIME	RECOVERY	TIME	Drawdown	Recovery	TIME	Drawdown	Recovery	TIME	Drawdown	
(MIN)	DOWN (M)	(L/S)	MIN	(M)	(min)	m	(m)	(min)	(m)		(min)	(m)	
1	2.19		1	17.90	1			1			1		
2	3.41		2	15.50	2			2			2		
3	4.74		3	14.57	3			3			3		
5	5.80	4.41	5	13.25	5			5			5		
7	6.57		7	12.23	7			7			7		
10	8.39	4.41	10	11.20	10			10			10		
15	10.16		15	9.65	15			15			15		
20	12.70	4.40	20	9.03	20			20			20		
30	13.65		30	7.65	30	0.00		30	0.00		30	0.00	
40	15.10	4.41	40	7.03	40			40			40		
60	16.51		60	6.10	60	0.00		60	0.00		60	0.00	
90	17.56	4.40	90	5.54	90			90			90		
120	18.14		120	5.01	120	0.00		120	0.00		120	0.00	
150	18.70	4.42	150	4.75	150			150			150		
180	18.90		180	4.60	180	0.00		180	0.00		180	0.00	
210	19.11	4.41	210	4.43	210			210			210		
240	19.30		240	4.25	240	0.00		240	0.00		240	0.00	
300	19.76	4.41	300	3.80	300			300			300		
360	20.03		360	3.61	360	0.00		360	0.00		360	0.00	
420	20.12	4.42	420	3.44	420			420			420		
480	20.35		480	3.27	480	0.00		480	0.00		480	0.00	
540	20.42	4.41	540	3.11	540			540			540		
600	20.66		600	3.05	600	0.00		600	0.00		600	0.00	
720	20.80	4.42	720	2.81	720	0.00		720	0.00		720	0.00	
840	21.04		840	2.63	840	0.00		840	0.00		840	0.00	
960	21.22	4.40	960	2.46	960	0.00		960	0.00		960	0.00	
1080	21.46		1080	2.29	1080	0.00		1080	0.00		1080	0.00	
1200	21.61	4.42	1200	2.17	1200	0.00		1200	0.00		1200	0.00	
1320	21.80		1320	2.02	1320			1320			1320		
1440	22.05	4.41	1440	1.94	1440			1440			1440		
1560			1560		1560			1560			1560		
1680			1680		1680			1680			1680		
1800			1800		1800			1800			1800		
1920			1920		1920			1920			1920		
2040			2040		2040			2040			2040		
2160			2160		2160			2160			2160		
2280			2280		2280			2280			2280		
2400			2400		2400			2400			2400		
2520			2520		2520			2520			2520		
2640			2640		2640			2640			2640		
2760			2760		2760			2760			2760		
2880			2880		2880			2880			2880		
3000			3000		3000			3000			3000		
3120			3120		3120			3120			3120		
3240			3240		3240			3240			3240		
3360			3360		3360			3360			3360		
3480			3480		3480			3480			3480		
3600			3600		3600			3600			3600		
3720			3720		3720			3720			3720		
3840			3840		3840			3840			3840		
3960			3960		3960			3960			3960		
4080			4080		4080			4080			4080		
4200			4200		4200			4200			4200		
4320			4320		4320			4320			4320		
Total time pumped(min):				1440		W/L	8.93		W/L	13.21		W/L	19.51
Average yield (l/s):				4.41									

FORM 5 F
CONSTANT DISCHARGE TEST & RECOVERY

BOREHOLE TEST RECORD SHEET

PROJ NO: P1815	MAP REFERENCE: S33.88239	PROVINCE: WESTERN CAPE
BOREHOLE NO: HABATA BH04	E019.76898	DISTRICT: ROBERTSON
ALT BH NO: 0		SITE NAME: HABATA FARM
ALT BH NO: 0		
BOREHOLE DEPTH: 96.80	DATUM LEVEL ABOVE CASING (m): 0.34	EXISTING PUMP: NEW BOREHOLE
WATER LEVEL (mbdl): 20.29	CASING HEIGHT: (magl): 0.30	CONTRACTOR: AB PUMPS
DEPTH OF PUMP (m): 64.00	DIAM PUMP INLET(mm): 210	PUMP TYPE: GW9602

CONSTANT DISCHARGE TEST & RECOVERY

TEST STARTED				TEST COMPLETED											
DATE: 28/06/2017	TIME: 12H00	DATE: 30/06/2017	TIME: 10H00	TYPE OF PUMP:		GW9602									
OBSERVATION HOLE 1				OBSERVATION HOLE 2		OBSERVATION HOLE 3									
NR: BH02				NR: BH03		NR: LGC BH01									
Distance(m): 210				Distance(m): 105		Distance(m): 1047									
Distance(m): 1047				Distance(m): 1047		Distance(m): 1047									
NR: HBH 02				NR: HBH 02		NR: HBH 02									
Distance(m): 1047				Distance(m): 1047		Distance(m): 1047									
TIME (MIN)	DRAW DOWN (M)	YIELD (L/S)	RECOVERY (MIN)	RECOVERY (M)	TIME (min)	Drawdown (m)	Recovery (m)	TIME (min)	Drawdown (m)	Recovery (m)	TIME (min)	Drawdown (m)	TIME (min)	Drawdown (m)	
1	1.89		1	13.76	1			1		5.70	1				
2	2.39		2	10.05	2			2		5.60	2				
3	2.66		3	8.64	3			3		5.53	3				
5	5.21	10.05	5	6.47	5			5		5.39	5				
7	8.85	11.06	7	6.26	7			7		5.28	7				
10	12.57		10	5.85	10			10		5.16	10				
15	15.46		15	5.40	15			15		5.02	15				
20	16.33	11.04	20	5.13	20			20		4.90	20				
30	17.10		30	4.85	30	0.05		30	1.04	4.75	30				
40	17.80		40	4.64	40			40		4.60	40				
60	18.74	11.11	60	4.32	60	0.05		60	1.52	4.40	60	0.00			
90	18.79		90	4.07	90			90	1.82	4.11	90			0.00	
120	18.91		120	3.84	120	0.08		120	2.05	3.92	120				
150	19.06	11.12	150	3.65	150	0.12		150	2.29	3.72	150	0.12			
180	19.24		180	3.51	180	0.15		180	2.47	3.59	180				
210	19.54	11.04	210	3.35	210	0.22		210	2.63	3.41	210				
240	19.82		240	3.21	240	0.28		240	2.80	3.39	240				
300	20.17	11.09	300	3.01	300	0.35		300	3.07	3.18	300				
360	20.78		360	2.83	360	0.49		360	3.33	2.90	360			0.00	
420	21.12	11.01	420	2.67	420	0.54		420	3.53	2.78	420				
480	21.62		480	2.52	480	0.58		480	3.80	2.68	480				
540	21.96	11.10	540	2.40	540	0.66		540	3.95	2.57	540				
600	22.40		600	2.32	600	0.71		600	4.35	2.46	600				
720	22.77	11.05	720	2.17	720	0.80		720	4.40	2.34	720				
840	23.10		840	2.08	840	0.92		840	4.51	2.24	840				
960	23.38	11.13	960	1.95	960	0.99		960	4.77	2.10	960				
1080	23.74		1080	1.82	1080	1.12		1080	5.20	1.95	1080				
1200	24.09	11.08	1200	1.74	1200	1.25		1200	5.40	1.87	1200	0.13		0.00	
1320	24.49		1320	1.67	1320	1.33		1320	5.61	1.78	1320				
1440	24.70	11.05	1440	1.44	1440	1.41		1440	5.80		1440	0.09		0.00	
1560			1560		1560			1560			1560				
1680			1680		1680			1680			1680				
1800			1800		1800			1800			1800				
1920			1920		1920			1920			1920				
2040			2040		2040			2040			2040				
2160			2160		2160			2160			2160				
2280			2280		2280			2280			2280				
2400			2400		2400			2400			2400				
2520			2520		2520			2520			2520				
2640			2640		2640			2640			2640				
2760			2760		2760			2760			2760				
2880			2880		2880			2880			2880				
3000			3000		3000			3000			3000				
3120			3120		3120			3120			3120				
3240			3240		3240			3240			3240				
3360			3360		3360			3360			3360				
3480			3480		3480			3480			3480				
3600			3600		3600			3600			3600				
3720			3720		3720			3720			3720				
3840			3840		3840			3840			3840				
3960			3960		3960			3960			3960				
4080			4080		4080			4080			4080				
4200			4200		4200			4200			4200				
4320			4320		4320			4320			4320				
Total time pumped(min):				1440	W/L	6.9		W/L	14.07		W/L	8.02		W/L	8.68
Average yield (l/s):															

FORM 5 F																	
CONSTANT DISCHARGE TEST & RECOVERY																	
BOREHOLE TEST RECORD SHEET																	
PROJ NO: P1815		MAP REFERENCE: S33.89397				PROVINCE: WESTERN CAPE											
BOREHOLE NO: HABATA BH08		E19.75197				DISTRICT: ROBERTSON											
ALT BH NO: 0						SITE NAME: HABATA											
ALT BH NO: 0																	
BOREHOLE DEPTH: 102.76		DATUM LEVEL ABOVE CASING (m): 0.30				EXISTING PUMP: NEW BOREHOLE											
WATER LEVEL (mbdl): 24.80		CASING HEIGHT: (magl): 0.40				CONTRACTOR: AB PUMPS											
DEPTH OF PUMP (m): 89.00		DIAM PUMP INLET(mm): 210				PUMP TYPE: GW9002											
CONSTANT DISCHARGE TEST & RECOVERY																	
TEST STARTED				TEST COMPLETED													
DATE:	01/07/2017	TIME:	16H00	DATE:	03/07/2017	TIME:		TYPE OF PUMP:	GW9002								
DISCHARGE BOREHOLE				OBSERVATION HOLE 1			OBSERVATION HOLE 2			OBSERVATION HOLE 3			OBSERVATION HOLE 3				
				NR:	LGC BH5		NR:	LGC BH9		NR:	LGC BH 01		NR:	HABATA 9			
				Distance(m):	242		Distance(m):	399		Distanc	696		Distance(m):	949			
TIME (MIN)	DRAW DOWN (M)	YIELD (L/S)	TIME (MIN)	RECOVERY (M)	TIME (min)	Drawdown (m)	Recovery (m)	TIME (min)	Drawdown (m)	Recovery (m)	TIME (min)	Drawdown (m)	TIME (min)	Drawdown (m)			
1	1.27		1	19.00	1			1			1		1				
2	3.80		2	18.74	2			2			2		2				
3	3.79		3	18.60	3			3			3		3				
5	5.24	7.32	5	17.95	5			5			5		5				
7	5.99		7	17.37	7			7			7		7				
10	11.62		10	17.03	10			10			10		10				
15	13.15		15	16.60	15			15			15		15				
20	13.95	7.31	20	16.34	20			20			20		20				
30	15.48		30	15.85	30	0.00		30	0.00		30	0.00	30	0.00			
40	16.38		40	15.52	40			40			40		40				
60	17.37	7.30	60	15.00	60	0.00		60	0.00		60	0.00	60	0.00			
90	18.37		90	14.27	90	0.00		90	0.00		90	0.00	90	0.00			
120	18.95		120	13.60	120	0.00		120	0.00		120	0.00	120	0.00			
150	19.52	7.51	150	13.02	150	0.00		150	0.00		150	0.00	150	0.00			
180	20.00		180	12.60	180	0.00		180	0.00		180	0.00	180	0.00			
210	20.45		210	12.20	210	0.00		210	0.00		210	0.00	210	0.00			
240	20.86	7.30	240	11.70	240	0.00		240	0.00		240	0.00	240	0.00			
300	21.40		300	11.08	300	0.00		300	0.00		300	0.00	300	0.00			
360	21.98		360	10.77	360	0.00		360	0.00		360	0.00	360	0.00			
420	22.67	7.31	420	10.04	420	0.00		420	0.00		420	0.00	420	0.00			
480	23.04		480	9.24	480	0.00		480	0.00		480	0.00	480	0.00			
540	23.85		540	9.00	540	0.00		540	0.00		540	0.00	540	0.00			
600	24.50	7.32	600	8.56	600	0.00		600	0.00		600	0.00	600	0.00			
720	25.70		720	7.49	720	0.00		720	0.00		720	0.00	720	0.00			
840	27.07		840	6.74	840	0.00		840	0.00		840	0.00	840	0.00			
960	29.50	7.33	960	5.67	960	0.00		960	0.00		960	0.00	960	0.00			
1080	31.67		1080	4.96	1080	0.00		1080	0.00		1080	0.00	1080	0.00			
1200	32.40		1200	4.30	1200	0.00		1200	0.00		1200	0.00	1200	0.00			
1320	32.80	7.32	1320		1320	0.00		1320	0.00		1320	0.00	1320	0.00			
1440	33.36		1440		1440	0.00		1440	0.00		1440	0.00	1440	0.00			
1560			1560		1560			1560			1560		1560				
1680			1680		1680			1680			1680		1680				
1800			1800		1800			1800			1800		1800				
1920			1920		1920			1920			1920		1920				
2040			2040		2040			2040			2040		2040				
2160			2160		2160			2160			2160		2160				
2280			2280		2280			2280			2280		2280				
2400			2400		2400			2400			2400		2400				
2520			2520		2520			2520			2520		2520				
2640			2640		2640			2640			2640		2640				
2760			2760		2760			2760			2760		2760				
2880			2880		2880			2880			2880		2880				
3000			3000		3000			3000			3000		3000				
3120			3120		3120			3120			3120		3120				
3240			3240		3240			3240			3240		3240				
3360			3360		3360			3360			3360		3360				
3480			3480		3480			3480			3480		3480				
3600			3600		3600			3600			3600		3600				
3720			3720		3720			3720			3720		3720				
3840			3840		3840			3840			3840		3840				
3960			3960		3960			3960			3960		3960				
4080			4080		4080			4080			4080		4080				
4200			4200		4200			4200			4200		4200				
4320			4320		4320			4320			4320		4320				
Total time pumped(min):				1440		W/L	7.43		W/L	1.73		W/L	8,31		W/L	0,25	
Average yield (l/s):				7.32													

(Last Page)